AN EVALUATION OF THE LIGAND EFFECTS ON NEOPENTYL PHOSPHINE DERIVED PRECATALYSTS FOR N-ARYLATION REACTIONS AND FOR THE CROSS-COUPLING OF ARYL ACETYLENES WITH PROPARGYL ALCOHOLS AND AMIDES

by

CORRIE E. BURLAS

KEVIN H. SHAUGHNESSY, COMMITTEE CHAIR
SILAS C. BLACKSTOCK
ELIZABETH T. PAPISH
STEPHEN A. WOSKI
JASON E. BARA

A DISSERTATION

Submitted in partial fulfillment of the requirements
for the degree of Doctor of Philosophy
in the Department of Chemistry and Biochemistry
in the Graduate School of
The University of Alabama

TUSCALOOSA, ALABAMA

2022

ABSTRACT

Palladium catalyzed cross-coupling reactions are some of the most widely employed methods for forming new C-C and C-heteroatom bonds in both academic and industrial settings. Much of the focus on developing these catalytic systems has shifted to identifying more effective ligands to facilitate these transformations. Trialkyl phosphines are a powerful class of ligands that have garnered a lot of interest in recent decades due to their ability to effectively catalyze a wide variety of cross-coupling reactions. Much of the focus in the Shaughnessy group has been on evaluating a series of neopentyl (Np) alkyl phosphine ligands and their capacity to catalyze different C-C and C-N coupling reactions.

Specifically, I prepared and tested a series of air-stable $[(Np_3P)Pd(Ar)Br]_2$ and $(Np_3P)Pd(Ar)(amine)$ precatalysts for the coupling of sterically hindered aryl bromides and aniline derivatives. The amine adducts were less active than the bromine-bridged dimers, however, these precatalysts were more active than the catalyst generated in situ from $Pd_2(dba)_3$ and PNp_3. We also demonstrated a positive correlation between increasing the steric bulk of the aryl group and increased catalytic activity in these N-arylation reactions.

Recently the Shaughnessy group developed a method for the selective cross-coupling of terminal aryl alkynes with propargyl alcohols to afford linear (E) enynol products using a di-*tert*-butylneopentyl phosphine (DTBNpP) derived palladacycle. Inspired by these findings, I aimed to determine how the identity of the ligand would impact the selectivity of the cross-coupling reactions. I synthesized novel variants of the complex $[Pd(\mu\text{-}\kappa^2\text{-}O,O\text{-}OAc)(\kappa^2\text{-}C,P\text{-}(R)_2PCH_2C(Me)_2CH_2)]_2$ with R groups of varying size (R = cyclohexyl or isopropyl) in order to

evaluate the steric effects of the phosphine ligand backbone on the outcome of the cross coupling of terminal aryl acetylenes with propargyl alcohol and *N*-propargylphthalimide.

LIST OF ABBREVIATIONS AND SYMBOLS

[M]	metal
Ad	adamantane
Ar	aryl group
BASF	Badische Anilin und Soda Fabrik
br	broad
cod	1,5-cyclooctadiene
Cy	cyclohexyl
d	doublet
dba	dibenzylideneacetone
DCM	dichlormethane
DCyNpP	dicyclohexylneopentylphosphine
Dd	doubet of doublets
dippp	3-bis(diisopropylphosphino)propane
DiPrNpP	diisopropylneopentyl phosphine
dppf	1,1′-(diphenylphosphino)ferrocene
DTBNpP	di-*tert*-butylneopentyl phosphine
HOMO	highest occupied molecular orbital
Hz	Hertz
iPr	isopropyl

J	coupling constant (Hz)
kcal	kilocalories
L	ligand
LUMO	lowest unoccupied molecular orbital
m	meta
m	multiplet
Me	methyl
MeCN	acetonitrile
mol	mole
ND	not determined
NMR	nuclear magnetic resonance
Np	neopentyl
NPhth	*N*-Phthalimide
Nu	nucleophile
o	ortho
OAc	acetate
OTf	triflate
p	para
P(*t*-Bu)$_3$	tri-*tert*-butyl phosphine
PCy$_3$	tricyclohexylphosphine
Ph	phenyl
PPh$_3$	triphenylphosphine
R	alkyl group

RT	room temperature
s	singlet
t	triplet
t-Bu	*tert*-butyl
TBDNpP	*tert*-butyldineopentyl phosphine
THF	tetrahydrofuran
TNpP	trineopentyl phosphine
TTBP	tri-*tert*-butyl phosphine
X	halide

ACKNOWLEDGMENTS

First and foremost, I would Like to thank Dr. Kevin Shaughnessy for all of his guidance, patience, and support throughout my time at the University of Alabama. I would not have been successful without his mentorship, and I am forever thankful that I joined his research group. I would like to thank my committee members Dr. Silas Blackstock, Dr. Elizabeth Papish, Dr. Stephen Woski, and Dr. Jason Bara for their guidance and advice over the years. I would also like to acknowledge a committee member of mine who passed earlier this year, Dr. Michael Jennings, and thank him for all of his kindness, advice, and encouragement.

A special shoutout goes to my lab mates Dr. Benjamin Headford, Jordan Pierce, Andrea Núñez León, Emily McEachern, Makynna Koper, and Kehinde Ogunmola for their friendship and support. Thank you so much for all of the late nights, early mornings, seemingly endless afternoons, and general good times. You were my rocks, and I could not have done this without you all.

I also want to thank my high school chemistry teacher Gloria Fisher for helping me discover my passion for chemistry. Finally I would like to thank my family and friends for their constant encouragement and overwhelming love and support.

CONTENTS

LIST OF TABLES

LIST OF FIGURES

LIST OF SCHEMES

CHAPTER 1: A SURVEY OF PALLADIUM CATALYZED CROSS-COUPLING REACTIONS

1.1 Introduction to Palladium-Catalyzed Cross Coupling Reactions

Palladium-catalyzed cross coupling reactions have become a crucial method for the formation of carbon-carbon and carbon-heteroatom bonds in recent decades. Typically in these reactions an electrophilic substrate, such as aryl, alkenyl, or alkyl halide/pseudohalide, reacts with a nucleophile to form the coupled product. There are a number of named reactions that have been developed to make a wide variety of desirable new sp, sp^2, and even sp^3 carbon-carbon/heteroatom bonds (Figure 1.1).[1-9] Methodologies such as these are heavily relied upon for the synthesis of pharmaceuticals, agrochemicals, organic materials and natural products.[10-13]

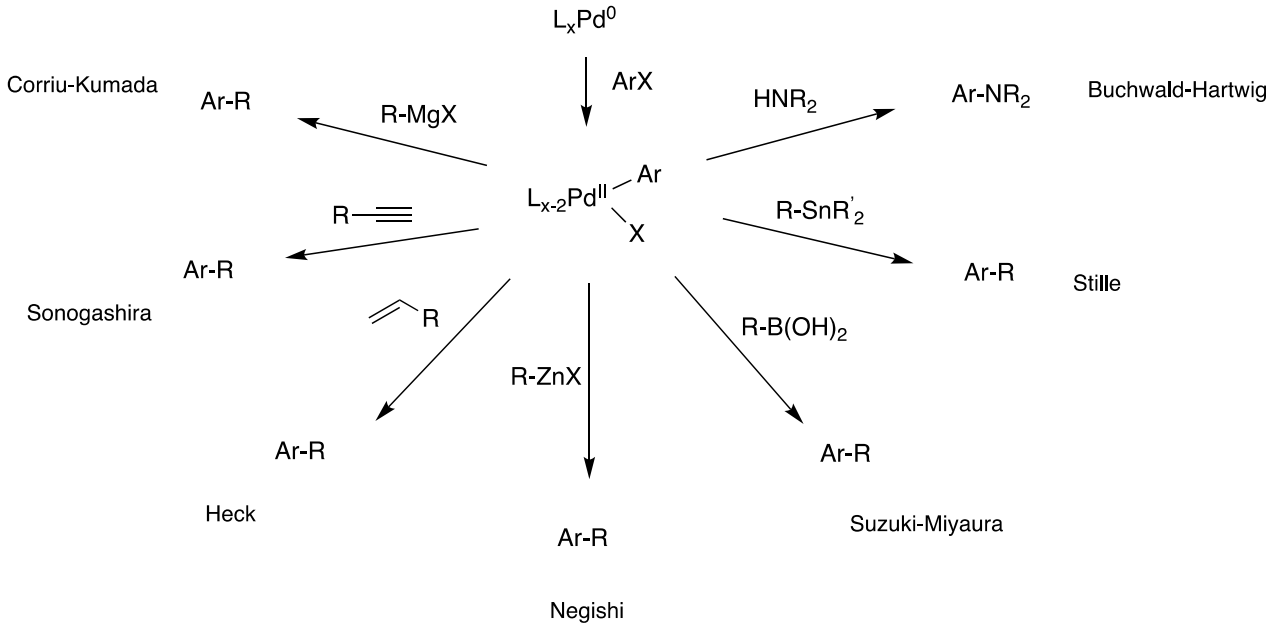

Figure 1.1: Examples of common palladium-catalyzed cross-coupling reactions.

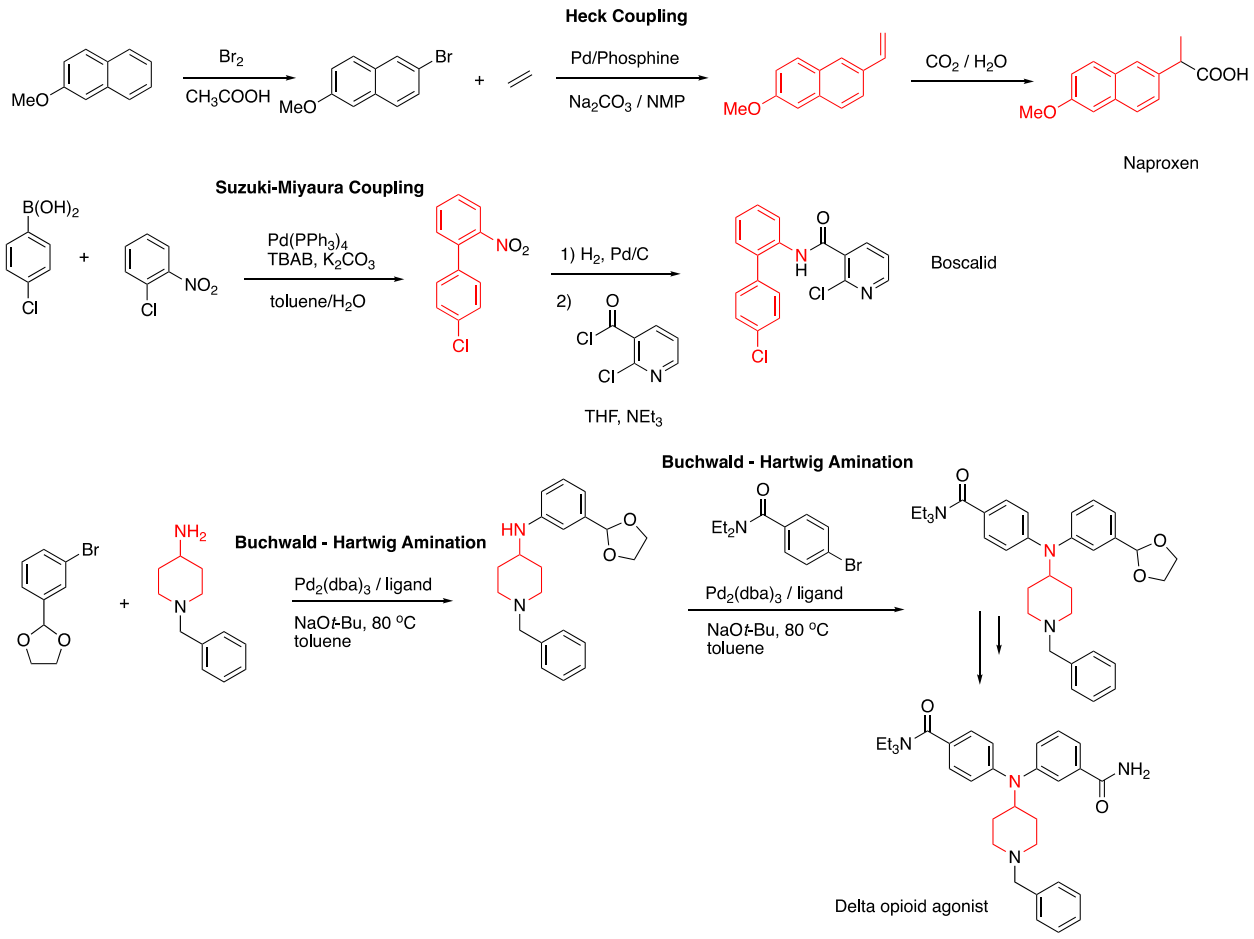

Figure 1.2: Examples of palladium-catalyzed cross-coupling reactions used in industrial processes.

For example, a Heck-type cross-coupling between and aryl bromide intermediate and ethylene is used to produce the common pain reliever Naproxen.[14] Boscalid is a fungicide developed by BASF in 2003. As of 2018, over 1000 tons of this fungicide are being produced annually. A key step in the synthesis of Boscalid is the Suzuki-Miyaura reaction of 1-chloro-2-nitrobenzene and 4-chloroboronic acid.[11] Successive Buchwald-Hartwig amination reactions can be used to generate an important intermediate in the synthesis of a delta opioid agonist (Figure 1.2).[15]

Although the overall mechanisms for these transformations vary depending on the coupling partners, they follow the same general catalytic cycle that involves a series of linked reactions including oxidative addition, transmetallation, and reductive elimination (Figure 1.3). All of these cross-coupling reactions require catalytically active L_nPd^0 to proceed. Generation of the active catalyst is typically accomplished using a Pd(II) or Pd(0) species, such as palladium(II) acetate ($Pd(OAc)_2$) or tris(dibenzylideneacetone)dipalladium(0) ($Pd_2(dba)_3$), and free ligand to form Pd(0) in situ.[13] Though palladium-catalyzed cross-coupling reactions are invaluable tools to obtain complex and useful organic motifs, there are always multiple ways in which they can be expanded and improved upon.

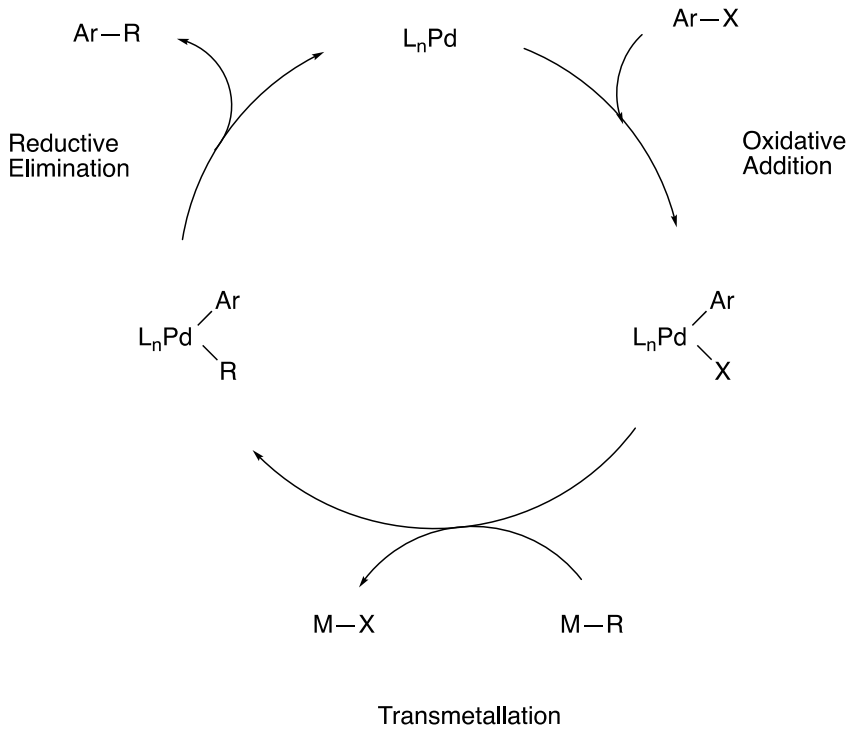

Figure 1.3: General mechanism for palladium-catalyzed cross-coupling reactions.

Since the beginning of what are now well-established methods for cross-coupling, researchers have been working to better understand what role the ligand plays in the different steps along the catalytic cycle. Triphenylphosphine (PPh_3) was the most popular ligand used during the early days of palladium catalysis. Although PPh_3 was, and still is, an effective choice of ligand for many cross-coupling reactions, certain classes of substrates will not effectively couple when PPh_3 is used. For example, electron-rich aryl chlorides are generally unreactive substrates under conditions that can easily couple their bromide and iodide counterparts. The low reactivity of aryl chlorides is due to the strength of the C-Cl bond (bond dissociation energies for PhX: Cl: 96 $kcalmol^{-1}$, Br: 81 $kcalmol^{-1}$, I: 65 $kcalmol^{-1}$). The stronger C-Cl bond makes the rate-limiting oxidative addition step that is necessary to continue along the catalytic cycle extremely slow, if not impossible, at temperatures under 140 °C.[16, 17] Challenges in activating difficult substrates, such as aryl chlorides or electron-rich heteroaryl halides, created a need for organic chemists to expand the library of ligands available for use in cross-coupling reactions.

1.2 Phosphine Ligands for Palladium Cross-Coupling

In 1979 Kumada was already noting the enhanced activity of palladium catalysts being used for the coupling of Grignard reagents and organic halides when employing the bidentate ligand 1,1′-(diphenylphosphino)ferrocene (dppf).[18] This bidentate ligand blocked open coordination sites on the metal and reduced the amount of β-hydride elimination observed in the alkylation reactions. By 1989, both Milstein and Osborn reported successful catalytic methods for the carbonylation of aryl chlorides using 3-bis(diisopropylphosphino)propane (dippp) and tricyclohexylphosphine (PCy_3), respectively (Figure 1.4).[19, 20] Milstein and Osborn were some of the first to acknowledge the enormity of the impact that both the steric and electronic nature of the ligand can have on the outcome and efficiency of catalytic reactions. Their reports suggest

that electron rich phosphines with a lot of steric bulk can significantly increase the catalytic activity of the metal they are bound to. The added electron density from the phosphine promotes oxidative addition and the steric bulk causes strain that facilitates reductive elimination to get back to a more stable geometry around the metal center.

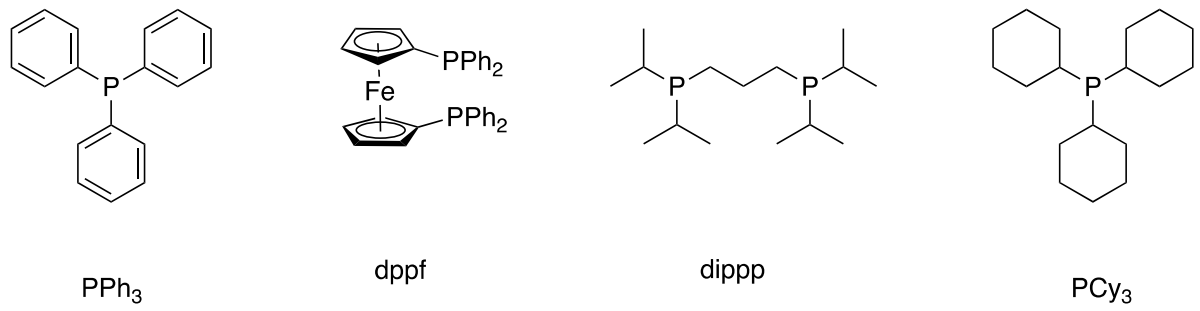

Figure 1.4: Examples of early tertiary phosphine ligands.

These observations ushered in a new era for the catalytic cross-coupling field. Substrates once thought of as not viable as cross-coupling partners were able to be added to the substrate scopes. Independently but concurrently, Buchwald and Hartwig reported improved protocols for coupling amines with aryl halides. Hartwig used the alkyl phosphine ligand tri-*tert*-butyl phosphine (P(*t*-Bu)$_3$) to facilitate room temperature animations of aryl chlorides and aryl bromides.[21, 22] Buchwald discovered that the catalytic activity of palladium in similar C-N coupling reactions and in Suzuki-Miyaura couplings could be enhanced by using dialkyl biaryl phosphine ligands.[23, 24] Fu and coworkers enhanced the efficiency and accessibility of multiple cross-coupling methods, such as Suzuki-Miyaura and Heck couplings, using the bulky alkyl phosphine ligands P(*t*-Bu)$_3$ and PCy$_3$.[25, 26]

Over the last several decades, these systems continue to be improved upon as catalysts with more complex tertiary phosphine ligands are synthesized. Some of the more notable advancements are Hartwig's dialkylferrocene phosphine ligand (QPhos) and Buchwald's

multiple generations of biaryl phosphines (Figure 1.5).[13] Beller and coworkers significantly expanded the scope of Suzuki-Miyaura cross-coupling reactions to include deactivated aryl chlorides using the extremely bulky diadamantyl alkyl phosphine ligand CataCXium A.[27] More recently, Carrow reported on an even more sterically hindered triadamantylphosphine ligand (PAd_3) that further enhances the efficiency and expands the substrate scope of Suzuki-Miyaura type reactions.[28]

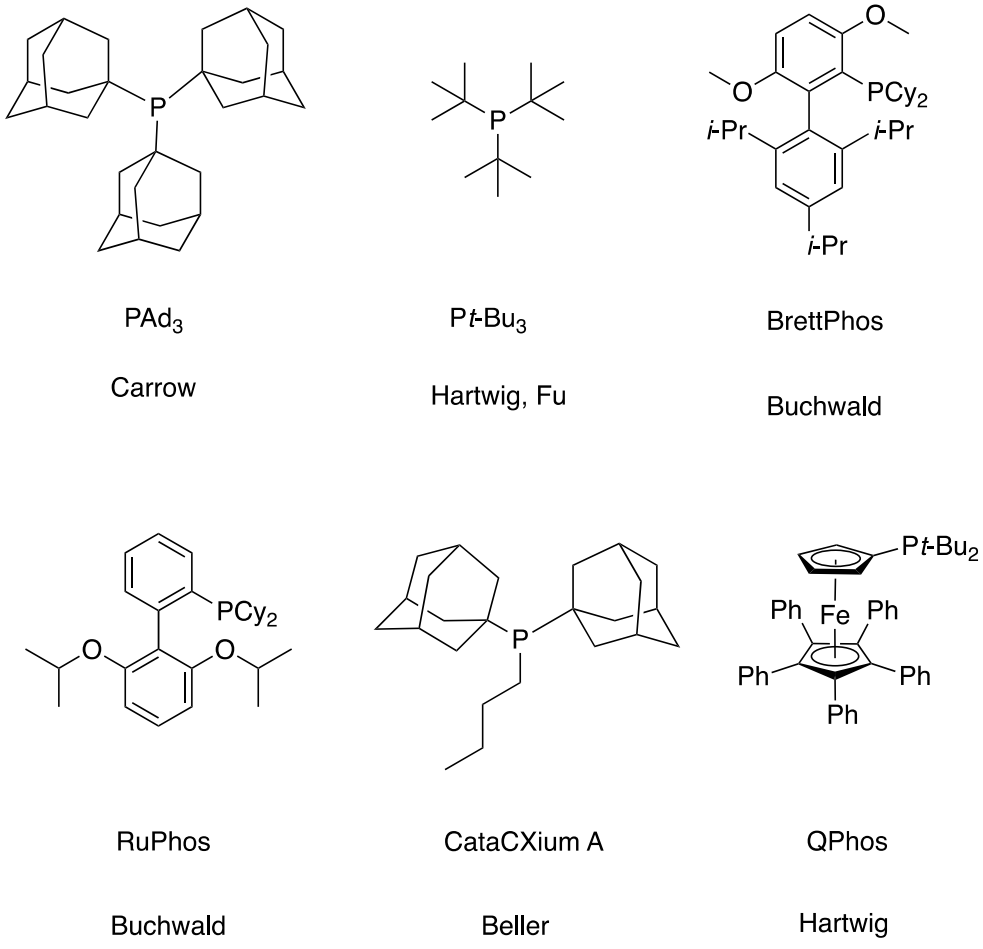

Figure 1.5: Examples of sterically hindered, electron rich phosphine ligands.

It is now widely understood that sterically demanding and electron rich phosphine ligands, such as P(*t*-Bu)$_3$ and PAd$_3$, can enhance the efficiency of catalysts in the cross-coupling reactions of an ever increasing broad range of aryl halides/pseudohalides, including aryl chlorides.[25, 29, 30] Investigations into why sterically hindered phosphines have this effect revealed that the active species in the catalytic reactions is a monoligated complex (LPd) when bulkier ligands are used. In contrast, less sterically hindered ligands are more likely to produce an active species with a 2:1 ratio of ligand to palladium (L$_2$Pd).[31-33] The larger the R group in PR$_3$ the more destabilized the L$_2$Pd species becomes. This induces ligand dissociation to promote the generation of a monoligated LPd complex that is electron deficient and therefore more reactive towards oxidative addition. These monoligated complexes where L is a sterically hindered phosphine are then further stabilized by the added σ-donation from the phosphorous that raises the energy of palladium's highest occupied molecular orbital (HOMO). This makes interaction with the lowest unoccupied molecular orbital (LUMO) of Ar-X more accessible and facilitates oxidative addition of the aryl substrates. Bulkier phosphine ligands are also known to enhance the efficiency of the reductive elimination step in palladium-catalyzed cross-coupling reactions by promoting the elimination of the added steric strain coming from the coupling substrates.

1.3 Neopentyl Phosphine

The Shaughnessy group has been investigating a series of phosphine ligands that contain one or more neopentyl moieties to use to develop complexes to use for a variety of cross-coupling reactions (Figure 1.6). The methylene in the neopentyl substituent gives the group additional conformational flexibility compared to other sterically demanding substituents of comparable size such as P*t*-Bu$_3$.[34] The added flexibility allows the coordination sphere of the palladium to accommodate more sterically demanding aryl ligands.

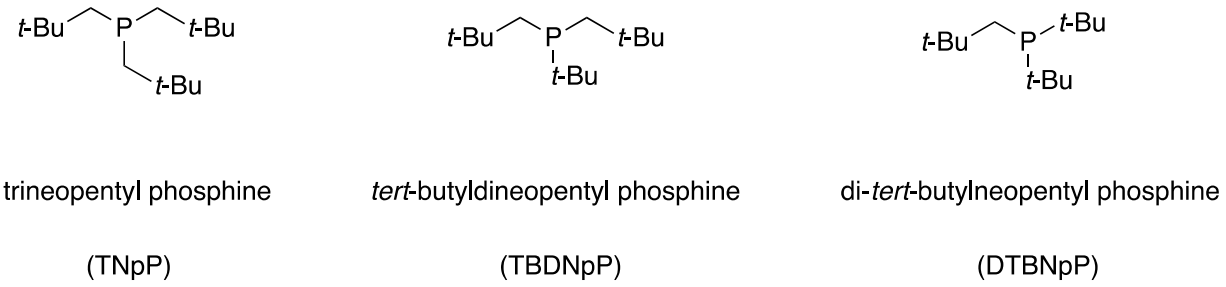

trineopentyl phosphine (TNpP)

tert-butyldineopentyl phosphine (TBDNpP)

di-*tert*-butylneopentyl phosphine (DTBNpP)

Figure 1.6: Examples of neopentyl phosphine ligands examined by Shaughnessy and coworkers.

The complex formed in situ from $Pd_2(dba)_3$ and trineopentyl phosphine (TNpP) displayed a high efficiency for coupling a wide range of sterically encumbered aryl bromides and chlorides with sterically hindered anilines.[35] More rigid catalysts with ligands such as P*t*-Bu_3 or di-*tert*-butylneopentyl phosphine (DTBNpP) struggle to effectively catalyzed cross-coupling reactions of di-*ortho*-substituted aryl halides with bulky aryl amines. Shaughnessy and coworkers have demonstrated that neopentyl phosphine ligands can be used to form catalysts in situ that can effectively facilitate a variety of C-C and C-N coupling reactions, including Heck, Suzuki, Sonogashira cross-coupling reactions, and Buchwald-Hartwig aminations.[35-38]

1.4 Conclusion

Palladium-catalyzed cross-coupling reactions are extremely valuable methods for constructing new C-Cand C-heteroatom bonds. These reactions take advantage of simple precursors and combine them to make more complicated structures. Phosphine ligands are some of the most powerful ligand types, and can be used to enhance cross-coupling reactions. The steric and electronic parameters of the ligands on palladium can have huge impacts on product formation and coupling efficiency. This feature can potentially be exploited to control the outcome of a cross-coupling reaction.

CHAPTER 2: EVALUATING THE EFFECT OF ARYL LIGAND IDENTITY ON CATALYTIC PERFORMANCE OF TRINEOPENTYLPHOSPHINE ARYLPALLADIUM COMPLEXES IN N-ARYLATION REACTIONS

This chapter is based on previously published work (*Organometallics* 2020, **39**, 20, 3618–3627) and has been reformatted for this dissertation.

2.1 Introduction

Trialkyl phosphines are extremely easy to oxidize, which makes their shelf-life short, storage difficult, and usage less appealing because they typically require specialized air-free handling. Oftentimes, catalytic systems using ligands like trialkyl phosphines or 2-biaryl phosphines will form the active catalyst in situ by mixing excess free ligand with a palladium source. The most common palladium sources are palladium(II) complexes, such as $Pd(OAc)_2$ or $PdCl_2$. This process can be very effective, but it gives chemists less control over the active species formation and requires using potentially pyrophoric, and often expensive free ligand. Also, the palladium(II) sources have to undergo a two-electron reduction before the active species is generated. This extra step can be avoided by using $Pd_2(dba)_3$, but at the risk of the released dba ligand inhibiting the coupling reaction.[39, 40]

One method to circumvent these issues is to develop preformed palladium ligand precatalysts that can effectively generate the active species under the catalytic reaction conditions. These precatalysts would ideally be air stable, easily formed, have the ideal atom economical ratio of 1:1 for L:Pd, and either be Pd(0) or able to readily to generate the active

LPd(0) species necessary for the catalysis to begin.[41] Examples of precatalysts that have had success are shown in Figure 2.1.[42]

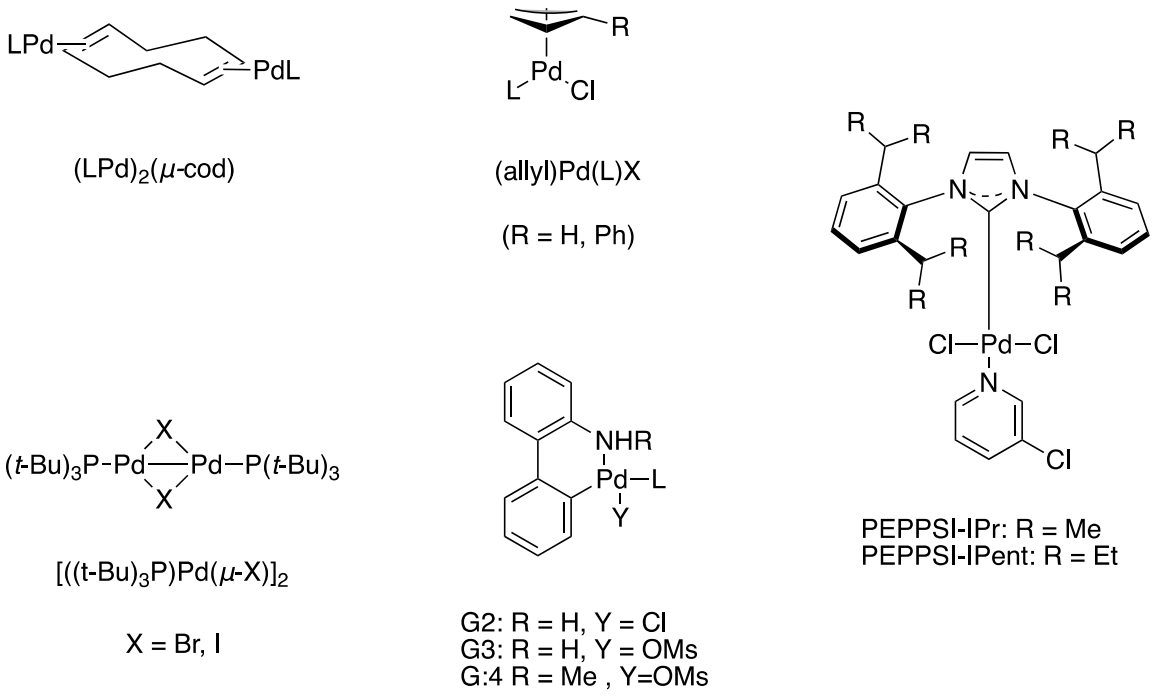

Figure 2.1: Examples of palladium precatalysts.

All of the examples mentioned in Figure 2.1 lie off of their respective catalytic cycles. Therefore, they all must undergo one or more steps before the catalytically active LPd(0) is generated. Activating the catalysts can be slow or inefficient, resulting in other off-cycle species and lowering overall catalyst activity. Allylpalladium precatalysts are known to readily form inactive μ-allylpalladium(I) dimers.[43] Alternatively, precatalysts can sometimes release species that inhibit the cross-coupling reaction during catalyst activation, such as the carbazole released by the G2 and G3 Buchwald palladacycles.[44] A precatalyst that either lies on the catalytic cycle or in rapid equilibrium with an on-cycle species could potentially circumvent the aforementioned

issues. When considering the catalytic cycle for Buchwald-Hartwig amine arylation cross-coupling reaction, three stable species that are on-cycle or in catalytically viable equilibrium with an on-cycle species could be viewed as potential precatalysts (Figure 2.2).

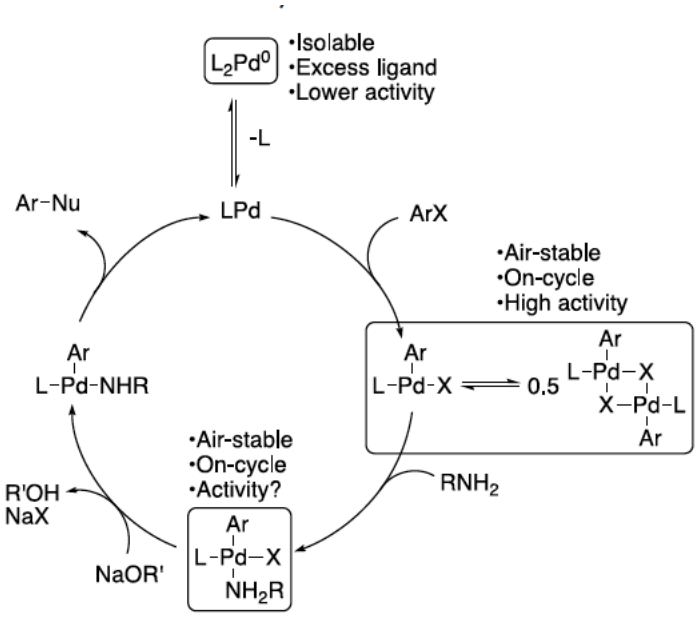

Figure 2.2: General mechanism of N-arylation cycle.

The $L_2Pd(0)$ species have been explored and used extensively, but has an undesirable L:Pd ratio of 2:1. The excess ligand can decrease catalyst activity by shifting equilibrium away from the active LPd species. Investigations into the mechanism of the Pd/PNp_3 catalyzed *N*-arylation reaction by the Shaughnessy group found that the $Pd(PNp_3)_2$ complex was much less active than palladium aryl species $([PNp_3)Pd(Ar)(Br)]_2$.[45] Initially, Buchwald reported using (AlPhos)Pd(Ar)X (X = Br and OTf) precatalysts for the fluorination of aryl bromides. Since then, complexes with the general formula $[LPd(Ar)X]_n$ have been shown to be significantly more active than the precatalysts in Figure 2.2 and comparable complexes formed in situ for a variety of coupling reactions by a number of groups.[46-51]

The aryl palladium complex ($[LPd(Ar)X]_n$ can be either a stable 3-coordinate species (n = 1) or a halide bridged dimer (n = 2) depending on the properties of the ligand, aryl group, and halide.[52] These arylpalladium precatalyst can be converted to the active LPd(0) species by addition of the nucleophilic coupling partner followed by reductive elimination. The halide bridged dimer is an off-cycle species that can easily enter the cycle if it is in equilibrium with the 3-coordinate complex or by the nucleophilic reagent splitting the dimer.

In C-N cross-coupling reactions, the amine coordinates to the $[LPd(Ar)X]_n$ species to form LPd(amine)(Ar)X, which is an isolable on-cycle intermediate in the absence of a base. The amine adduct is a deprotonation and reductive elimination away from the 3-coordinate active LPd(0) species. Therefore, the LPd(amine)(Ar)X complex is another viable option to consider as a stable precatalyst.

Coupling sterically hindered 2,6-di-*ortho*-substituted aryl halides with bulky amines is challenging when commonly used ligands, such as P(*t*-Bu)$_3$ or Sphos, are used. There have been some successful methods developed with *N*-heterocyclic carbene palladium complexes, diketiminate palladium complexes, proazaphosphatrane-derived catalysts and iminoproazaphosphatrane phosphine/palladium systems.[53-57] The Shaughnessy group has previously reported that TNpP-supported catalysts are particularly effective at coupling sterically demanding aryl halides.[58, 59] In this chapter, I will discuss the use of air-stable complexes $[(Np_3P)Pd(Ar)Br]_2$ and $(Np_3P)Pd(Ar)(HNR_2)Br$ as precatalysts for the cross-coupling of sterically demanding aryl bromides and bulky aniline derivatives. Emphasis will be on determining how the identity of the aryl group on palladium affects catalytic efficiency and the relative activity of $[(Np_3P)Pd(Ar)Br]_2$ and $(Np_3P)Pd(Ar)(HNR_2)Br$ as catalyst sources.

2.2 Results and Discussion

2.2.1 Synthesis of Palladium(II) Precatalysts

The bromine bridged arylpalladium complexes used for this analysis were synthesized using conditions previously reported by the Shaughnessy group.[34] The aryl groups on these complexes were selected to have zero (**1**), one (**2**), or two (**3**) ortho substituents in order to determine how altering the steric environment would affect the catalytic performance in the coupling of sterically hindered arylamines with sterically hindered aryl bromides.

Freshly made (cod)Pd($CH_2TMS)_2$, 1.0 equivalent of PNp_3, and an excess of the aryl bromide in pentane gave complexes with the general formula [(Np_3P)Pd(Ar)Br]$_2$ (**1, 2, 3**) in good to moderate yields (Scheme 2.1). It is possible to make the phenyl derivative **1** and the *ortho*-methoxy variant **2** by reacting Pd($PNp_3)_2$ with an excess of the appropriate aryl bromide in toluene at 70 °C.[35] This method is ineffective at producing **3** starting from 2-bromo-*m*-xylene, however, due to in situ degradation of the dimer via C-H activation into a palladacycle and *m*-xylene. The resulting precatalysts were all characterized by ^{1}H, ^{13}C, and ^{31}P NMR spectroscopy, and **1** and **2** were further characterized using elemental analysis.

Scheme 2.1: Synthesis of [(Np_3P)Pd(Ar)Br]$_2$ bromine bridged dimers.

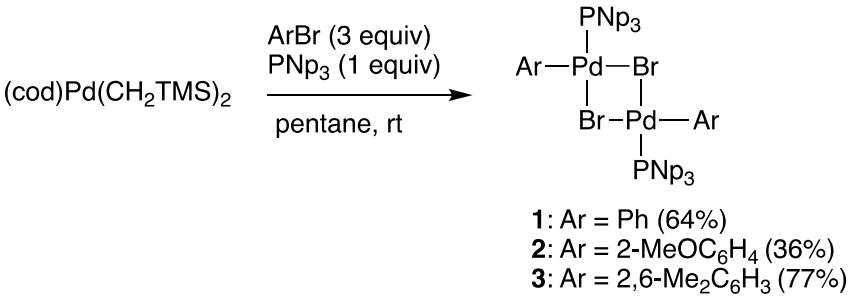

The dimers **1** and **3** were converted to their respective amine adducts via treatment with either a secondary or primary amine (morpholine or isobutylamine, respectively) in methylene chloride (Scheme 2.2). Complexes **4, 5,** and **6** were characterized using ^{1}H, ^{13}C, and ^{31}P NMR spectroscopy. Amine adduct **4** was further characterized via elemental analysis. ^{1}H NMR analysis showed no evidence of the amine behaving as an anionic amido ligand. All expected amine protons were visible in the spectrum, indicating that the amines coordinate as neutral ligands. These complexes were able to be stored in ambient conditions with no signs of degradation over several months.

Scheme 2.2: Synthesis of amine adducts from the bromine bridged dimers ($[(Np_3P)Pd(Ar)Br]_2$).

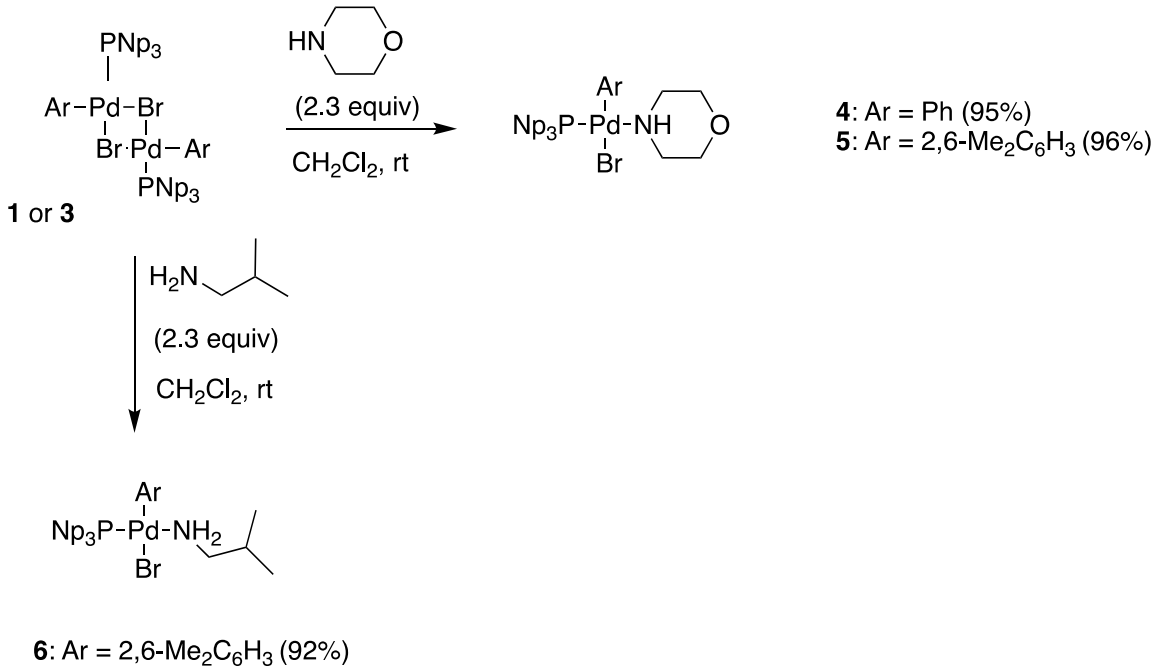

2.2.2 Analysis of the Catalytic Effectiveness of the Palladium(II) Precatalysts

In order to compare the effect of adding steric bulk to the aryl group on the catalyst source, the reaction profiles for the three dimeric precatalysts (**1, 2, 3**) in the coupling of a sterically hindered arylamine with a bulky aryl bromide were evaluated. The rates of conversion in the reaction of 2,6-diisopropylaniline with 1-bromo-2,4,6-triisopropylbenzene were monitored by GC at three separate temperatures for each precatalyst (Scheme 2.3).

Scheme 2.3: Reaction of 1-bromo-2,4,6-triisopropylbenzene with 2,6-diisopropylaniline in the presence of the bromine bridged precatalysts (**1-3**) and sodium *t*-butoxide in toluene at varying temperatures.

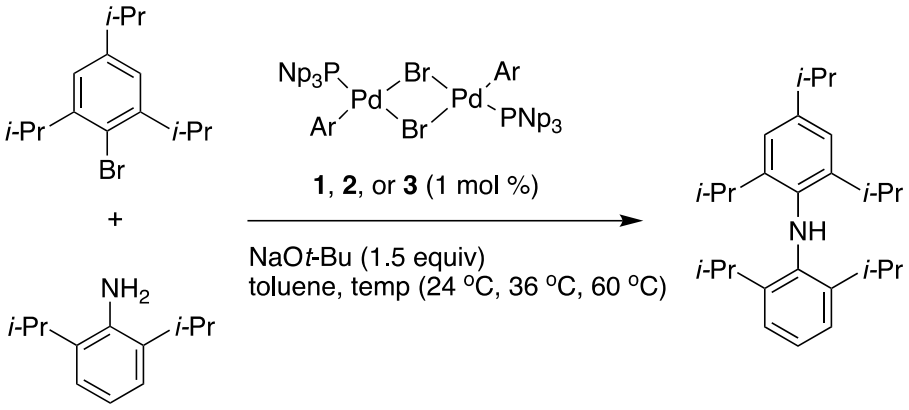

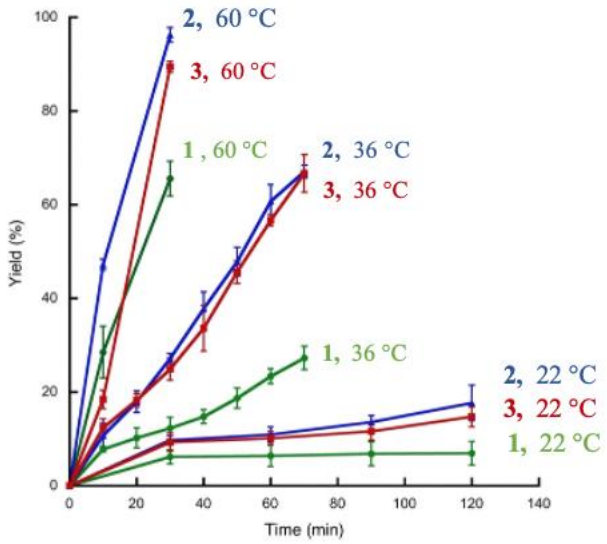

Figure 2.3: Reaction profiles for the coupling of 1-bromo-2,4,6-trisipropylbenzene and 2,6-diisopropylaniline using precatalysts (**1 – 3**) as a function of temperature (Scheme 2.3).

At room temperature the overall conversion was low for all three species. The unsubstituted phenyl variant (**1**) had the lowest overall conversion compared to the *o*-methoxy substituted (**2**) and the *m*-xylene (**3**) variants, but the overall yield never surpassed 20% in any of these cases. When the temperature was increased to 36 °C, the precatalysts with substituents on the aryl group showed significantly increased overall conversion. Both the *o*-methoxyphenyl and *m*-xylene based precatalysts reached 65% yield after 1 hour, but the phenyl variant showed much slower conversion and overall yield.

At 60 °C the catalytic activity of the three bromine-bridged complexes followed the same general trend as the reactions run at lower temperatures. There was also a sharp increase in rate of conversion. Both precatalysts **2** and **3** achieved over 90% conversion in 30 minutes, whereas precatalyst **1** only reached 65% conversion in the same timeframe. The anisole complex (**2**) had the fastest rate and the highest overall yield.

The amine adducts (**4, 5, 6**) were tested under the same conditions as the halide bridged complexes. At room temperature and at 36 °C, the amine precatalysts all showed low conversion yields and rapid catalyst deactivation. At 60 °C the complexes with 2,6-dimethylphenyl ligands (**5** and **6**) gave significantly higher reaction rates than that of the unsubstituted phenyl ligand morpholine adduct (**4**) (Figure 2.4). The isobutylamine complex (**6**) and the morpholine adduct (**5**) showed comparable initial rates, but the isobutylamine complex became inactive after 30 minutes and leveled out at about 45% conversion. The morpholine precatalyst retained its activity longer and achieved an overall higher conversion yield of 60%. When comparing between the halide bridged complexes and their amine adducts, the rate of conversion and the maximum yields of the amine adducts (**4, 5, 6**) are notably lower than for the bromine-bridged dimers **1** and **3** (Figure 2.5).

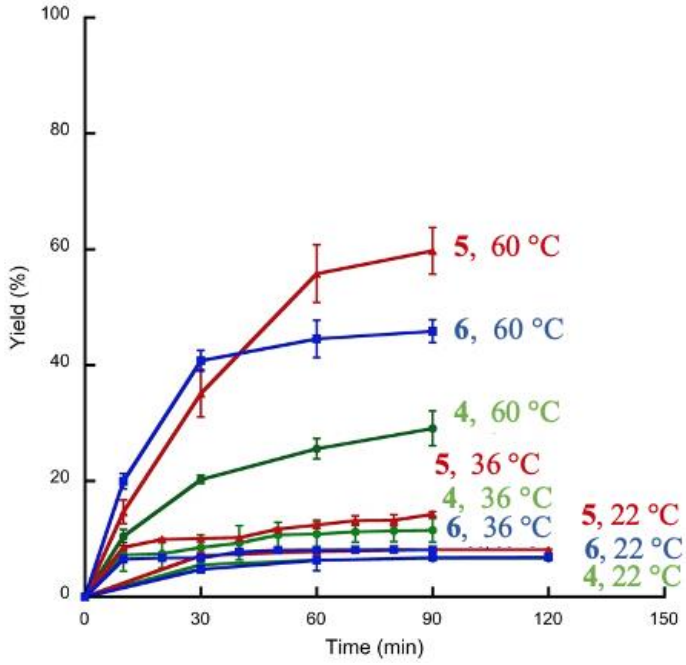

Figure 2.4: Reaction profiles for the coupling of 1-bromo-2,4,6-triisopropylbenze and 2,6-diisopropylaniline using the amine adduct precatalysts (**4, 5, 6**) as a function of temperature.

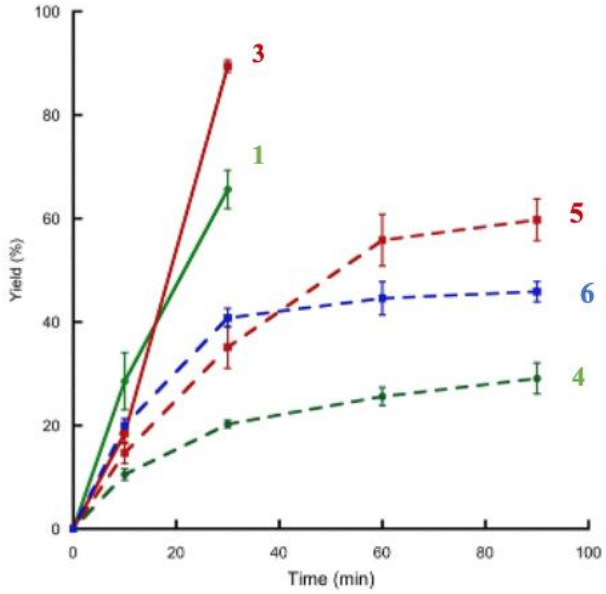

Figure 2.5: Comparison of aryl palladium precatalysts **1** and **3** (solid lines) and their amine adducts: **4, 5, 6** (dotted lines) in the coupling of 1-bromo-2,4,6-triisopropylbenzene and 2,6-diisoproylaniline at 60 °C (Scheme 2.3).

When taking both synthetic efficiency and catalytic performance into account, the *m*-xylene bromine bridged dimer (**3**) was the most efficient of the precatalysts evaluated. In order to compare the effectiveness of complex **3** to the pre-catalyst generated in situ from the well-known conditions that employ $Pd_2(dba)_3$ (0.5 mol%) and trineopentylphosphine (1 mol %), the reaction of 1-bromo-2,4,6-triinsopropylbenzene and 2,6-diisoproylaniline under catalytic conditions was profiled at 22, 36, and 60 °C (Figure 2.6).

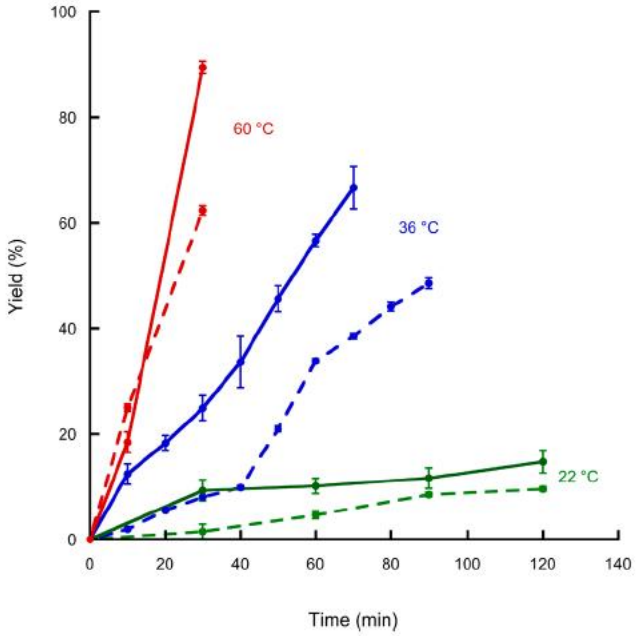

Figure 2.6: Reaction profiles for the coupling of 1-bromo-2,4,6-triinsopropylbenzene and 2,6-diisoproylaniline using precatalyst **3** (solid lines) and $Pd_2(dba)_3$/TNpP (dotted lines) as a function of temperature.

At 22 and 36 °C, complex **3** performed better than the $Pd_2(dba)_3$/TNpP system. The bromine bridged dimer produced an overall higher conversion to product and had a significantly higher initial rate. At 60 °C, the two systems gave similar reaction profiles, but precatalyst **3** gave 90% conversion after 30 min whereas the in-situ generated catalyst from $Pd_2(dba)_3$/TNpP gave only 62% conversion. The reactions performed using the $Pd_2(dba)_3$/TNpP conditions showed an induction period prior to reaching the maximum rate at lower temperatures (22 and 36 °C). Previous studies by the Shaughnessy group revealed that the displacement of dba by PNp_3 is slow at room temperature.[45] Therefore, it is likely that the concentration of active species is much higher early in the reaction when using the *m*-xylene bromine bridged dimer than when using $Pd_2(dba)_3$/TNpP, especially at lower temperatures. Another factor that may be playing a

role here is the generation of free dba ligand, which has been shown to be an inhibitor in cross-coupling reactions. This would lead to slower rates once the active species was formed.

Based on the catalytic cycle (Scheme 2.2), the bromine bridged dimers (**1, 2, 3**) initiate the cycle through the reaction with an amine and a base followed by reductive elimination to generate (PNp_3)Pd(0). The identity of the aryl group should not have any effect on the reaction after this initial process. Therefore, the differences in the effectiveness of these precatalysts are likely due to differences in the rate and efficiency of forming the active species. Amine coordination would be expected to be most favorable with the least hindered aryl groups; however, the trend observed for this set of dimers did not match what was expected. The unsubstituted phenyl ligand (**1**) was the least efficient across a range of temperatures, while the anisole ligand (**2)** and the more sterically demanding *m*-xylene ligand (**3**) performed comparably relative to each other and overall better than the unsubstituted variant. It is unclear how the aryl group is affecting this process. Reductive elimination from the more substituted **3** is expected to be slower than for the other two bromine dimers due to the increased steric bulk.

Previous studies in the Shaughnessy group have shown that [(PNp_3)Pd(Ar)Br] complexes produce $Pd(Np_3P)_2$ and ArNHPh within minutes after being exposed to aniline and sodium *t*-butoxide at 80 °C. Due to the fast rate of this process, obtaining kinetic data for the reaction of the bromide bridged dimers has proven unsuccessful.

The amine adducts undergo base-promoted reductive elimination at rates that are slow compared to the catalytic reaction. The rates measured are much slower than those reported for other complexes with the general formula LPd(Ar)(amine)(X). The exact reason for this is not clear, but it is consistent with the lower coupling efficiency observed compared to the bromine-bridged dimers. Current investigations by the Shaughnessy group suggest that the amine adducts

may be in equilibrium with a palladacycle species. Palladacycles are known to form more readily in basic environments, and the amines may be facilitating C-H activation of the ligand to facilitate the cyclization.

2.3 Conclusions

Trineopentylphosphine supported aryl palladium halide complexes have been shown to be effective catalysts for the coupling of sterically hindered aryl bromides with sterically hindered anilines. The di-*ortho*-substituted aryl palladium complex (**3**) had a higher coupling rate compared to the catalyst generated in situ from $Pd_2(dba)_3$ and PNp_3. There was a positive correlation between steric bulk of the aryl group bound to the palladium and the coupling efficiency. Mono- and di-*ortho*-substituted aryl palladium complexes **2** and **3** give increased rates of overall conversion than the phenylpalladium complex (**1**), which suggests that the structure of the palladium-bound aryl group has a measurable effect on the performance of the catalyst.

Amine adducts have a decreased coupling rate compared to the halide bridged dimer precatalysts (**1**-**3**). Analysis of the base-promoted reductive elimination is unexpectedly slow for these species. This result suggests that generation of the active LPd(0) occurs more slowly for the amine adducts than the bridged precatalysts. The thermodynamically disfavored displacement of the amine by the aniline appears to be required to activate the amine adducts (**4**-**6**).

In order to gain a better understanding of the effects of the aryl ligands on the cross-coupling reaction, it would be useful to examine a larger series of precatalysts under the catalytic conditions. Having an *ortho*-methyl substituted complex to compare to phenyl complex **1** and di-*ortho*-substituted aryl palladium complex **3** would give better insight into the effects of

increasing sterics alone. It would also be interesting to further increase the steric demand of the aryl ligand by using precatalysts with larger alkyl substituents on the aryl ligand.

Complex **2** has an *ortho*-methoxy substituent on the aryl ligand, which introduces potential electronic differences affecting the results. Generating complexes with electron donating and electron withdrawing aryl substituents at varying locations on the phenyl ring would allow us to better determine how the electronic parameters of the ligand affect the reaction.

2.4 Experimental

General Procedures and Materials: Reagents were purchased from commercial sources and used as received unless specifically noted. Toluene was refluxed over sodium and THF was refluxed over sodium/benzophenone for at least an hour under a nitrogen atmosphere and both freshly distilled before use. Pentane was dried over CaH_2, distilled, and degassed via three freeze-pump-thaw cycles prior to use. PNp_3,[60] (cod)Pd(CH_2TMS),[61] and **3**[34] were prepared following reported methods. Reaction temperatures refer to previously equilibrated oil bath temperatures. Reactions were conducted under a nitrogen atmosphere using double manifold inert-atmosphere techniques, unless noted otherwise. All GC samples were measured using a Shimadzu GC-2014 Gas Chromatograph using an Alltech Econo-Cap EC-5 capillary column (5%phenylpolysiloxane 95%-methylpolysiloxane; 30 m x 0.32 mm I.D. x 0.25 µm) with a 10°C/min increasing rate from 150 to 250 °C. NMR spectra were collected on a Brüker 500 MHz spectrometer. ^{31}P NMR spectra were obtained under gated decoupling mode at fixed scans through the length of the experiment with the aid of an automated data collection program.

PNp_3. A solution of LiBr (174 mg, 2.00 mmol) , CuI (190 mg, 1 mmol), and PCl_3 (873 µL, 10 mmol) in 40 mL of THF was cooled to -78 °C. Neopentylmagnesium bromide (1M in THF, 40 mL, 40 mmol) was added under N_2 counter flow. The reaction mixture was allowed to warm to room temperature and stirred for 16 h. The solution was concentrated under reduced pressure before 60 mL of degassed ether was added. The ether solution was cooled to 0 °C and quenched using saturated aqueous ammonium chloride (40 mL). The resulting air-stable mixture was extracted using ether (20 mL x3), dried over Na_2SO_4, and concentrated under reduced pressure. The crude product was recrystallized in methanol to yield needle-like crystalline solid (90%). $^{31}P\{^1H\}$ NMR (202.5 MHz, $CDCl_3$): δ -57.5 ppm

(cod)Pd(CH_2TMS)$_2$. A solution of (trimethylsilyl)methylmagnesium chloride (1M in ether, 12.8 mL, 12.8 mmol) in degassed ether (28 mL) was added to a solution of $PdCl_2$(cod) in the same solvent (30 mL) at -78 °C. The solution was warmed to -10 °C and stirred for 30 min. The resulting mixture was concentrated under reduced pressure. Keeping the temperature at or below -10 °C for the rest of the procedure, the residue was extracted with chilled, degassed hexane (30 mL x2). The combined hexane filtrates were evaporated to dryness in vacuo to give a thermally unstable off-white solid. The product was used immediately without characterization.

[(PNp_3)Pd(C_6H_5)(μ-Br)]$_2$ (1). Trineopentylphosphine (120 mg, 0.492 mmol) and bromobenzene (154 µL, 1.476 mmol) were combined in 12 mL of pentane in a two neck flask under N_2 atmosphere. Freshly made (cod)Pd(CH_2TMS)$_2$ (190 mg, 0.488 mmol) was added under N_2 counterflow. The reaction was stirred at 22 °C for 22 h. The resulting slurry was concentrated and filtered to give a light-grey solid. The grey solids were dissolved in DCM (5 mL) and filtered through Celite. The filtrate was collected and dried in vacuo to produce an air-stable white solid (160 mg, 64%). ^{1}H NMR (500 MHz, C_6D_6, 295 K): δ 7.72 (br, 2H), 7.06 (br, 2H), 6.91 (br, 1H), 1.72 (d, J = 10.5 Hz, 6H), 1.22 (brs, 27H). ^{13}C NMR (125 MHz, C_6D_6, 295 K): δ 152.9, 135.8, 123.4, 108.0, 40.2 (d, $J_{C\text{-}P}$ = 20.0 Hz), 33.5, 32.6. ^{31}P{^{1}H} NMR (202.5 MHz, C_6D_6, 295 K): δ 7.9. Elemental Analysis: calcd for $C_{42}H_{76}Br_2P_2Pd_2$: C, 49.67; H, 7.54; N, 0.0. Found: C, 50.56; H, 7.72; N, 0.0.

[(PNp_3)Pd(2-$MeOC_6H_3$)(μ-Br)]$_2$ (2). Trineopentylphosphine (100 mg, 0.410 mmol) and 2-bromoanisole (160 µL, 1.285 mmol) were combined in 12 mL of pentane in a two neck flask and reacted with (cod)Pd(CH_2TMS)$_2$ (160 mg, 0.411 mmol) following the same method as **1** to give an air stable yellow solid (80 mg, 36%). ^{1}H NMR (500 MHz, C_6D_6, 295 K): δ 7.79 (br, 1H), 6.99 (m, 1H), 6.89 (m, 1H), 6.49 (d, J = 8.2 Hz, 1H), 3.98 (s, 3H), 1.76 (brs, 6H), 1.29 (br, 27H).

^{13}C NMR (125 MHz, C_6D_6, 295 K): δ 162.1 (d, J_{C-P} = 12.5 Hz), 141.4, 138.2 (d, J_{C-P} = 13.8 Hz), 126.0, 122.4 (d, J_{C-P} = 3.75 Hz), 112.4 (d, J_{C-P} = 25.0 Hz), 56.5 (d, J_{C-P} = 11.3 Hz), 41.3 (brs), 37.7, 34.0. $^{31}P\{^1H\}$ NMR (202.5 MHz, C_6D_6, 295 K): δ 11.21, 11.17, 9.75, 9.69 (stereoisomeric mixture 1:1:0.2:0.2). Elemental Analysis: calcd for $C_{44}H_{80}Br_2O_2P_2Pd_2$: C, 49.13; H, 7.50; N, 0.0. Found: C, 48.93; H, 7.53; N, 0.0.

[(PNp$_3$)Pd(2,6-Me$_2$C$_6$H$_3$)(*μ*-Br)]$_2$ (3). Trineopentylphosphine (97 mg, 0.398 mmol) and 2-bromo-*m*-xylene (160 μL, 1.20 mmol) were combined in 12 mL of pentane in a two neck flask and reacted with (cod)Pd($CH_2TMS)_2$ (160 mg, 0.411 mmol) following the same method as **1** to give an air stable light yellow green solid (164 mg, 77%). ^{1}H NMR (500 MHz, C_6D_6, 295 K): δ 7.05-6.93 (m, 1H), 6.88 (d, *J* = 7.2 Hz, 2H), 3.59 (brs, 1H), 3.08 (d, *J* = 12.5 Hz, 2H), 2.83 (s, 6H), 2.73 (m, 6H), 2.68 (m, 2H), 2.02 (brs, 2H), 1.54 (s, 18H), 1.36 (s, 4H), 0.76 (s, 9H). ^{13}C NMR (125 MHz, C_6D_6, 295 K): δ 160.0, 140.0, 127.0, 124.6, 67.8, 49.4, 43.9 (d, J_{C-P} = 9.7 Hz), 33.5, 32.8, 26.9. $^{31}P\{^1H\}$ NMR (202.5 MHz, C_6D_6, 295 K): δ 7.6, 6.4 (stereoisomeric mixture 77:23)

(PNp$_3$)Pd(morpholine)(Ph)Br (4). [(PNp$_3$)Pd(C_6H_5)Br]$_2$ (**1**, 67.6 mg, 0.067 mmol) was dissolved in methylene chloride (8 mL) under nitrogen. Morpholine (13.0 μL, 0.150 mmol) was added into the solution. After stirring for 1 h, the volatiles were removed to provide an air-stable white solid (75 mg, 95%) that was analytically pure. ^{1}H NMR (500 MHz, C_6D_6, 295 K): δ 7.56 (d, *J* = 8.8 Hz, 2 H), 7.07(t, *J* = 7.4 Hz, 2H), 6.98 (t, *J* = 7.2 Hz, 1H), 3.53 (brs, 1H), 3.11 (d, *J* = 11.3 Hz, 2H), 2.60 (m, 6H), 1.99 (d, *J* = 9.9 Hz, 6H), 1.30(s, 27H). ^{13}C NMR (125 MHz, C_6D_6, 295 K): δ 158.0, 135.2, 123.8, 67.7, 48.7, 40.5 (d, J_{C-P} = 23.8 Hz), 33.6, 32.8. $^{31}P\{^1H\}$ NMR (202.5 MHz, C_6D_6, 295 K): δ 7.8. Elemental analysis: calcd for $C_{25}H_{47}BrNOPPd$: C, 50.47; H, 7.96; N, 2.35. Found: C, 50.57; H, 7.96; N, 2.33.

(PNp$_3$)Pd(morpholine)(2,6-Me$_2$C$_6$H$_3$)Br (5). [(PNp$_3$)Pd(2,6-Me$_2$C$_6$H$_3$)Br]$_2$ (**3**, 70 mg, 0.065 mmol) was dissolved in methylene chloride (8 mL). Then, morpholine (13.0 μL, 0.150 mmol) was added into the solution. After stirring for 1 h, the volatiles were removed under a vacuum to provide a white solid (78 mg, 96%). Colorless single crystals were formed after slow evaporation of a benzene solution. ^{1}H NMR (500 MHz, C_6D_6, 295 K): δ 7.05−6.93 (m, 1H), 6.88 (d, *J* = 7.2 Hz, 2H), 3.59 (br, 1H), 3.08 (d, *J* = 12.5 Hz, 2H), 2.83 (s, 6H), 2.73 (m, 6 H), 2.68 (m, 2 H), 2.02 (brs, 2H), 1.54 (s, 18 H), 1.36 (s, 4H), 0.76 (s,9H). ^{13}C NMR (125 MHz, C_6D_6, 295 K): δ 160, 140.0, 127.0, 124.6, 67.8, 49.4, 43.9 (d, J_{C-P}= 9.7 Hz), 33.3, 32.8, 26.9. P{^{1}H} NMR (202.5 MHz, C_6D_6, 295 K): δ 12.0

(PNp$_3$)Pd((CH$_3$)$_2$CHCH$_2$NH$_2$)(2,6-Me$_2$C$_6$H$_3$)Br (6). [(PNp$_3$)Pd(2,6-Me$_2$C$_6$H$_3$)Br]$_2$ (**3**, 50 mg, 0.047 mmol) was dissolved in methylene chloride (6 mL). Then, isobutylamine (10.0 μL, 0.101 mmol) was added into the solution. After stirring for 1 h, the volatiles were removed under a vacuum to provide a white solid (52 mg, 92%). ^{1}H NMR (500 MHz, C_6D_6, 295K): δ 6. 90 (m, 3H), 2.86 (s, 6H), 2.75 (brs, 2H), 2.27 (s, 4H), 2.23 (br, 1H), 2.03 (brs, 2H), 1.56 (brs, 18H), 1.36 (br, 6H), 0.93 (br, 2H), 0.78 (brs, 9H). ^{13}C NMR (125 MHz, C_6D_6, 295 K): δ 159.7, 140.2, 126.9, 124.6, 52.1, 43.9, 33.3 (d, J_{C-P} = 35 Hz), 30.2, 27.0, 19.5. P{^{1}H} NMR (202.5 MHz, C_6D_6, 295 K): δ 16.9.

General Buchwald-Hartwig Amination Procedure: The palladium precatalyst (**1 – 6** (0.5 mol %, L:PNp$_3$ 1:1) or Pd$_2$(dba)$_3$/PNp$_3$ (0.5 mol % Pd and 1 mol % PNp$_3$)) were weighed into a 5 mL screw-capped vial and evacuated and backfilled (x3) with nitrogen. The vial was then taken into a nitrogen-filled glovebox. A stir bar and NaO*t*-Bu (1.5 equiv) was added before being sealed and taken out of the glovebox and attached to a Schlenk line. 1-Bromo-2,4,6-triisopropylbenzene (1 mmol, 250 μL), 2,6-diisopropylaniline (1.2 equiv, 225 μL) and 4 mL of

toluene were added, and the vial was placed in an oil bath set at the appropriate temperature (22, 36, or 60 °C). The reaction was monitored by GC.

2.5 Appendix – Chapter 2

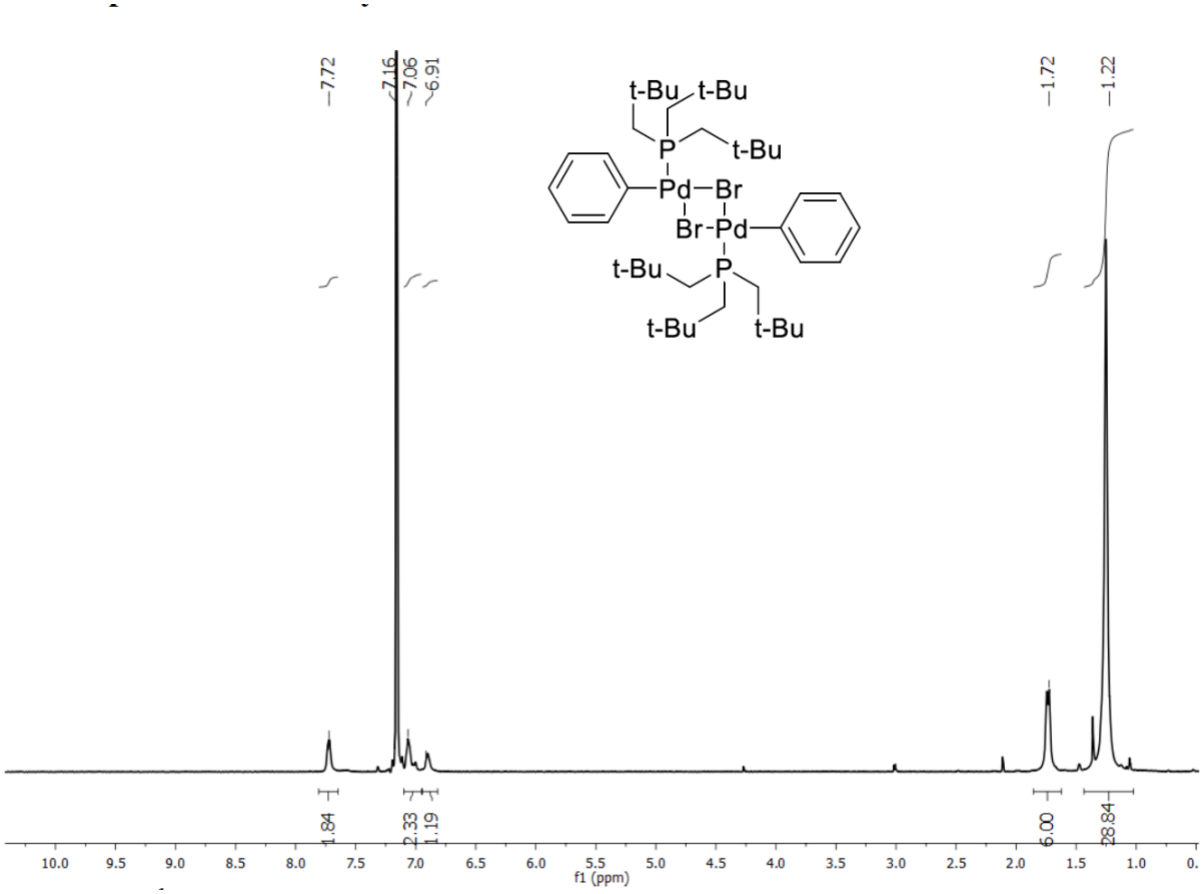

Figure A1: ^{1}H NMR (500 MHz, C_6D_6) spectrum of **1**.

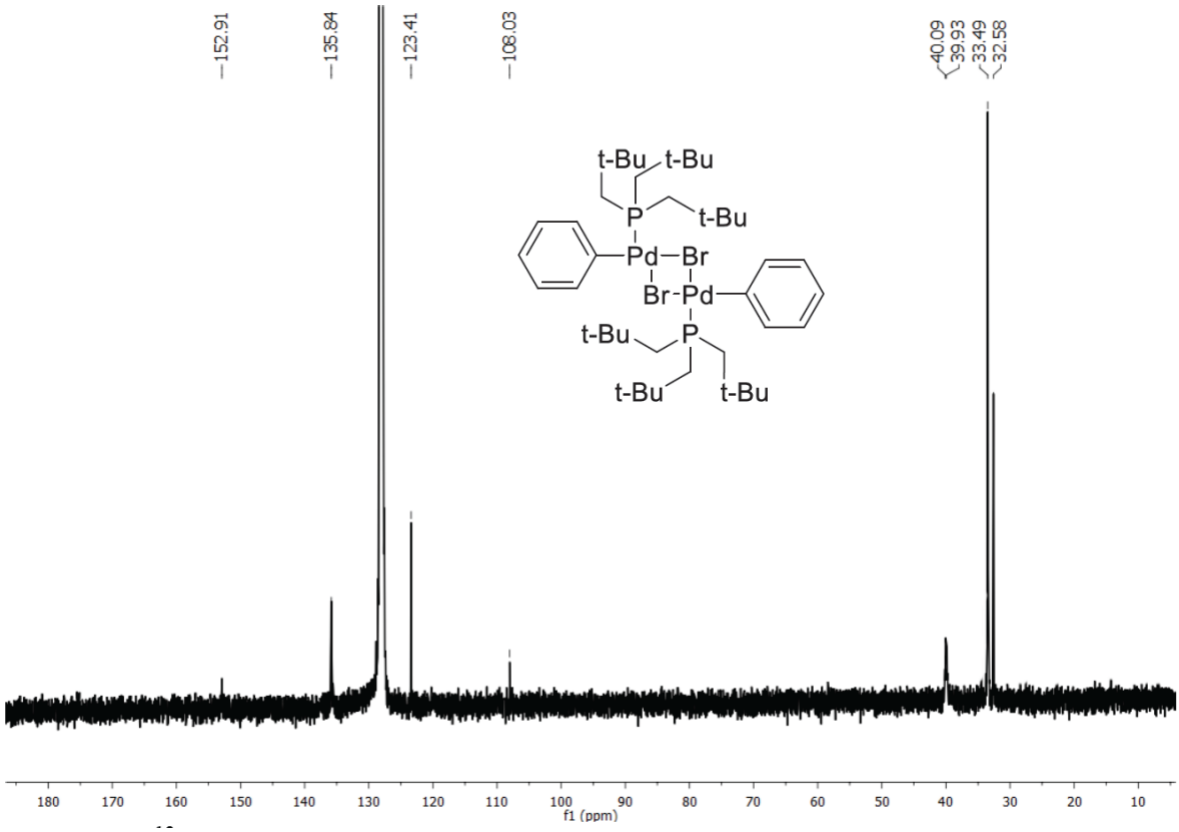

Figure A2: ^{13}C NMR (125 MHz, C_6D_6) spectrum of **1**.

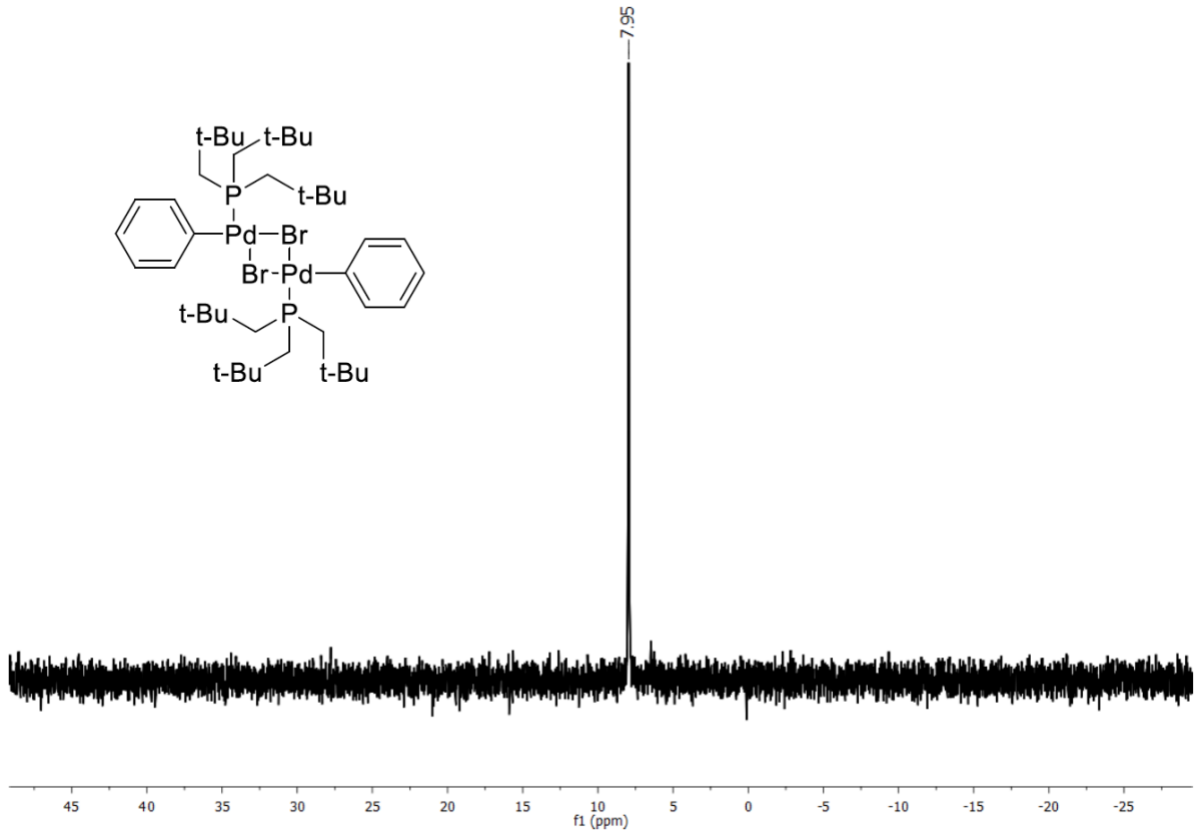

Figure A3: $^{31}P\{H\}$ NMR (202.5 MHz, C_6D_6) spectrum of **1**.

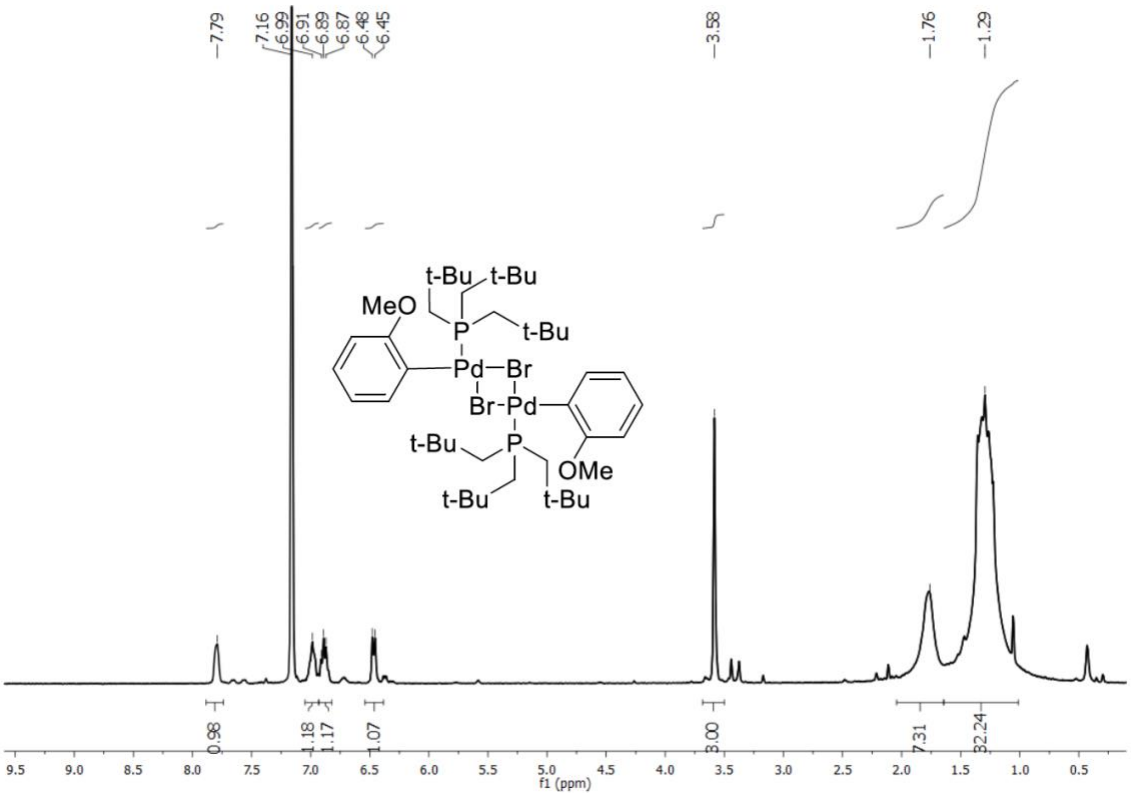

Figure A4: ^{1}H NMR (500 MHz, C_6D_6) spectrum of **2.**

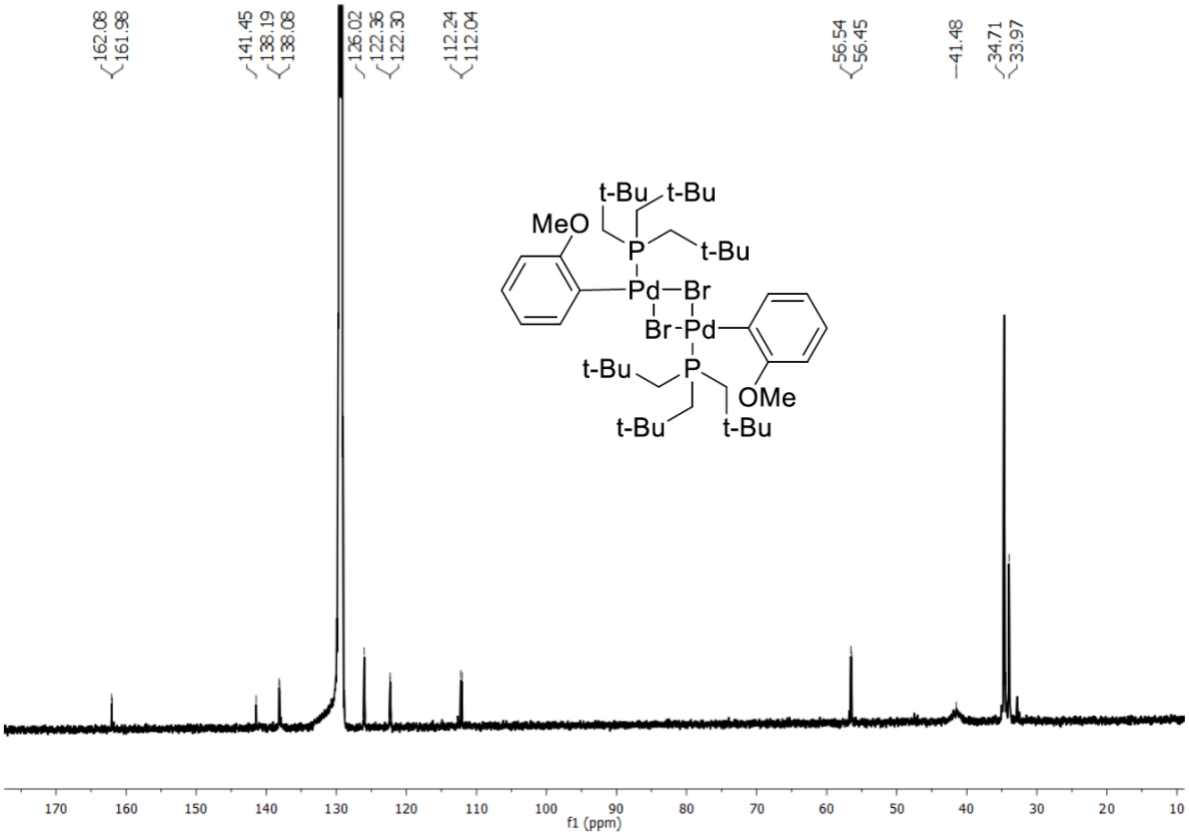

. **Figure A5:** ^{13}C NMR (125 MHz, C_6D_6) spectrum of **2**.

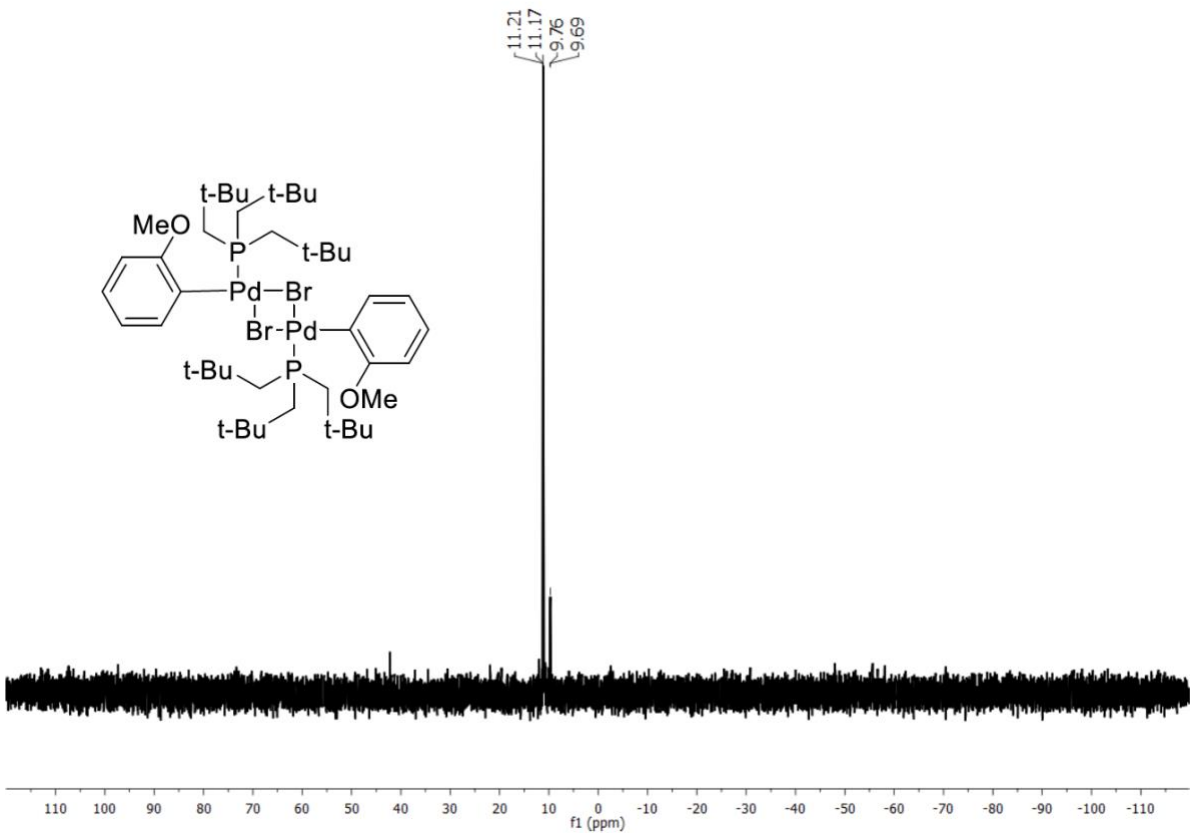

Figure A6: $^{31}P\{H\}$ NMR (202.5 MHz, C_6D_6) spectrum of **2**.

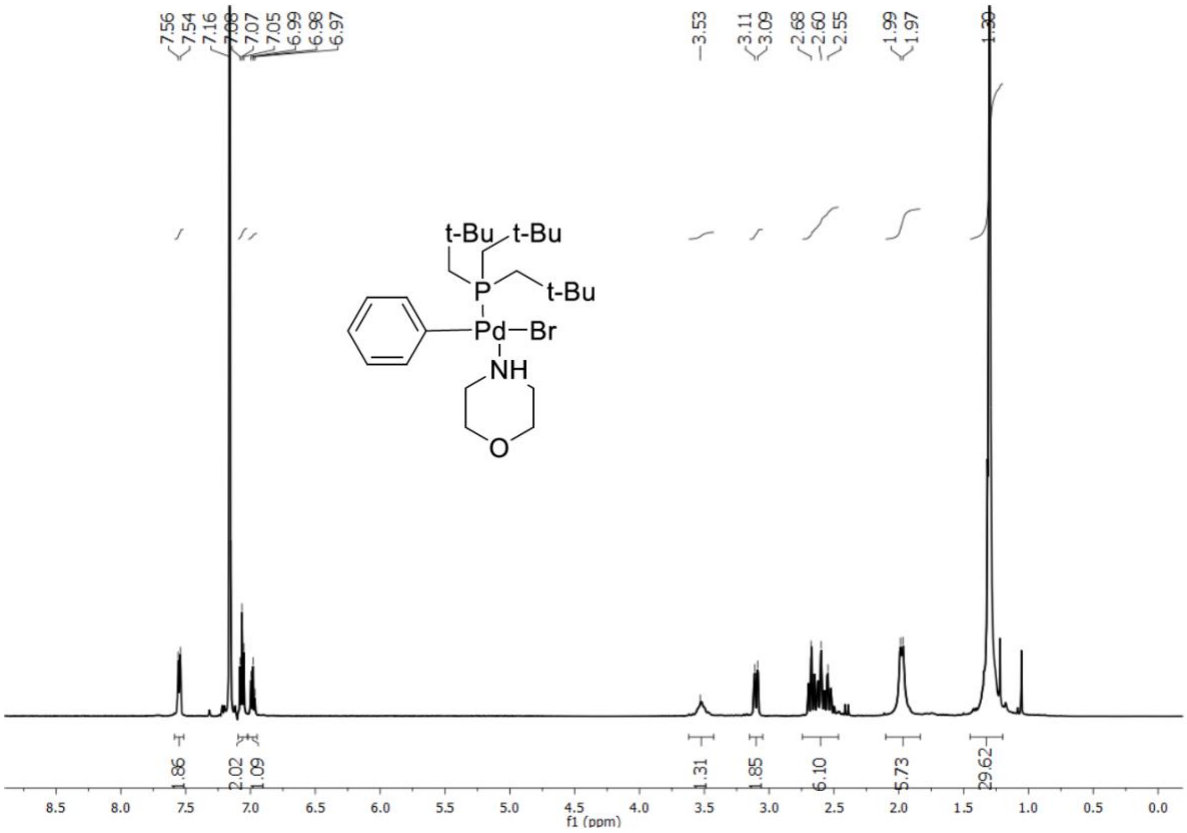

Figure A7: ^{1}H NMR (500 MHz, C_6D_6) spectrum of **4.**

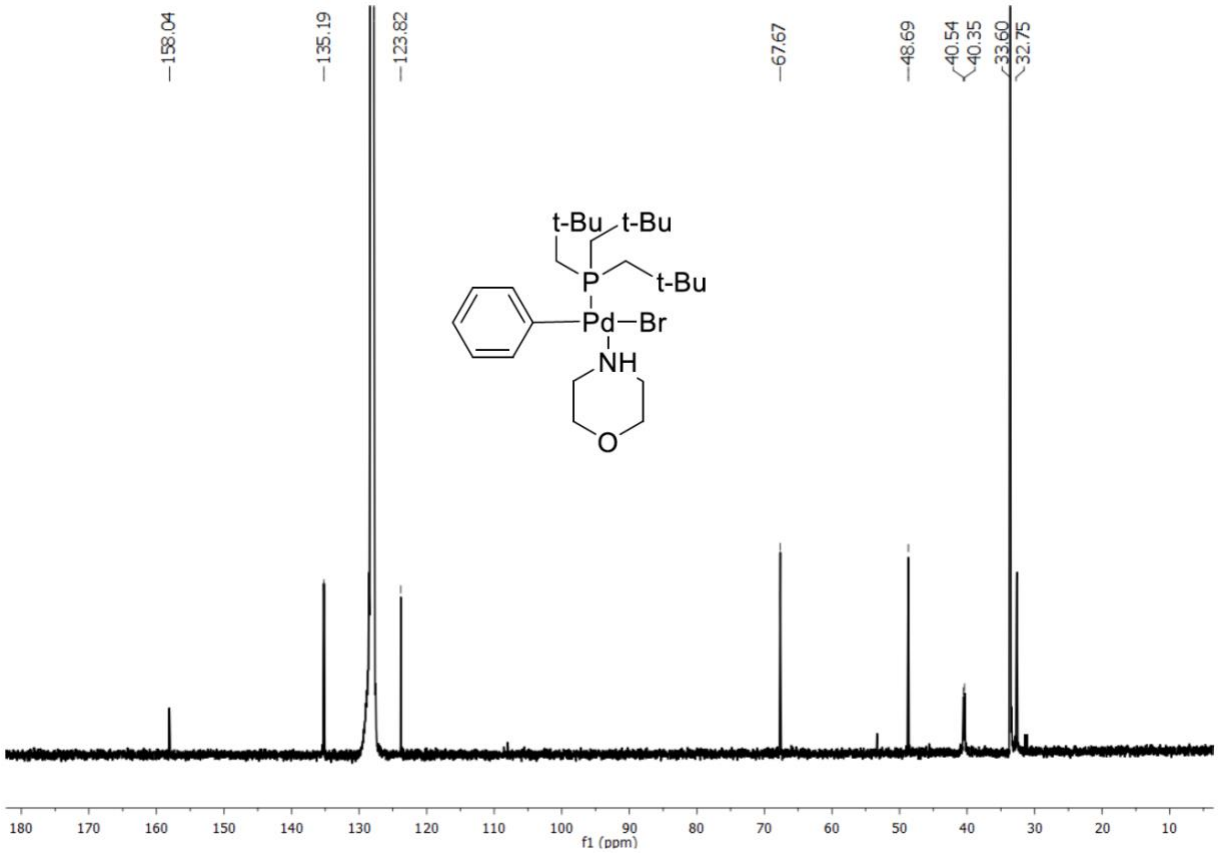

Figure A8: ^{13}C NMR (125 MHz, C_6D_6) spectrum of **4**.

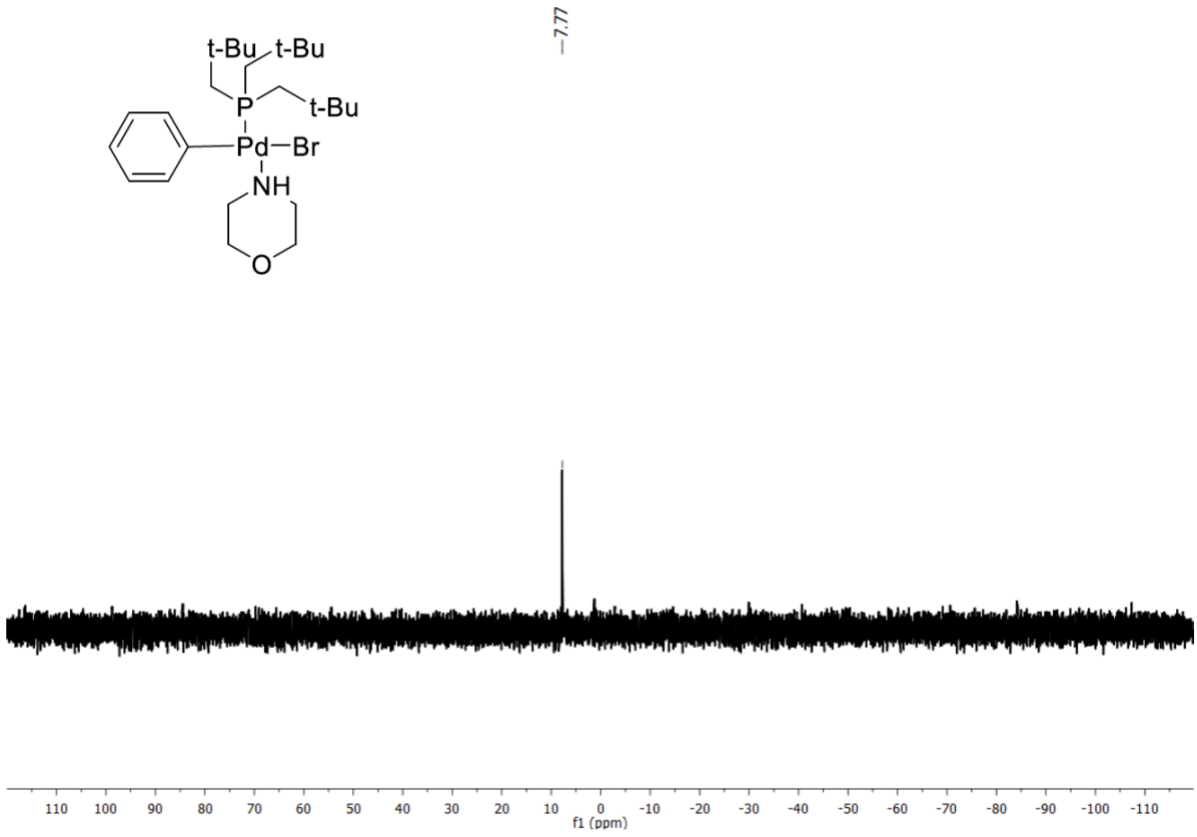

Figure A9: $^{31}P\{H\}$ NMR (202.5 MHz, C_6D_6) spectrum of **4.**

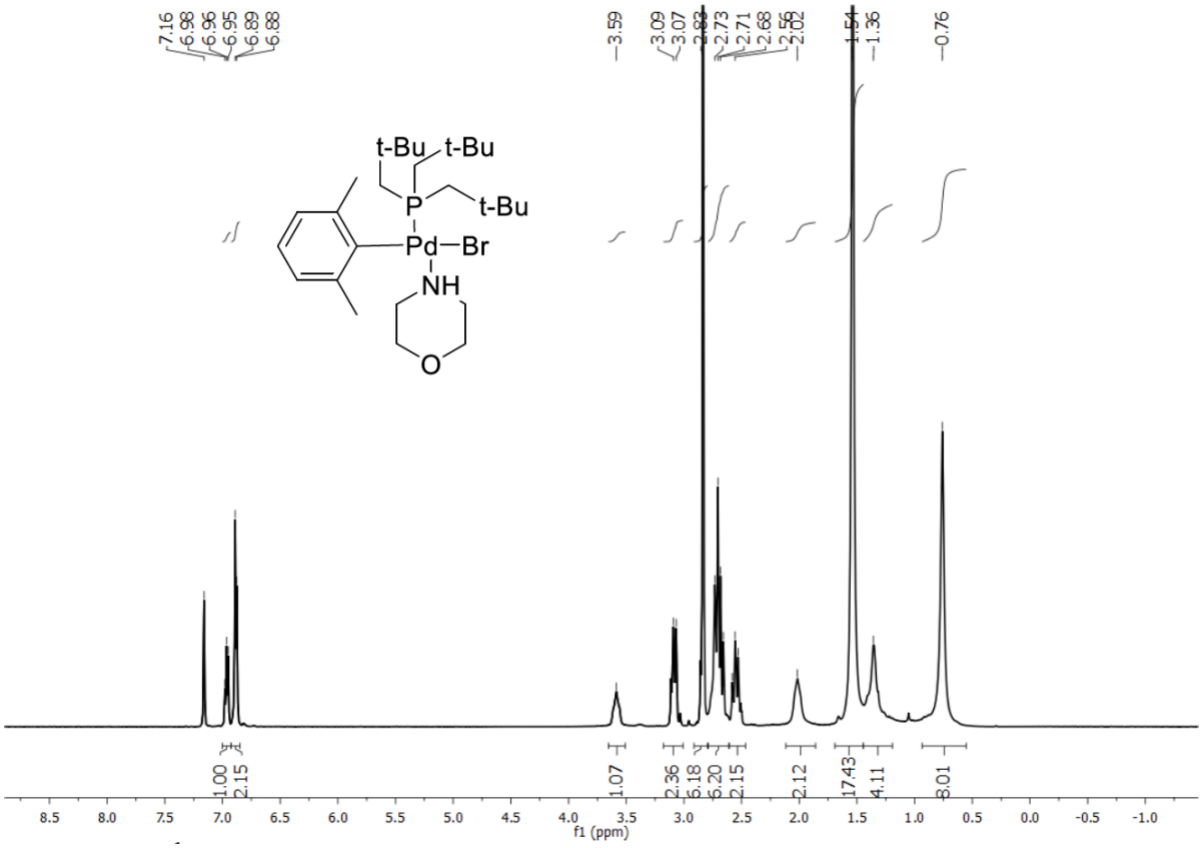

Figure A10: ^{1}H NMR (500 MHz, C_6D_6) spectrum of **5.**

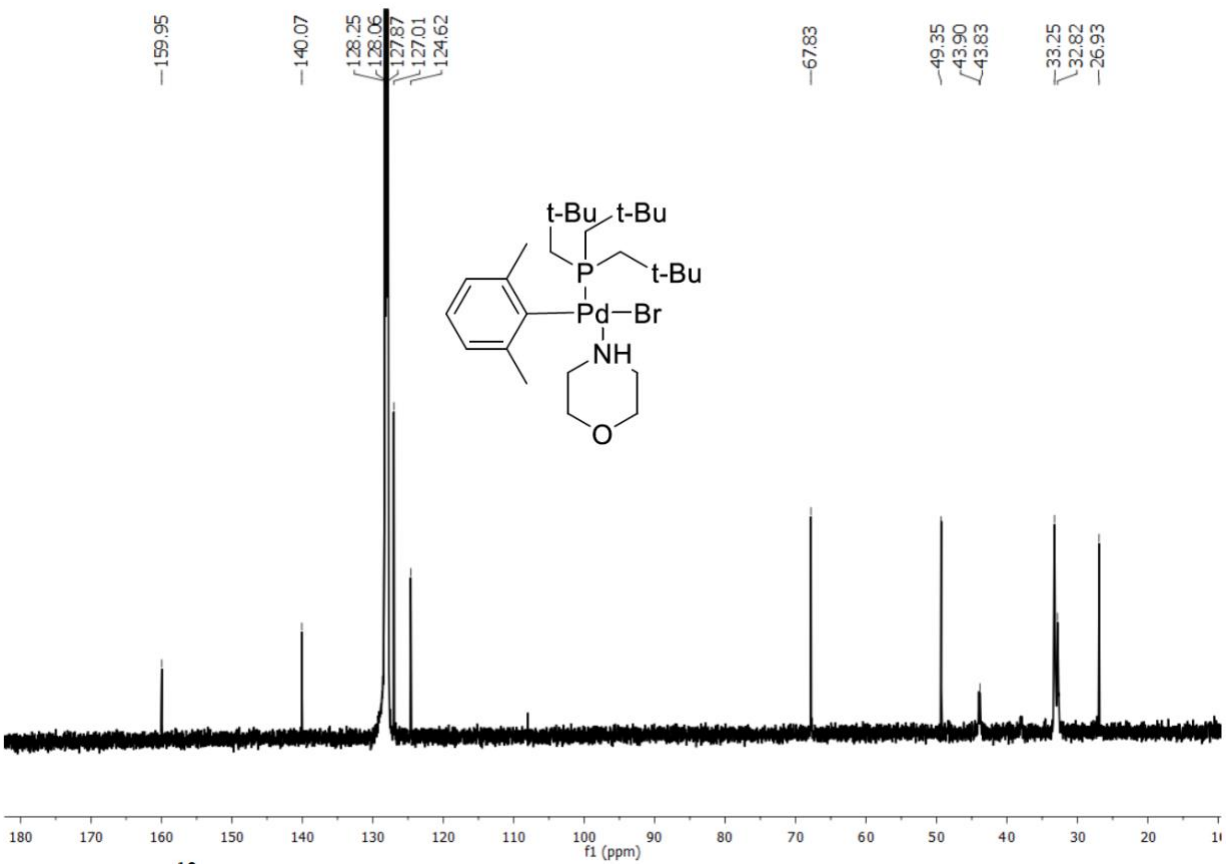

Figure A11: ^{13}C NMR (125 MHz, C_6D_6) spectrum of **5**.

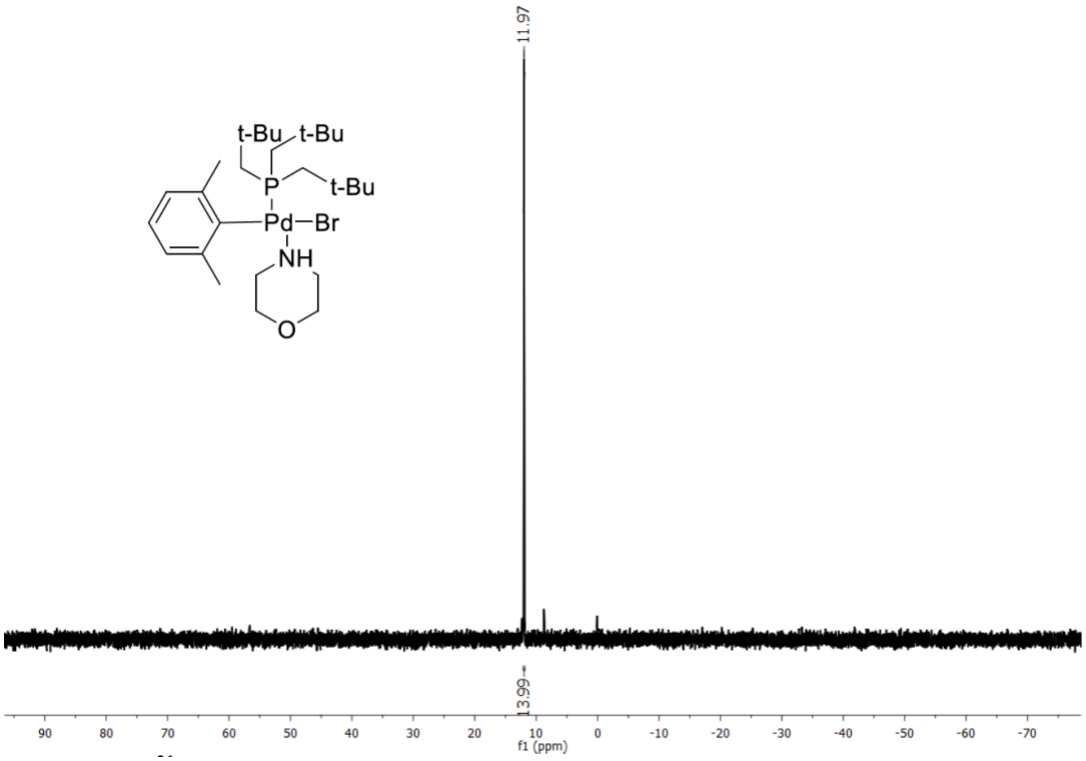

Figure A12: $^{31}P\{H\}$ NMR (202.5 MHz, C_6D_6) spectrum of **5**.

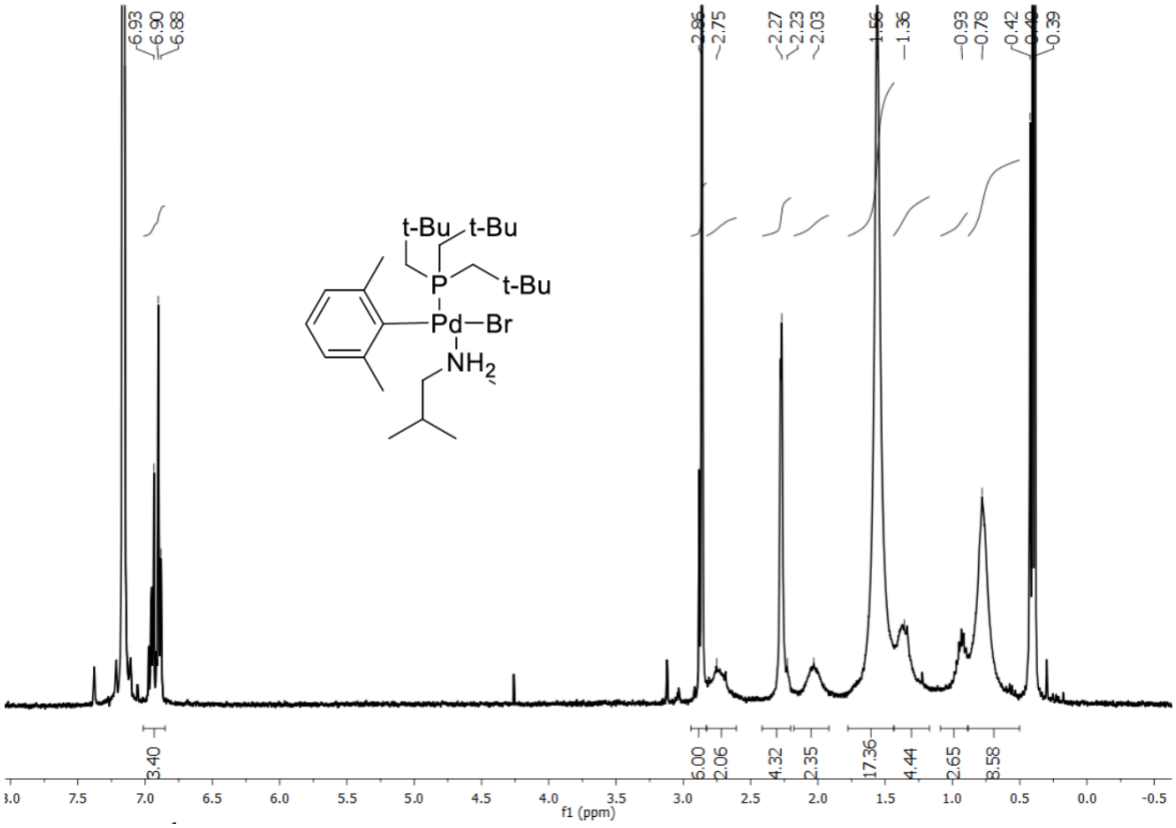

Figure A13: ^{1}H NMR (500 MHz, C_6D_6) spectrum of **6.**

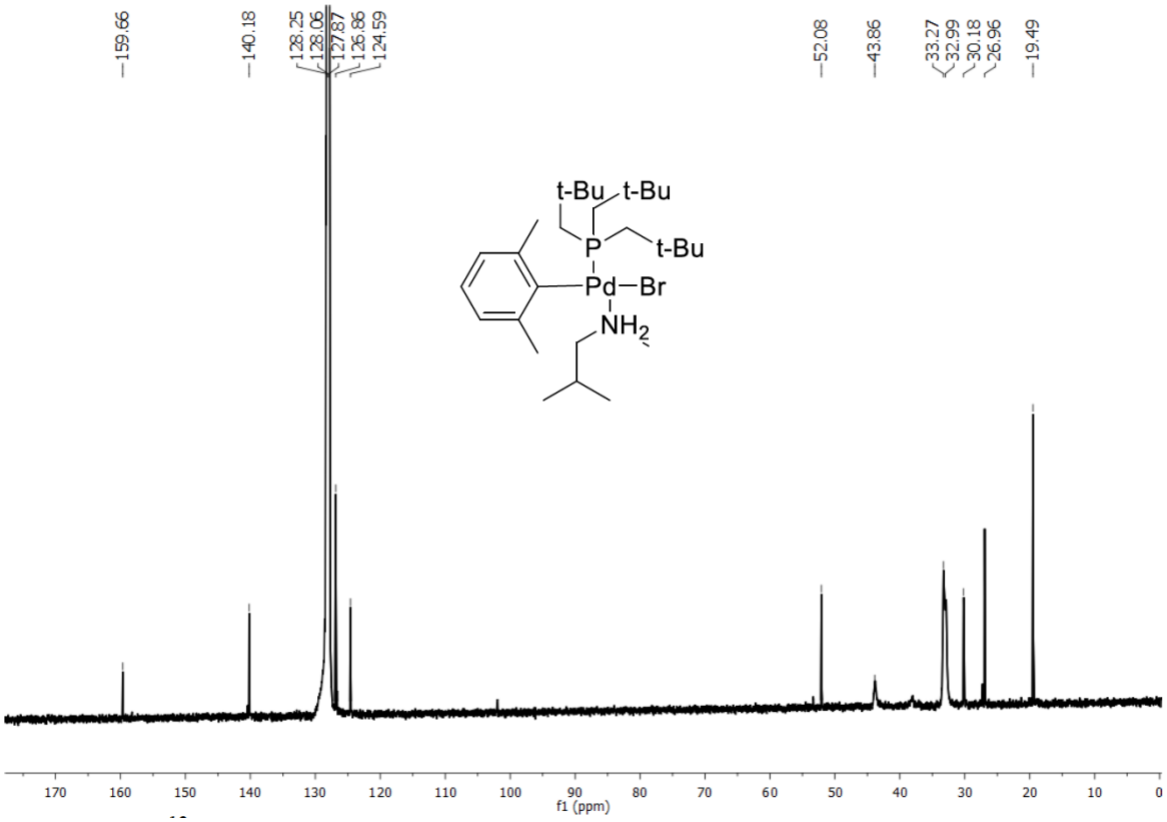

Figure A14: ^{13}C NMR (125 MHz, C_6D_6) spectrum of **6**.

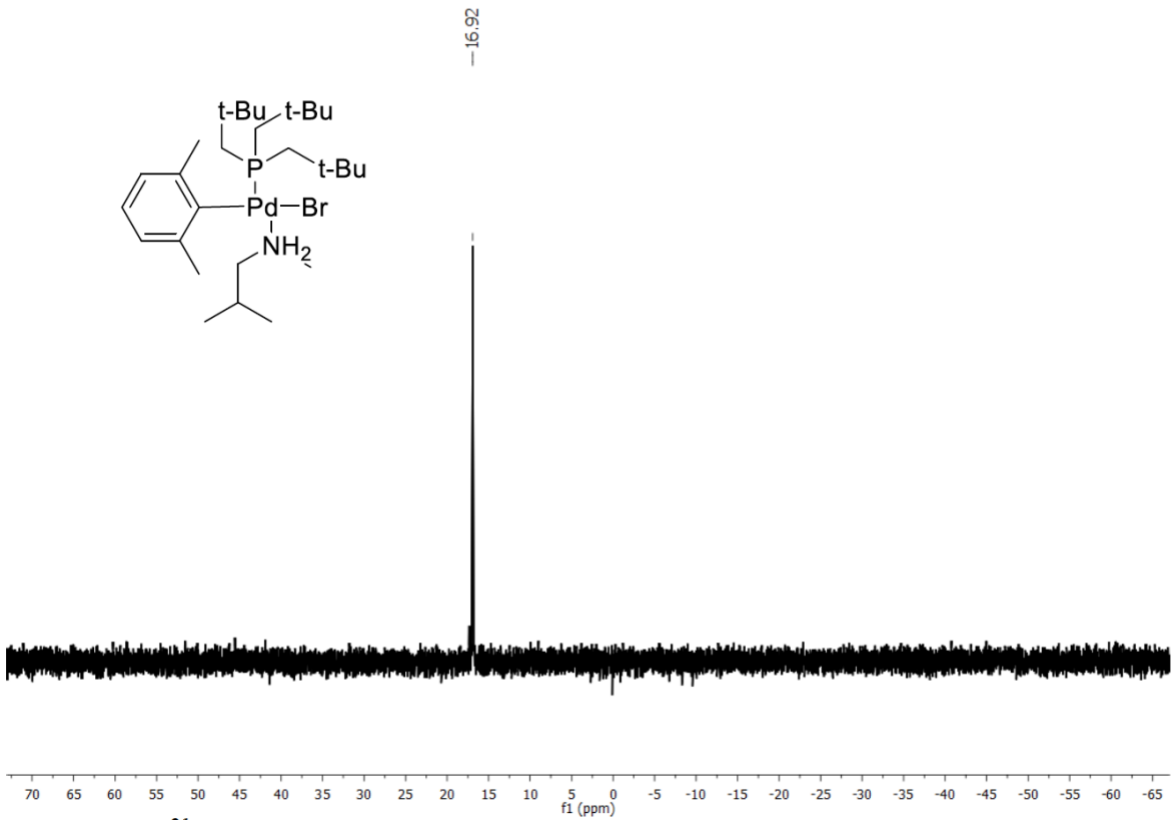

Figure A15: $^{31}P\{H\}$ NMR (202.5 MHz, C_6D_6) spectrum of **6**.

CHAPTER 3: TRIALKYLPHOSPHINE DERIVED PALLADACYCLES AS CATALYSTS FOR THE CROSS-COUPLING OF TERMINAL ARYL ACETYLENES WITH TERMINAL PROPARGYL ALCOHOLS AND AMIDES: AN EVALUATION OF THE LIGAND EFFECTS

3.1 Introduction

Conjugated 1,3-enynes are synthetically versatile and important motifs that are found in many natural products and pharmaceuticals.[62] The 1,3-enynes are also extremely useful as building blocks when constructing heterocycles and other complex molecules.[63] There are several known methods for synthesizing these compounds, including Sonogashira coupling reactions of vinyl halides with terminal alkynes, Wittig reactions of conjugated alkynals, and dehydration of propargylic alcohols.[64-66] Direct catalytic coupling of alkynes to produce conjugated enynes is a particularly attractive method given that alkynes are so readily available, however, developing methods to achieve these transformations are not as straight forward as it seems.

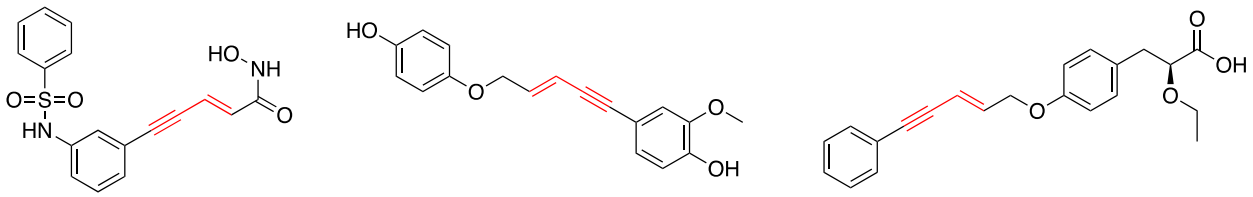

Oxmflatin

bioactive compound extracted from Asparagus Cochinchinensis

drug candidate NNC 61-4655

Figure 3.1: Examples of molecules with a 1,3 enyne motif highlighted in red.

Scheme 3.1: Regioisomers possible in the dimerization of terminal alkynes.

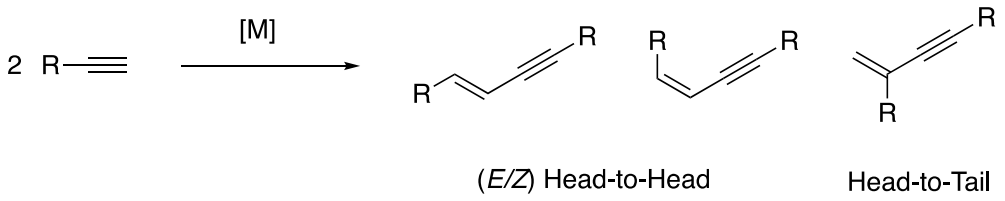

Metal-catalyzed dimerization of alkynes has the potential to produce three different enyne regioisomers (Scheme 3.1).[67] The dimerizations can occur in either a head-to-head (E/Z) or head-to-tail fashion. Several mechanistic investigations into metal-catalyzed dimerization reactions revealed that there are multiple reaction pathways this can occur.

One reaction pathway involves a terminal alkyne first forming a metal acetylide species that then coordinates to another alkyne via a carbometallation mechanism. The regiochemical outcome of this process is dependent on which orientation the alkynes coordinate to the metal sphere relative to one another (Figure 3.2) Elimination of the enyne product occurs through either protonolysis or a metathesis reaction that generates another metal acetylide.

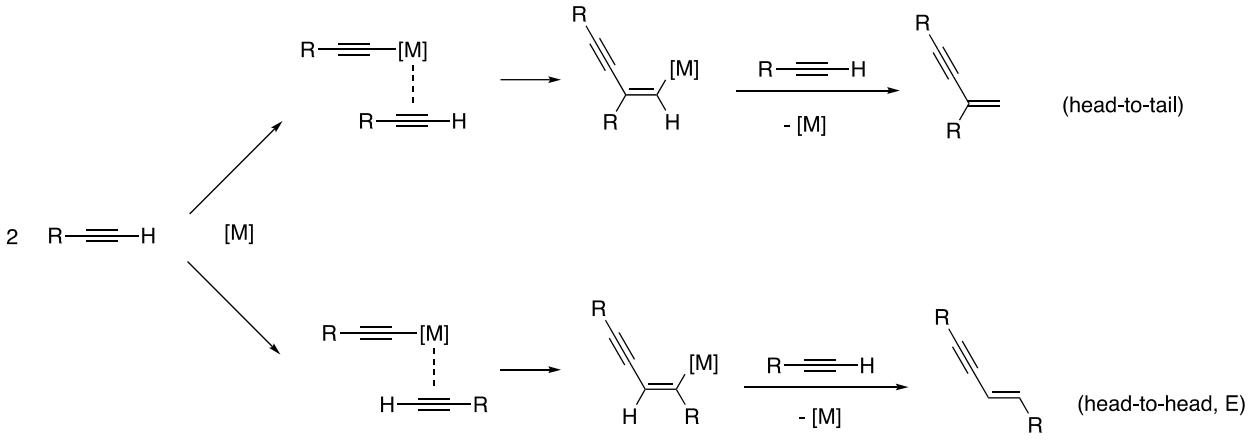

Figure 3.2: Metal acetylide-carbometallation pathway for alkyne cross-coupling reactions.

A second mechanistic pathway than can occur in the dimerization of terminal alkynes is referred to as a hydrometallation-reductive elimination process (Figure 3.3). In this pathway, the metal catalyst inserts into the alkynyl C-H bond to generate a hydrido(alkynyl)metal species. Spectroscopic evidence of these types of intermediates was first reported in 1990 for the dimerization of alkynes by $RhCl(PMe_3)_3$.[68] In the same report, the alkynyl(vinyl)metal species that are produced in the second step by insertion of another alkyne into the M-H bond were also observed. As in the metal acetylide-carbometallation pathway, regiocontrol of the products is influenced here by the orientation of the two alkynes relative to each other during insertion into the C-H bond. Reductive elimination generates the head-to-tail or the (E)-head-to-head isomer.

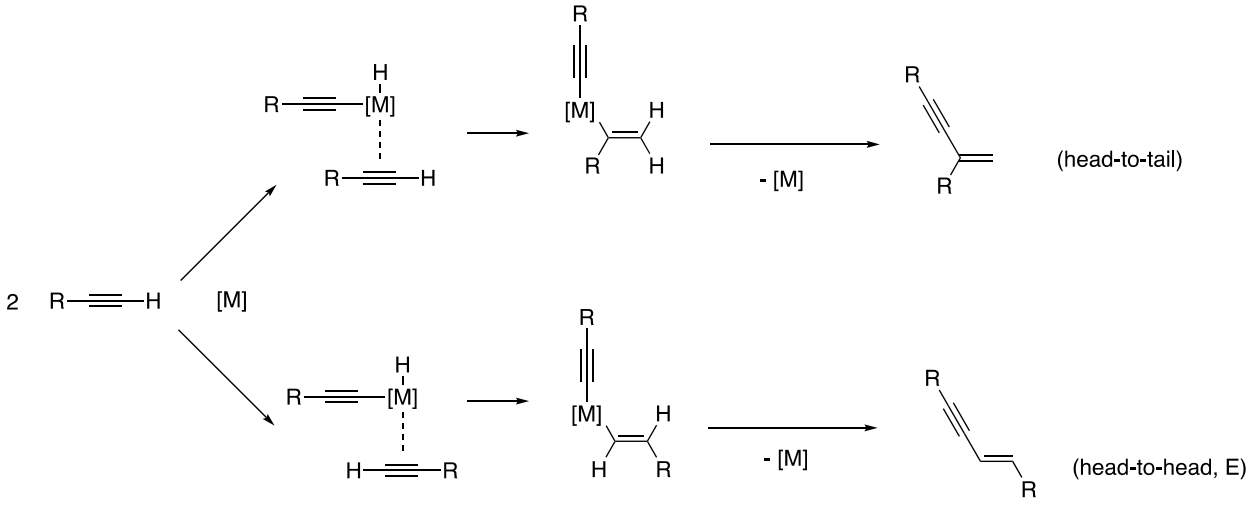

Figure 3.3: Hydrometallation-reductive elimination pathway for alkyne cross-coupling reactions.

A third possible reaction pathway exists in which the interaction of two terminal alkynes with a transition metal may generate a metal acetylide–vinylidene intermediate, which can equilibrate between its rotameric forms. Migration of the acetylide ligand to the α-carbon of the

vinylidene generates an enynylmetal species from which either the (E)- or (Z)- head-to-head isomer is derived. (Figure 3.4)

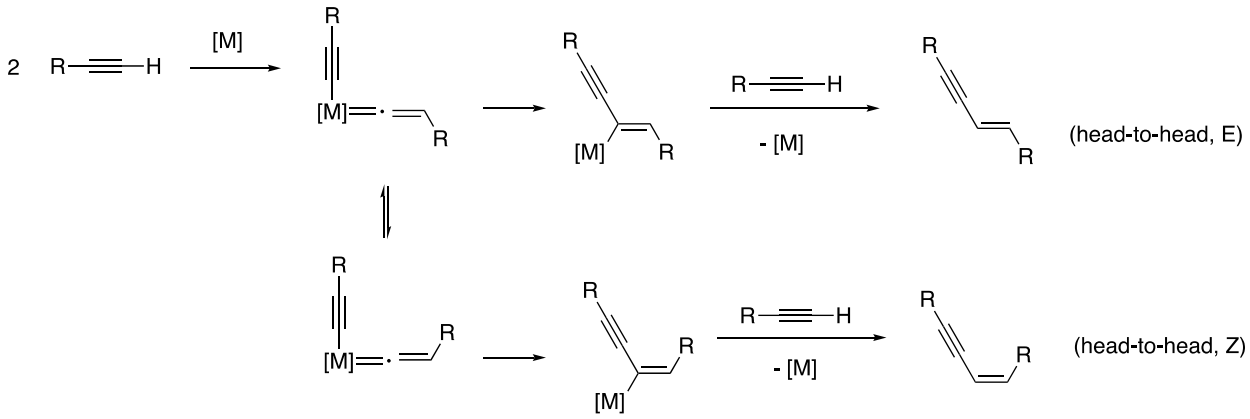

Figure 3.4: Metal Acetylide-Vinylidene Pathway alkyne cross-coupling reactions.

Considering that multiple different reaction pathways exist for catalytically coupling alkynes and that there may be more than one mechanism occurring simultaneously, a lot of effort has been put forth to develop selective methods that generate the desired regioisomeric enyne. There are now many reports of catalytic systems using different transition metals as catalysts to generate head-to-tail and head-to-head *E*-selective enyne products. The pincer-ligated species (PCP)Ir (PCP = κ^3-C_6H_3-2,6-(CH_2P*t*-Bu_2)) by Goldman and the NHC carbene complex $Pd(IPr)_2$ (IPr = 1,3-bis(2,6-diisopropylphenyl)imidazol-2-ylidene)) in the presence of bulky phosphines demonstrate sole selectivity for the formation head-to-head *E*-enynes.[67, 69]

Boese and Goldman reported a rhodium-catalyzed dimerization system using $[Rh(PMe_3)_2Cl]_2$ where the distribution of products was a function of the steric bulk of the substrate.[70] (Figure 3.5) The sterically hindered *tert*-butylacetylene was selective only for the head-to-head product, whereas the smaller acetylenes, such as phenylacetylene, was selective for

the head-to-tail isomer. These results demonstrated the level of influence the steric environment has on the outcome of the distribution of products.

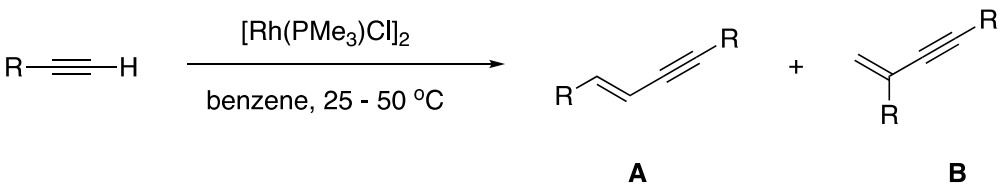

R	% Yield of **A** (head-to-head product)	% Yield of **B** (head-to-tail product
n-propyl	37	63
t-butyl	100	0
phenyl	0	100

Figure 3.5: Product distribution of the rhodium-catalyzed dimerization of alkynes reported by Boese and Goldman.[70]

Z-Selective enyne formation tends to be more difficult to selectively generate due to the inherent energetic disadvantage between cis- and trans alkenes, but there has been some success in this area. Schafer and Platel demonstrated a zirconium-catalyzed dimerization that preferentially formed the head-to-head *Z*-enyne.[71] In general, the regioselectivity of the metal-catalyzed dimerization of terminal alkynes can be controlled by altering the steric environment of the catalyst/and or substrate.

The aforementioned problems surrounding the regioselectivity of catalytic dimerization reactions are increased exponentially when considering the catalytic cross-coupling of two different alkynes. Rather than the three regioisomeric enynes that can be generated when coupling two of the same alkyne, a total of twelve different products, including stereo- and

constitutional isomers of the homocoupled and cross-coupled products, can be formed when two different alkynes are used (Scheme 3.2). Special attention must be paid to the coupling substrates to ensure there is one alkyne that is more likely to act as the acceptor and one that is primed to act as the donor to avoid homocoupling the substrates. Due to the increased challenge of controlling chemoselectivity on top of regioselectivity, far fewer methods have been developed for the cross-coupling of two different terminal alkynes.

Scheme 3.2: Possible isomeric products when two different alkynes are coupled.

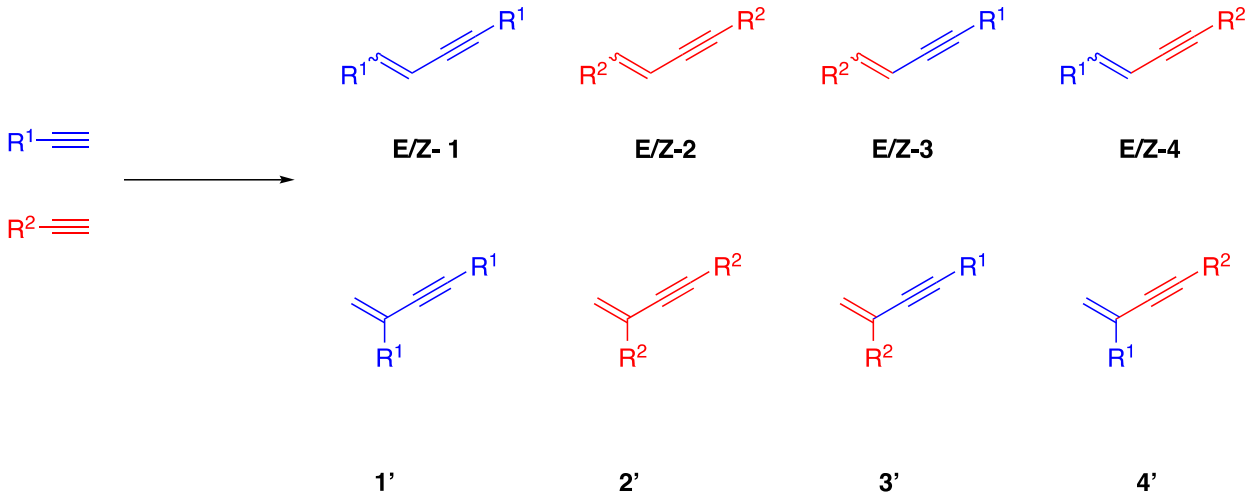

Silyl alkynes can be selectively cross-coupled with both aryl and alkyl alkynes to produce either *E/Z* head-to-head enynes or head-to-tail enynes depending on the choice of catalyst. Milstein and coworkers used an iron complex [Fe(H)(BH_4)(iPr-PNP)] (iPr-PNP = 2,6-$C_5H_3N(CH_2P^iPr_2)_2$) to selectively homocouple terminal alkynes and cross-couple aryl acetylenes with silyl alkynes to generate the *Z*-head-to-head product.[72] Perez-Torrente and Oro developed an NHC-derived rhodium(I)-catalyzed system that was selective for head-to-tail enyne products.[73] Miura and coworkers were able to generate an in situ catalyst using $[RhI(cod)]_2$ and

Xantphos that selectively cross-coupled silyl alkynes and bulky terminal alkynes to produce *E* head-to-head enyne products (Figure 3.6).[74]

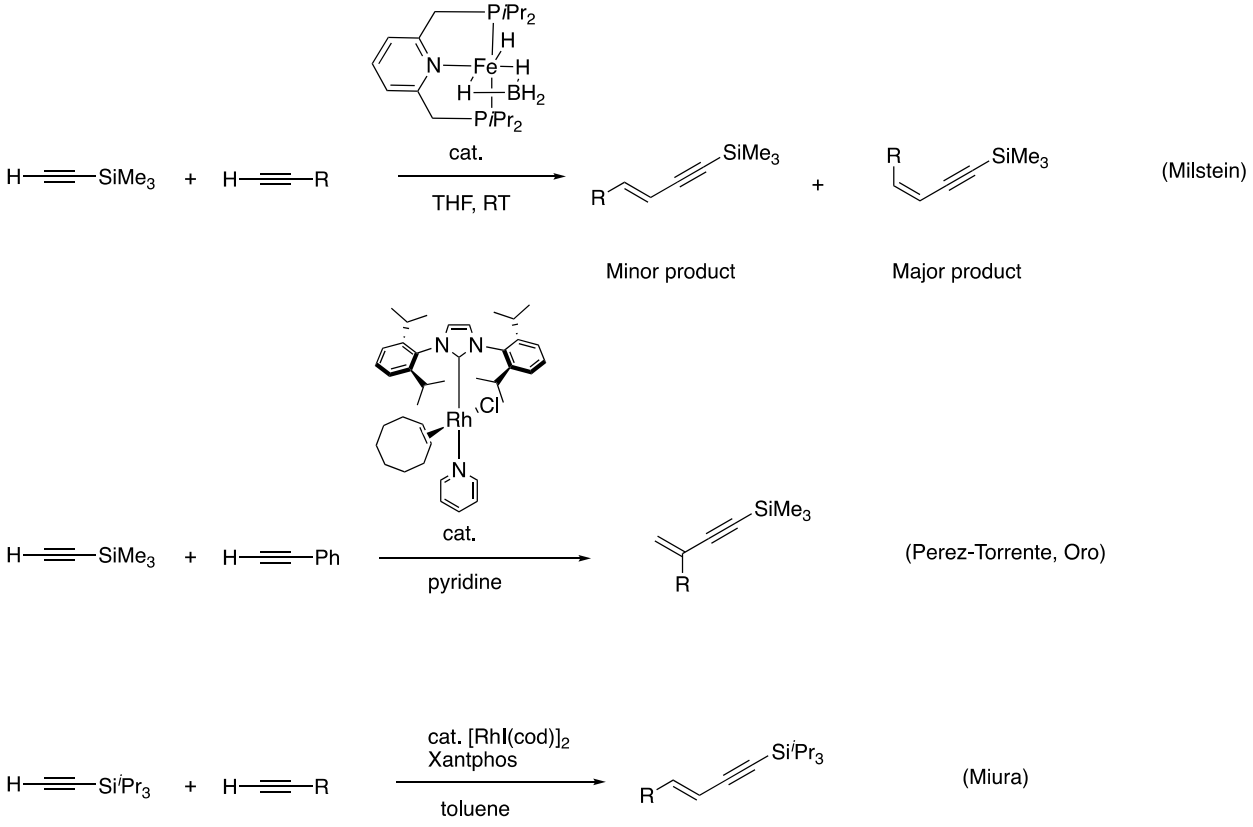

Figure 3.6: Examples of selective catalytic cross-coupling of terminal alkynes.

Previously, the Shaughnessy group had reported in situ generation of a catalyst using $Pd_2(dba)_3$ and a tertiary phosphine (PR_3 = DTBNpP or PNp_3) that could catalyze Heck type cross-couplings of aryl bromides and alkenes.[38] During investigation into the mechanism of the Heck couplings, an unknown peak was observed in the phosphorous NMR spectra at 94 ppm when DTBNpP was used as the ligand. No neopentyl phosphine-derived palladacycles had been reported in the literature before; however, it was hypothesized that this species was a

palladacycle based on the fact that neopentyl phosphines are known to be capable of cyclometalating with metals such as platinum and iridium.[75]

The palladacycle derived from alkyl phosphine P*t*-Bu$_3$ had been reported by Stambuli.[76] Using an adaptation of Stambuli's procedure, Shaughnessy and coworkers synthesized an acetate-bridged palladacycle derived from DTBNpP and Pd(OAc)$_2$ (**7**).[77] The acetate-bridged dimer was converted to a bromide-dimer to compare the resulting species to the unknown peaks observed in the mechanistic studies of the Heck cross-couplings when DTBNpP was used as the ligand. (Figure 3.7) The ^{31}P spectrum for the bromide-bridged DTBNpP dimer matched the spectrum of the unknown peak at 94 ppm observed in the Heck reactions.

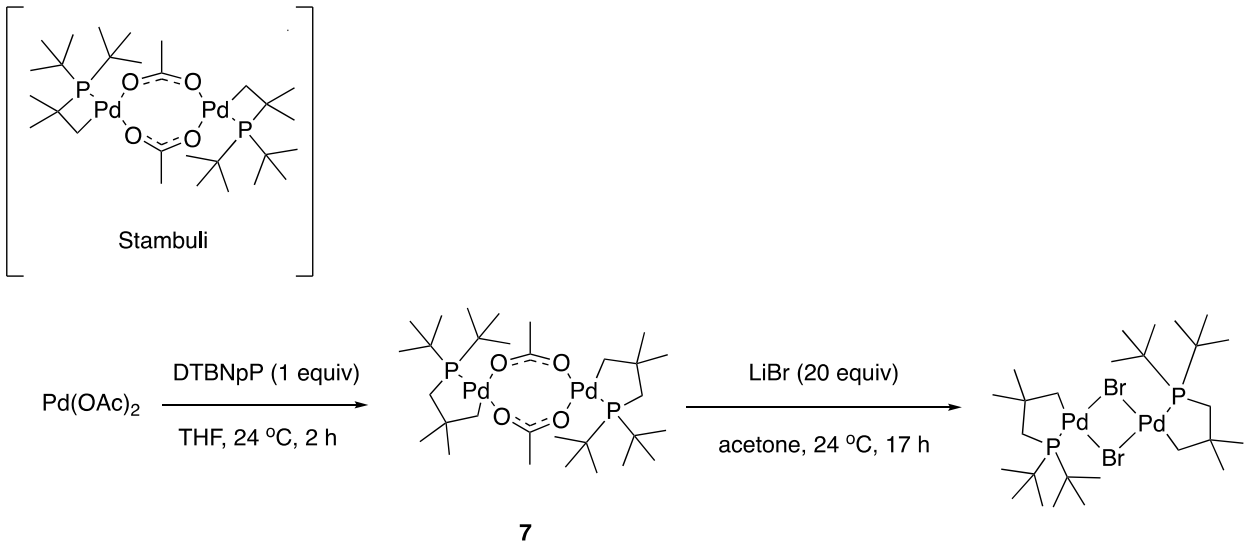

Figure 3.7: Method adapted from Stambuli used to generate **7**.

The bromine-bridged palladacycle species identified in the Heck cross-coupling reactions was a part of the catalyst deactivation pathway for that catalytic system, however, the acetate-bridged DTBNpP dimer (**7**) was shown to promote the selective cross-coupling of terminal aryl alkynes with both propargyl alcohols and propargyl amides to synthesize linear *E*-enynol

or -enynamide products, respectively (Scheme 3.3).[77] The reaction also showed strong selectivity for coupled products in which the propargyl coupling partner is the alkyne acceptor. It was less selective for which alkyne acted as the alkyne donor, as demonstrated by the propensity for cross-coupled and homo-coupled propargyl products, but not homo-coupled arylalkyne products. This report by Shaughnessy and coworkers was the first cross-coupling method for coupling alkynes with propargyl alcohols or amides that preferentially afforded *E* head-to-head enyne products.

Scheme 3.3: DTBNpP acetate-bridged palladacycle dimer (**7**) catalyzed coupling of aryl acetylenes with propargyl alcohols and amides.

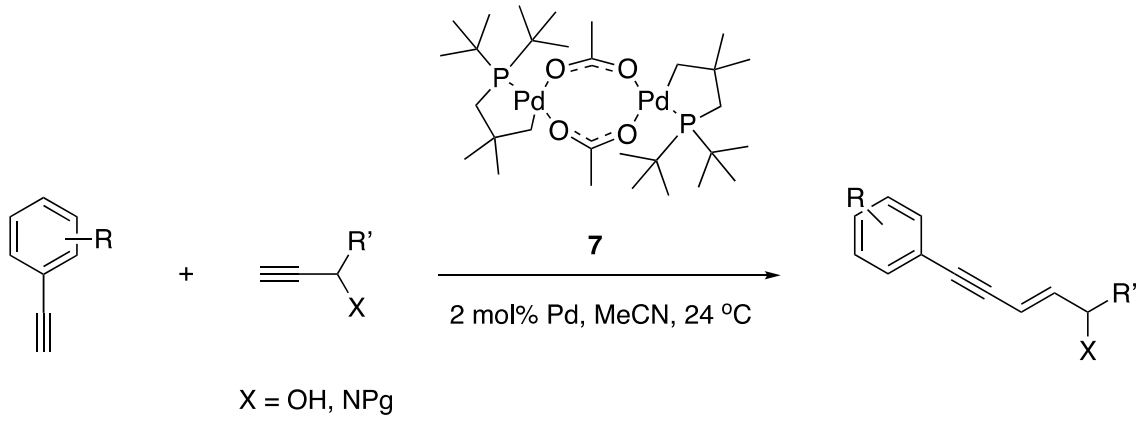

The palladacycle precatalyst appears to play an important role in determining the regioselectivity of the cross-coupling reaction. The TTBP-derived palladacycle first reported by Stambuli was less selective with overall lower yield than palladacycle **7**. In situ generated catalyst using DTBNp and $Pd(Oac)_2$ gave **V-a** (Figure 3.8) as the major isomer but was less efficient and less selective than precatalyst **7**. Other in situ generated catalysts such as *o*-tolyphosphine, TDMPP, or TNpP with $Pd(OAc)_2$, displayed significant selectivities for the head-to-tail product (**V-b**). It is clear that the both nature of the ligand and the type of catalytic system

have an impact on the chemo- and regioselectivity of the cross-coupling reaction. The acetate-bridged palladacycle was more selective and had the highest single isomer selectivity compared to similar precatalysts and in situ generated palladium catalyzed systems.

The cycle is believed to follow the reaction pathway described above in Figure 3.2. The catalytic cycle begins with **7** dissociating from the acetate-bridged dimer into the monomeric species **I** (Figure 3.8). The arylacetylene undergoes acetate-assisted C-H activation to generate the acetylide species **II**. The acetylide-bridged complex shown in Scheme 3.4 is likely in equilibrium with complex **II**, which accounts for both the catalytic competency of the species and the fact that the acetylide-bridged complex is less efficient due to lying in equilibrium with the on-cycle species. Complex **II** then coordinates propargyl alcohol to produce **III**. The stereochemistry of this intermediate is unknown, but it is believed that this is the point in the cycle where the regioselectivity of the transformation is determined. The likely conformation of **III** when palladacycle **7** is used will have the bound acetylide cis- to the phosphorous to allow for the incoming alkyne to have a more accessible space to coordinate away from the *t*-Bu groups on the phosphorous atom. The direction that the second alkyne coordinated (**III-a** or **III-b**) sets up the path for the migratory insertion to generate complex **IV** (**a** or **b**). Protonolysis by the acetic acid produced when generating **II** completes the cycle and regenerates the active species **I**.

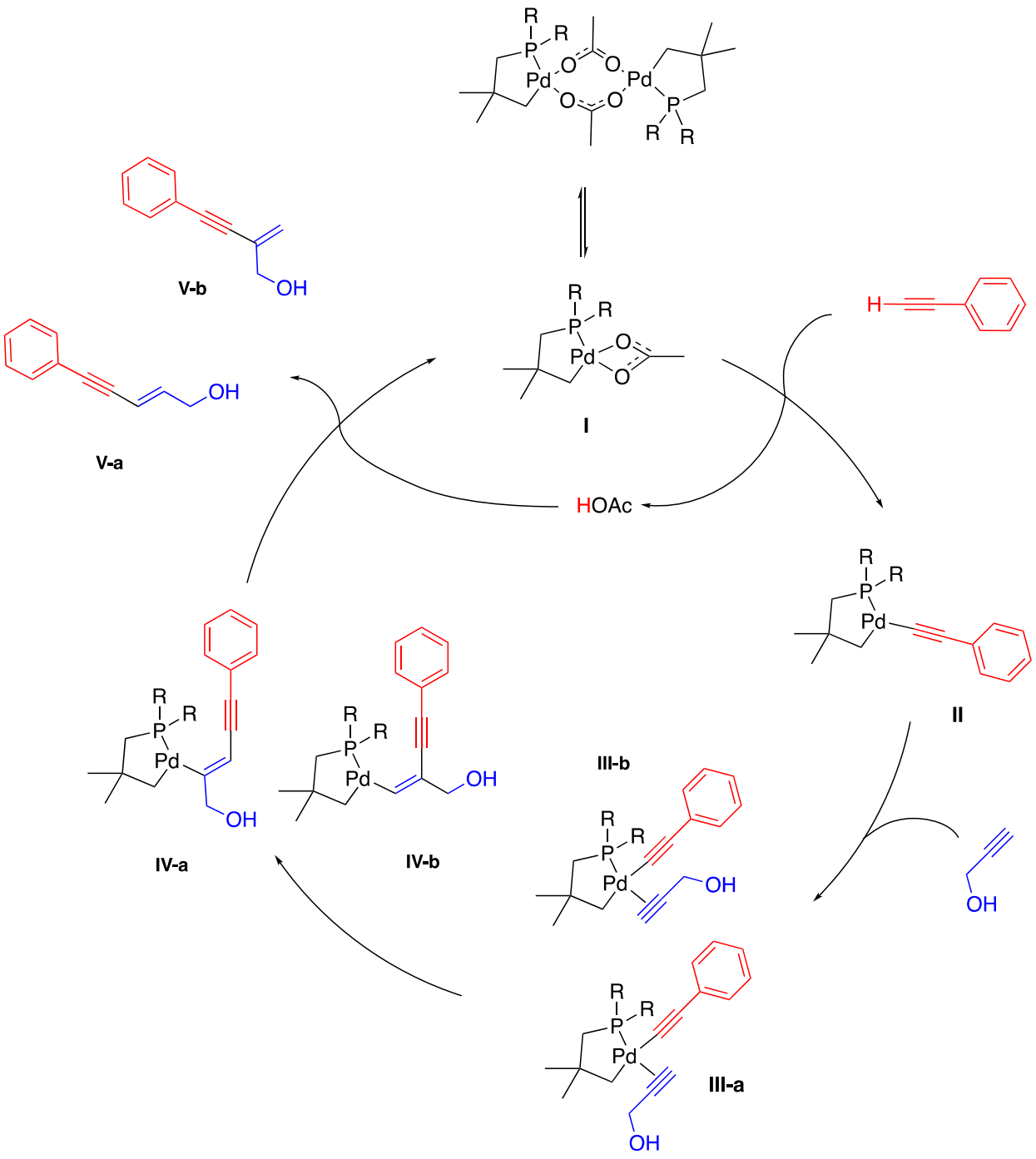

Figure 3.8: Catalytic cycle proposed by Shaughnessy and coworkers for the cross-coupling of phenylacetylene with propargyl alcohol catalyzed by palladacycle **7**.

Scheme 3.4: Preparation of the acetylide species derived from **7**.

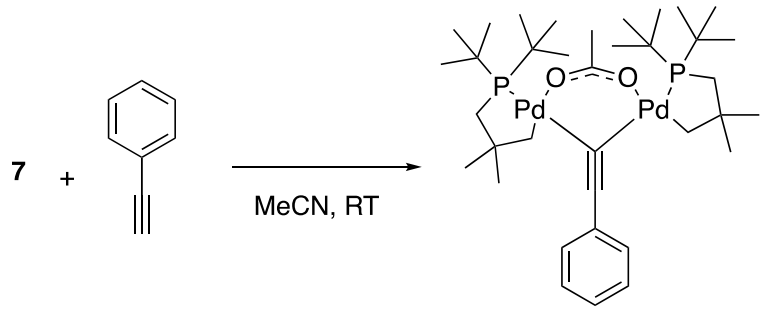

During mechanistic studies of the cross-coupling reaction shown in Scheme 3.3, a peak in the ^{31}P NMR spectrum of the reaction mixture revealed a previously unidentified peak around 80 ppm. It was hypothesized that the peak could be an acetylide complex derived from **7** (Scheme 3.4). This hypothesis was confirmed when the acetylide complex was synthesized separately and characterization matched the peak at 80 ppm in the ^{31}P NMR spectrum. The acetylide complex was catalytically competent for the cross-coupling reaction, albeit with slightly reduced conversion. This suggests that the acetylide species is involved in the cycle or in equilibrium with an on-cycle intermediate.

Given the success of **7** in the synthesis of linear (*E)*-enyne products (Scheme 3.1), I wanted to examine the effects of manipulating the steric features of the ligand on palladacycle formation and on the selectivity and efficiency of the cross-coupling reaction.

3.2 Results and Discussion

3.2.1 Synthesis of Alkylphosphines (**8-12**)

A series of ligands with the general formula $(R^1)_2PR^2$ (where R^1: *tert*-butyl, isopropyl, cyclohexyl, or phenyl and R^2: neopentyl or (trimethylsilyl)methyl were synthesized in order to

examine the effect altering the steric hindrance and electronics of the neopentyl phosphine backbone has on the ability of the acetate-bridged palladacycle to catalyze the alkyne cross-coupling (Scheme 3.3). Under inert conditions, 1.5 equivalents of the neopentyl Grignard reagent (or (trimethylsilyl)methyllithium reagent) was added slowly to a stirring solution of the dialkylchlorophosphine (1 equiv) with 0.2 equivalents of lithium bromide and 0.1 equivalents of copper(I) iodide in dry THF cooled to 0 °C. The temperature was maintained at 0 °C for a period of 2 hours before being allowed to warm to ambient temperature. The reaction was monitored by ^{31}P NMR spectroscopy. After complete alkylation of the chlorophosphine, the solution was concentrated in vacuo.

Scheme 3.5: Synthesis of alkylphosphines **8-12**.

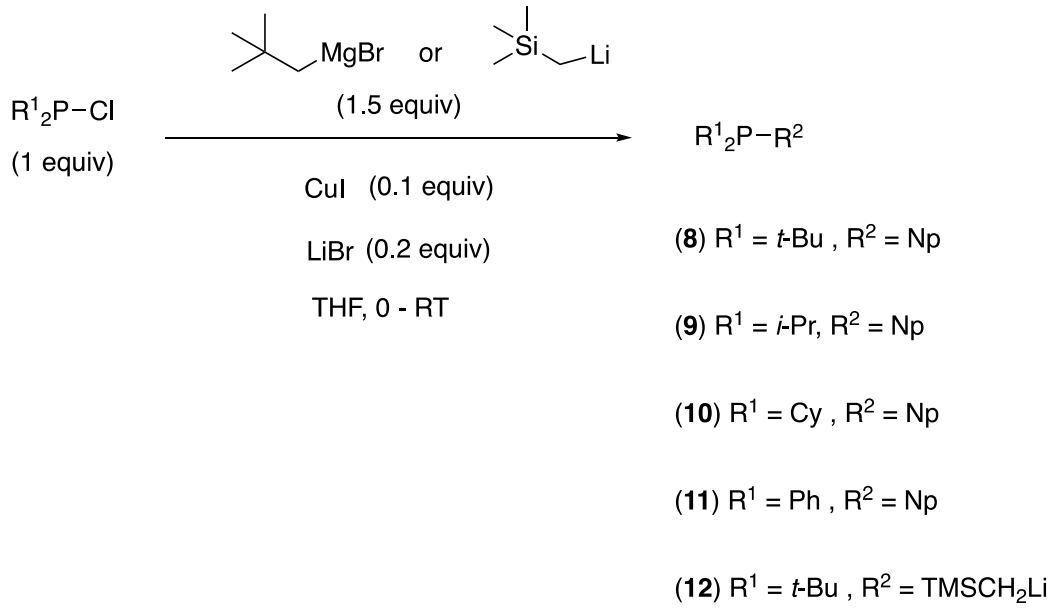

3.2.2 Synthesis of Phosphonium Tetrafluoroborate Salts (**13**-**17**)

Free phosphines typically require air-free conditions during preparation and storage. The diphenylneopentylphosphine (DPhNpP) (**11**) was relatively stable in the air and could be kept for

over a week without evidence of oxidation. Phosphines **8**–**10** and **12** are much more air-sensitive and would oxidize if not used immediately for complexation or if not stored in the glove box. In order to circumvent the aforementioned issues and to make purification easier, the alkyl phosphines were converted to their respective tetrafluoroborate salts before work-up following the procedure by Fu (Scheme 3.6).[78]

Scheme 3.6: Synthesis of phosphonium tetrafluoroborate salts **13**-**17**.

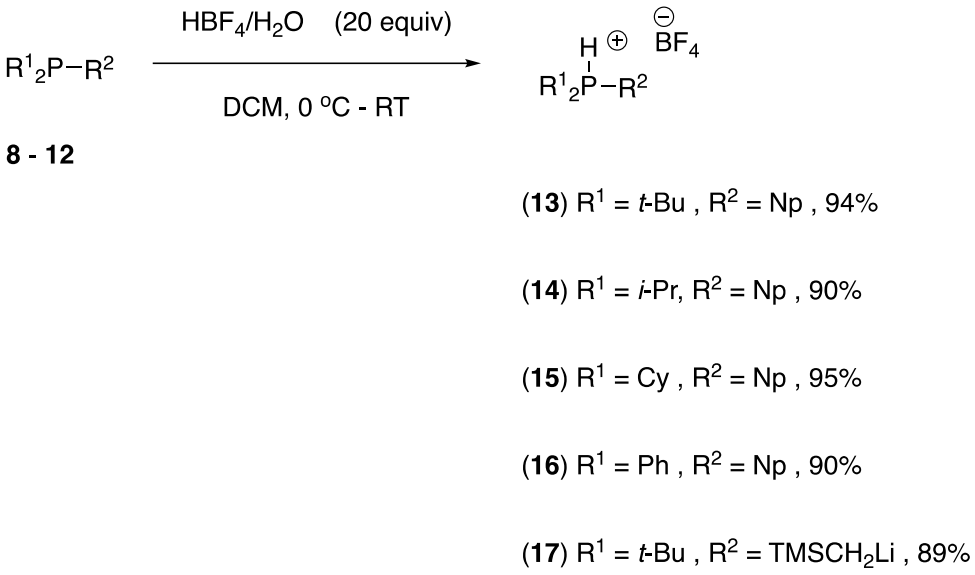

3.2.3 Formation of Acetate-bridged Palladacycle Precatalysts (**7**, **18**, **19**)

Palladacycles **7**, **18**, and **19** were prepared using an adapted version of a method developed by Stambuli (Scheme 3.7).[79] The phosphonium salts (**16** – **18**) were deprotonated in situ under air-free conditions by stirring them in a solution of THF and 1.2 equivalents of sodium *tert*-butoxide for approximately 3 hours before being transferred to a stirring solution of 1 equivalent of palladium(II) acetate in THF. The resulting solution was concentrated, extracted with DCM, dried over Na_2SO_4, and washed with cold pentane to yield a powdered product. The

palladacycle precatalysts were characterized by ^{1}H, ^{13}C, and ^{31}P NMR spectroscopy. Attempts to complex ligands **16** and **17** were not successful. When attempting to cyclometalate the DPhNpP ligand **16,** the resulting species would decompose to palladium black and free ligand Its unclear why they were both unsuccessful, however, I suspect the di-*tert* butyl(trimethylsilyl)methylphosphine ligand **17** having a silicon atom in place of a carbon atom inhibited cyclization due to the increased bite angle the 5-membered ring would have to adopt.

Scheme 3.7: Synthesis of palladacycles **7**, **18**, and **19.**

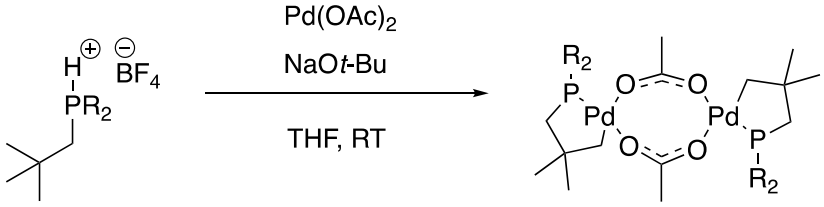

13 - 17

(**7**) R = *t*-Bu , 90%

(**18**) R = *i*-Pr , 91%

(**19**) R = Cy , 88%

Crystallographic data for the halide-bridged DTBNpP-derived palladacycle dimer has been reported, however, attempts to grow crystals of the acetate-bridged precatalysts **7**, **18**, and **19** were unsuccessful.[45] The palladacycles can be characterized by relatively broad peaks in the ^{31}P NMR spectra. The broadness of the peaks can be attributed to the fluxional nature of the complex. Acetate-bridged phosphapalladacycles tend to adopt a non-rigid structure that exist in equilibrium with the monomeric species due to the nature of the weakly bound acetate ligands to open coordination sites at the metal. At lower temperatures the broad peak will resolve into three sharper resonances (Figure 3.9). These peaks likely correspond to the monomeric version of the

palladacycle plus the *cis*- and *trans*-isomers of the dimer. This natural equilibrium of the acetate complex likely explains the unsuccessful attempts to grow crystals for structure determination in comparison to the halide-bridged examples (Scheme 3.8).

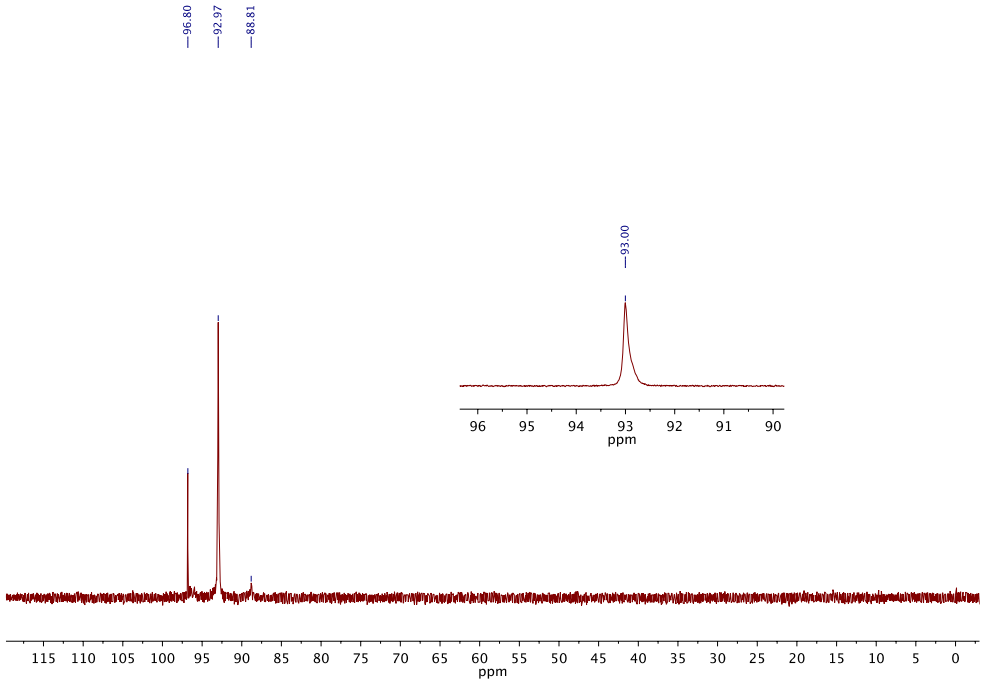

Figure 3.9: The ^{31}P NMR spectrum of precatalyst **7** in $CDCl_3$ at 24 °C (top) and at -40 °C (bottom).

Scheme 3.8: Equilibrium of palladacycle isomers in solution.

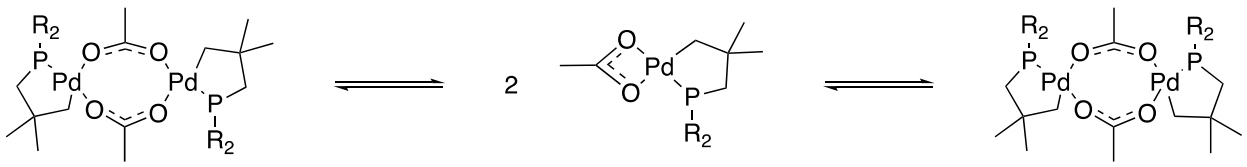

trans- *cis*-

3.2.4 Evaluation of Ligand Effects

In order to determine the effects the ligand has on the product selectivity in the cross-coupling of terminal arylacetylenes with propargyl alcohols and propargyl amides, the method using DTBNpP palladacycle **7** reported by Shaughnessy and coworkers was repeated using DiPrNpP and DCyNpP precatalysts **18** and **19** (Scheme 3.9).[77] Arylacetylenes with electron withdrawing substituents, electron donating substituents, and a heterocyclic moiety were selected to be coupling partners with propargyl alcohol and propargyl phthalimide.

Scheme 3.9: Reaction of arylacetylenes with propargyl alcohol (or propargyl phthalimide) catalyzed by palladacycles **7**, **18**, or **19**.

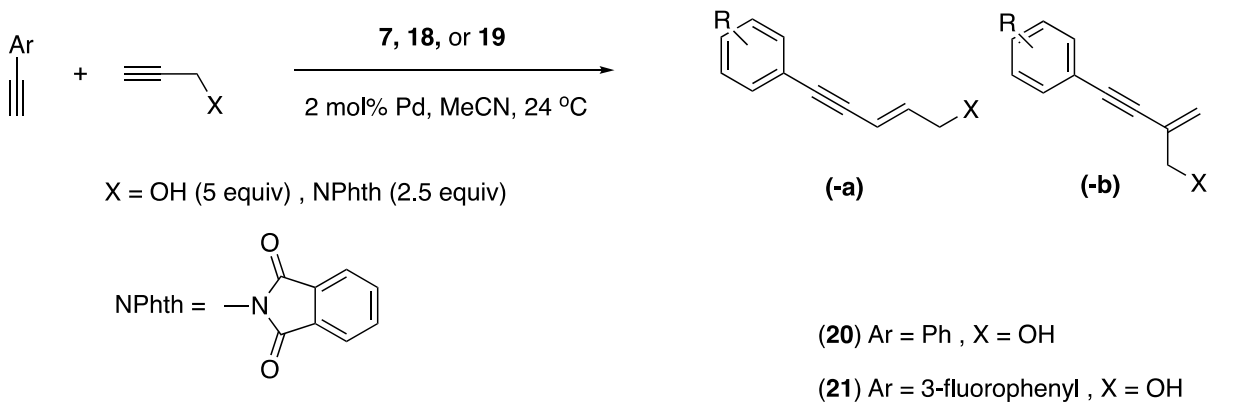

(**20**) Ar = Ph , X = OH

(**21**) Ar = 3-fluorophenyl , X = OH

(**22**) Ar = 4-methoxyphenyl , X = OH

(**23**) Ar = 3-thiophenyl , X = OH

(**24**) Ar = Ph , X = Nphth

(**25**) Ar = 3-fluorophenyl , X = Nphth

(**26**) Ar = 4-methoxyphenyl , X = Nphth

(**27**) Ar = 3-thiophenyl , X = Nphth

Under inert conditions, the phenylacetylene derivative and the propargyl alcohol (or *N*-propargylphthalimide) were added in 1:5 ratio (1:2.5 for *N*-propargyl phthalimide) to the catalyst (2 mol %) in acetonitrile and allowed to stir for 24 hours at room temperature. The resulting

distribution of products was evaluated using ^{1}H NMR spectroscopy and an internal standard (Tables 3.1 and 3.2). For products **22** and **26** the internal standard is hexamethylcyclotrisiloxane. All other conditions used anisole as the internal standard. An example of the analysis of a crude reaction mixture is shown in Figure 3.10. The main products were separated out of the mixture using column chromatography when possible and identified using ^{1}H NMR spectroscopy.

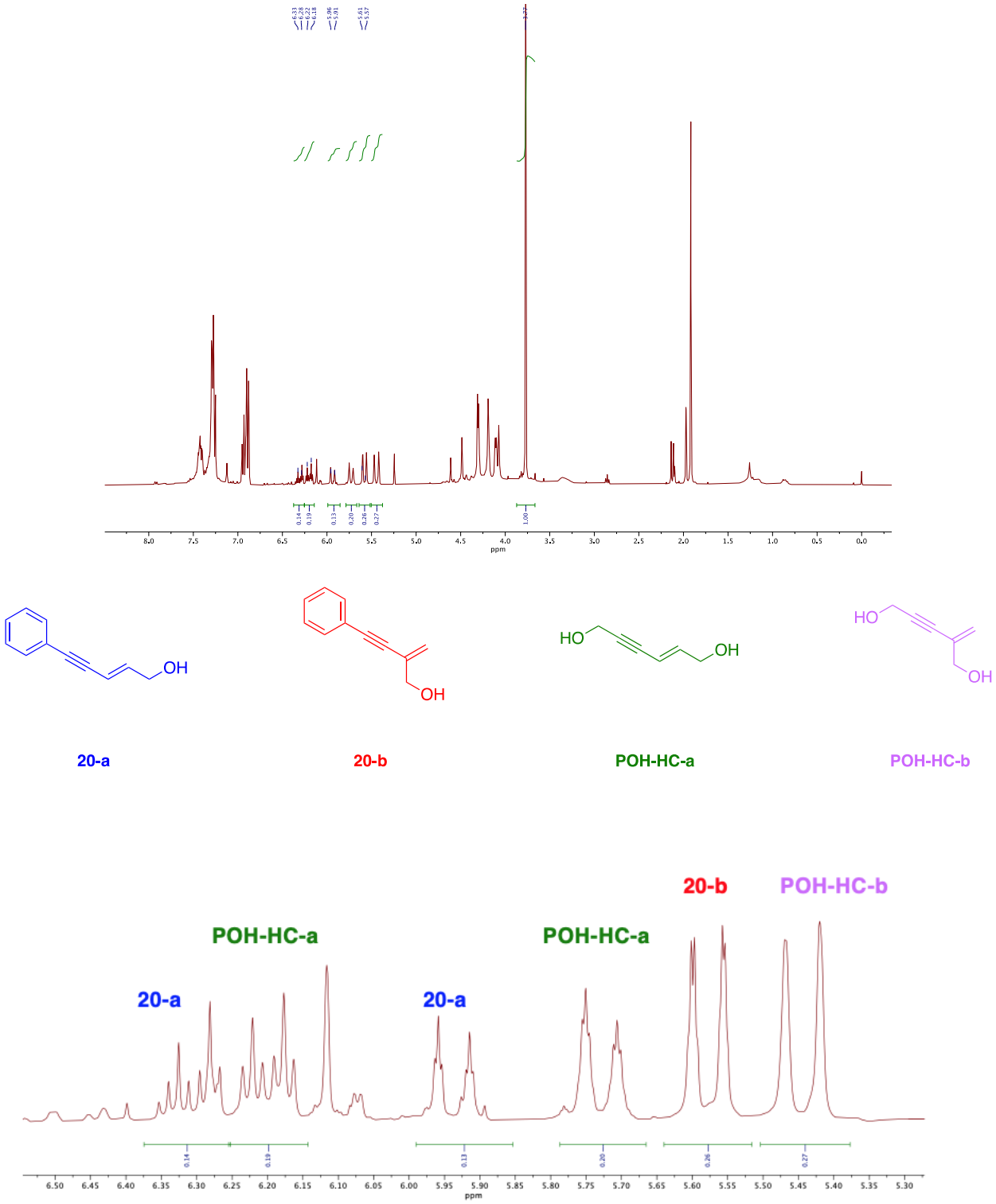

Figure 3.10: Analysis of the ^{1}H NMR spectrum of the crude reaction mixture of phenylacetylene with propargyl alcohol to give products **20-a** and **20-b** and the isomeric propargyl alcohol homo-coupled products. Top = full spectrum showing anisole as the internal standard at 3.8 ppm. Bottom = zoomed in alkene region.

Table 3.1: Distribution of isomeric products when X = OH (Scheme 3.9).

Precatalyst	yield	**20-a**	**20-b**	**POH-HC-a**	**POH-HC-b**
7	72%	1	0	2	-
18	69%	1	0.96	1.4	1
19	57%	1	3.75	2	3.6
		21-a	**21-b**	**POH-HC-a**	**POH-HC-b**
7	ND	ND	ND	ND	ND
18	55%	1	2.8	0	0.8
19	48%	1	3	0	2.1
		22-a	**22-b**	**POH-HC-a**	**POH-HC-b**
7	61%	1	0	-	-
18	74%	1	5	4	6
19	44%	1	6	3	6
		23-a	**23-b**	**POH-HC-a**	**POH-HC-b**
7	63%	1	0	-	-
iPr	20%	1	5	4	6
Cy	0%	0	0	0	0

*ND = not determined. Precatalyst **7** data from Lauer and coworkers.[77]

When examining the product distribution in Table 3.1 for the cross-coupling with propargyl alcohol, the DTBNpP-palladacycle (**7**) is vastly more selective compared to the DiPrNpP and DcyNpP variants (**18** and **19**, respectively). Palladacycle **7** solely favors the *E* head-to-head linear enyne. Palladacycle **18** favors the head-to-tail enyne product in all cases other than when phenylacetylene is the aryl coupling partner. When there are no substituents on the aryl moiety the

ratio of cross-coupled products is approximately 1:1. Palladacycle **19** also has selectivity for the head-to-tail products (**20-23 -b**), and generates at least three times the amount of **20-23-b** as it does the head-to-head regioisomer (**20-23 -a**) regardless of the substitution pattern on the aryl group.

Precatalyst **7** was the most effective as far as yield is concerned, however, palladacycle **18** showed a comparable yield when the aryl coupling substrate is a phenylacetylene derivative, albeit with opposite selectivity. DTBNpP-derived palladacycle **7** was the most efficient when 3-alkynyl thiophene was the aryl substrate coupling with propargyl alcohol. Palladacycle **18** only produced a 20% yield of cross coupled products and **19** failed to catalyze the reaction at all. Complex **19** gave the lowest yields overall, but showed the most selectivity for the head-to-tail enyne products (**20-23 -b**).

Previous reports in our group demonstrated that palladacycle **7** was competent at cross-coupling several substituted propargyl alcohols with phenyl acetylene (Scheme 3.10).[77] A series of substituted propargyl alcohols to use as coupling substrates with phenyl acetylene under catalytic conditions using palladacycles **18** and **19** (Scheme 3.11 and Scheme 3.12). Unfortunately, palladacycles **18** and **19** were unable to catalyze the cross-coupling of **28 – 31** with phenyl acetylene. Trace amounts of multiple different enyne regioisomers were detected, however, all attempts to separate and characterize the products were unsuccessful due to the low yields.

Scheme 3.10: Reaction of phenylacetylene with substituted propargyl alcohols catalyzed by **7.**

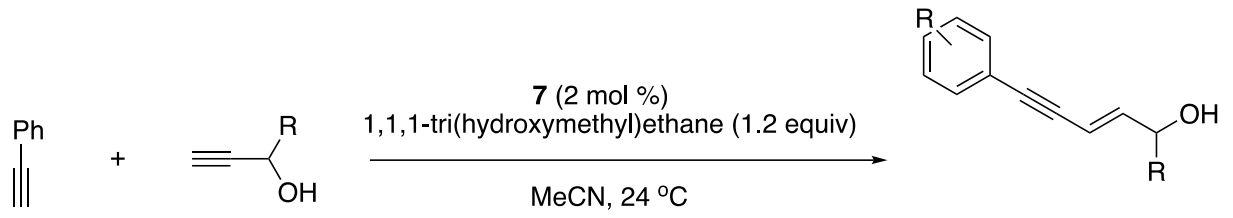

R = Aryl , alkenyl

5 examples

E head-to-head selective

61 - 73% yield

Scheme 3.11: Preparation of substituted propargyl alcohols **28 – 31**

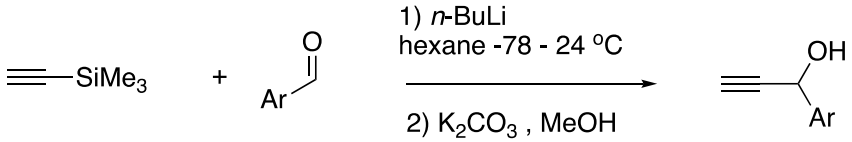

(28) Ar = Ph , 86%

(29) Ar = *o*-bromophenyl , 78%

(30) Ar = benzonitrile , 80%

(31) Ar = *p*-methoxyphenyl , 67%

Scheme 3.12: Reaction of phenylacetylene with substituted propargyl alcohols (**28-31**) catalyzed by **18** or **19.**

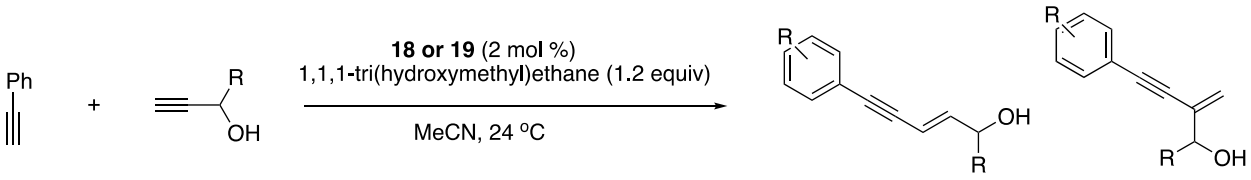

28 - 31

Table 3.2: Distribution of isomeric products when X = NPhth (Scheme 3.9).

Precatalyst	yield	**24-a**	**24-b**	**PNphth-HC-b**
	82%	3	1	ND
iPr	78%	1	2.6	0.8
Cy	87%	1	3.8	2.7
		25-a	**25-b**	**PNphth-HC-b**
7	ND	ND	ND	ND
iPr	29%	1	2.8	2.4
Cy	87%	1	3.1	2.4
		26-a	**25-b**	**PNphth-HC-b**
7	88%	3.7	1	ND
iPr	67%	1	3.6	0.4
Cy	56%	1	3.5	2.4
		27-a	**25-b**	**PNphth-HC-b**
7	72%	3	1	ND
iPr	70%	1	2.1	1.6
Cy	66%	1	3.4	2.4

* ND = not determined. Precatalyst **7** data from Lauer and coworkers.[77]

The product distribution in the cross-coupling of arylacetylenes with *N*-propargyl phthalimide followed a similar trend as the coupling reactions with propargyl alcohol. Complexes **18** and **19** displayed similar selectivities, with the DcyNpP-derived complex **19** slightly more selective for the head-to-tail regioisomer having product ratios approaching 1:4

24-27-a : **24-27-b** (Table 3.2). This preference for the head-to-tail enyne is almost the exact opposite of the selectivity displayed by the palladacycle **7**, where a 3:1 ratio of **24-27-a** : **24-27-b** isomers.

All three complexes showed comparable efficiencies when considering overall yield of cross-coupled products.

The DTBNpP-palladacycle **7** outpaced its DiPrNpP and DCyNpP varients (**18** and **19**) in terms of conversion. Generally accepted computational methods for approximating the individual steric bulk of phosphine ligands, such as Tolman's cone angle, show that P*t*-Bu$_3$ occupies a much larger space than almost all other trialkyl phosphines (Figure 3.11).[80] Tricyclohexylphosphine and P^{i}Pr$_3$ are less sterically encumbering, which suggests that conversion from **18** and **19** to the monomeric active species will be slower than the conversion is for **7** because the low coordinate palladium active species **I** (Figure 3.8) is less stabilized when there is better access to coordination sites on the palladium. Also, the reduction in steric bulk of **18** and **19** could cause the elimination of the enyne to occur at a slower rate than palladacycle **7**. Larger ligands cause more strain, and the palladium has more of a driving force to reduce the strain by eliminating the coordinated alkynes.

PR_3	Tolman cone angle
P*i*-Pr$_3$	160
PCy_3	170
P*t*-Bu	182

Figure 3.11: Tolman cone angles for selected PR$_3$ ligands.

The approximated differences in relative steric bulk of the phosphine backbones of **7**, **18**, and **19** may offer some insight into the product distributions observed. The regioselectivity in these reactions is most likely determined by the conformation of the alkyne that is favored for migratory insertion step in the cycle. (Figure 3.12) Steric bulk at the metal center would be expected to favor insertion to place the metal at the terminal carbon, leading to the head-to-tail enyne isomer. When the steric bulk of the phosphine ligand is decreased from *t*-Bu to *i*Pr or cyclohexyl, the selectivity for head-to-tail cross-coupled enyne product increases. The results observed suggest that the migratory insertion for **18** and **19** can occur in either orientation. If steric bulk was the only factor affecting the regioselectivity, palladacycle **19** would be expected to be less selective overall and **18** would be expected to be the most selective for head-to-tail product formation given that the DiPrNpP ligand theoretically occupies less space relative to the ligand backbones on **7** and **19.** This is not the case, however. Palladacycle **19** is the most selective for head-to-tail enyne formation and **18** is less selective on average but still trending more toward the head-to-tail product generation. This implies either that steric bulk is not the only factor at play in these transformations, and/or that the effect of steric hindrance generated by the phosphine ligand cannot be thought about in a linear fashion.

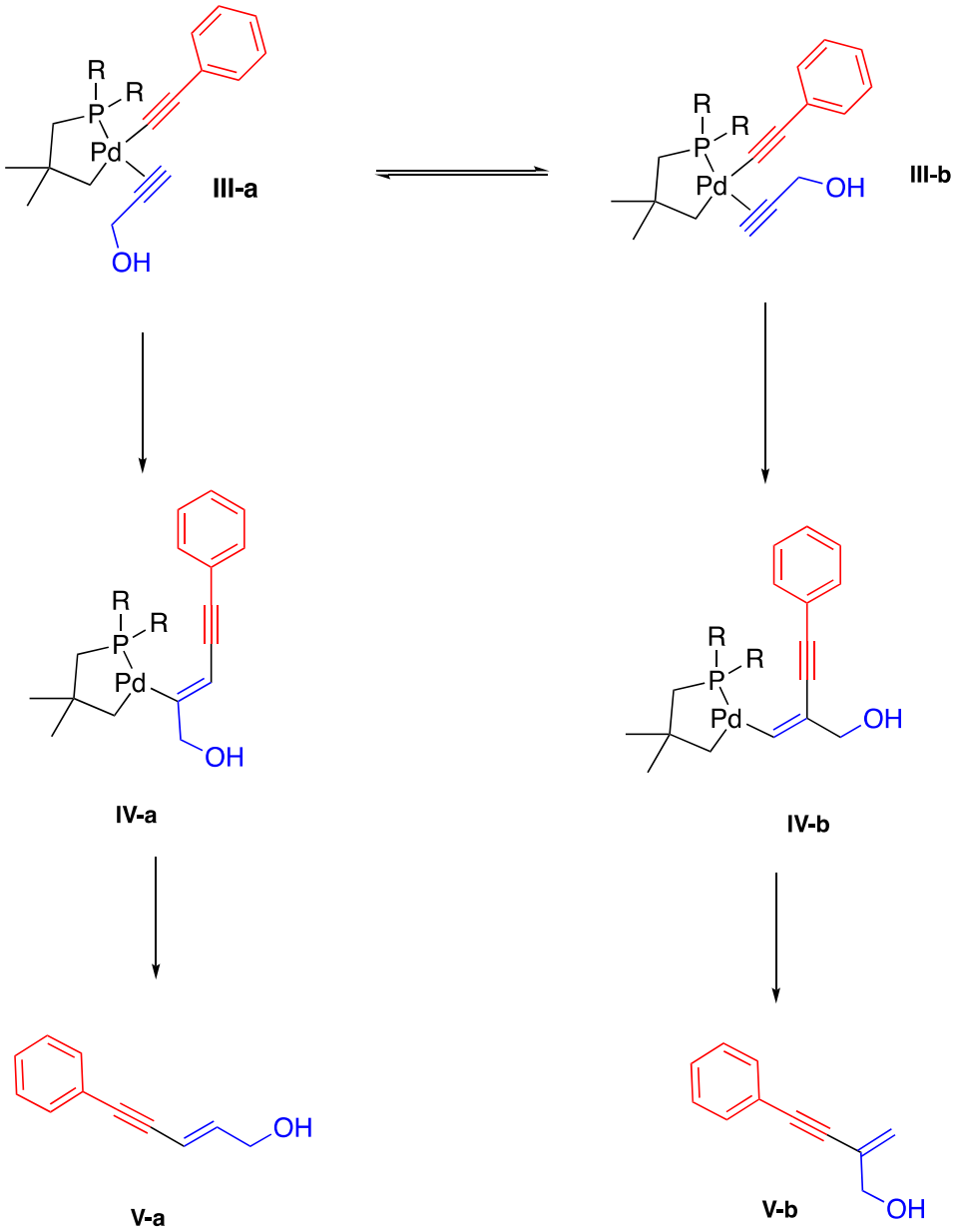

Figure 3.12: Mechanism for the migratory insertion step in the catalytic cycle.

3.3 Conclusions

Trialkyl neopentyl phosphine derived palladacycles **7**, **18,** and **19** are effective precatalysts for the catalytic cross-coupling of terminal arylacetylenes with terminal propargyl alcohols and propargyl amides. Depending on the steric parameters of the ligands, the distribution of regioisomeric enyne coupling products can be manipulated. Extremely bulky precatalyst **7** selectively delivers E enyne products, whereas palladacycles **18** and **19** with the less sterically hindered tri alkyl phosphine ligands yield the head-to-tail regioisomer.

In the future it would be helpful to analyze more coupling partners using the three different catalysts (**7, 18,** and **19**) to gain a better understanding of the catalytic efficiencies of the palladacycles. Also, expanding the library of ligands employed would allow for a more in depth examination of the steric effects the phosphine ligand has on the product distribution. Ligands **16** and **17** were not able to be cyclometalated, but one could envision altering the steric properties of the dialkylneopentylphosphine ligand by having larger alkyl substituents, such as adamantyl, and smaller alkyl groups such as methyl or ethyl to have more comparisons of product distribution to examine.

3.4 Experimental

General Procedures and Materials:

Reagents were purchased from commercial sources and used as received unless specifically noted. Toluene was refluxed over sodium, THF was refluxed over sodium/benzophenone, and MeCN was distilled over CaH_2 for at least an hour under a nitrogen atmosphere and both freshly distilled before use. Reaction temperatures refer to previously equilibrated oil bath temperatures. Assume all reactions were performed in an air-free environment by use of a glove box and Schlenk techniques. NMR spectra were collected on a Brüker 500 MHz spectrometer. ^{31}P NMR spectra were obtained under gated decoupling mode at fixed scans through the length of the experiment with the aid of an automated data collection program.

Synthesis of Phosphonium Tetrafluoroborate Salts (**13**, **14**, **15**, **16**, **17**):

The dialkyl chlorophosphine (1 equiv), lithium bromide (0.2 equiv), and copper(I) iodide (0.1 equiv) were added to a flask with THF and cooled to 0 °C. Neopentyl bromide or trimethylsilylmethyl lithium (1.5 equiv) was added to the stirring solution. The reaction was stirred and monitored by ^{31}P NMR spectroscopy. After alkylation is complete, the reaction was concentrated in vacuo. The resulting mixture was diluted with N_2 sparged DCM and cooled to 0 °C. Excess HBF_4/H_2O (48 wt%) was added via syringe. The reaction was allowed to stir for a period of 1-4 hours. The reaction was exposed to air and washed with brine. The product was dried over Na_2SO_4, filtered over celite, and concentrated in vacuo. The resulting white solid was triturated in hot ether to yield a white, crystalline powder.

[(t-Bu)$_2$HPNp]BF$_4$ (13). A flask containing chlorodi-(*t*-butyl)phosphine (190 μL, 1 mmol), LiBr (1.70 mg, 0.02 mmol), CuI (1.90 mg, 0.01 mmol), and THF (10 mL) was cooled to 0 °C. Neopentyl magnesium bromide (1M in THF) (4.9 mL, 3 mmol) was added and the reaction stirred for approximately 17 hours before being concentrated. The resulting solution was diluted with 10 mL of DCM and cooled to 0 °C. HBF_4/H_2O (48 wt%) (5mL) was added and the reaction stirred for 3 hours before being washed with brine, dried over Na_2SO_4, filtered over celite, concentrated, and triturated with hot ether. After filtration a white, crystalline solid was collected. (286 mg, 94%). ^{1}H NMR (500 MHz, $CDCl_3$): δ 6.81 – 5.87 (d, *J*= 472.4 Hz, 1H) 2.25 (dd, *J* = 11 Hz, 3.8 Hz, 2H), 1.50 (d, *J* = 16.4 Hz, 18 H) , 0.34 (s, 9H). ^{31}P NMR (202.5 MHz,$CDCl_3$): δ 28.6 (d, *J* = 481.1 Hz).

[(*i*-Pr)$_2$HPNp]BF$_4$ (14). A flask containing diisopropylphosphine (159 μL, 1 mmol), LiBr (1.70 mg, 0.02 mmol), CuI (1.90 mg, 0.01 mmol), and THF (10 mL) was cooled to 0 °C. Neopentyl magnesium bromide (1M in THF) (4.9 mL, 3 mmol) was added and the reaction stirred for approximately 14 hours before being concentrated. The resulting solution was diluted with 10 mL of DCM and cooled to 0 °C. HBF_4/H_2O (48 wt%) (5mL) was added and the reaction stirred for 3 hours before being washed with brine, dried over Na_2SO_4, filtered over celite, concentrated, and triturated with hot ether. After filtration a white, crystalline solid was collected. (248 mg, 90%). ^{1}H NMR (500 MHz, $CDCl_3$): δ 6.69 – 5.72 ($^1J_{P\text{-}H}$ = 474.2Hz, $^3J_{P\text{-}H}$ = 4.3 Hz, dp, 1H) 2.76 (m, 2 H) 2.09 (*J* = 11.9, 4.5 Hz, dd 2H), 1.47 (*J* = 7.2 Hz, d, 3H), 1.44 (*J* = 7.2 Hz, d, 3H), 1.42 (*J* = 7.1 Hz, d, 3H), 1.39 (*J* = 7.2 Hz, d), 1.19 (s, 9H). ^{31}P{^{1}H} NMR (202.5 MHz,$CDCl_3$): δ 21.54.

[(Cy)$_2$HPNp]BF$_4$ (15). A flask containing chlorodicyclohexylphosphine (159 μL, 1 mmol), LiBr (1.70 mg, 0.02 mmol), CuI (1.90 mg, 0.01 mmol), and THF (10 mL) was cooled to 0 °C.

Neopentyl magnesium bromide (1M in THF) (4.9 mL, 3 mmol) was added and the reaction stirred for approximately 14 hours before being concentrated. The resulting solution was diluted with 10 mL of DCM and cooled to 0 °C. HBF_4/H_2O (48 wt%) (5mL) was added and the reaction stirred for 3 hours before being washed with brine, dried over Na_2SO_4, filtered over celite, concentrated, and triturated with hot ether. After filtration a white, crystalline solid was collected. (248 mg, 90%). ^{1}H NMR (500 MHz, $CDCl_3$): δ 6.51 – 5.57 (d, J_{H-P} = 470.5, 1H), 2.50 (m, 2 H) 2.09 – 1.16, m, 12H). ^{31}P NMR (202.5 MHz,$CDCl_3$): δ13.2 (J= 469.9), d, 1H).

[(Ph)$_2$HPNp]BF$_4$ (16). A flask containing chlorodiphenylphosphine (159 μL, 1 mmol), LiBr (1.70 mg, 0.02 mmol), CuI (1.90 mg, 0.01 mmol), and THF (10 mL) was cooled to 0 °C. Neopentyl magnesium bromide (1M in THF) (4.9 mL, 3 mmol) was added and the reaction stirred for approximately 14 hours before being concentrated. The resulting solution was diluted with 10 mL of DCM and cooled to 0 °C. HBF_4/H_2O (48 wt%) (5mL) was added and the reaction stirred for 3 hours before being washed with brine, dried over Na_2SO_4, filtered over celite, concentrated, and triturated with hot ether. After filtration a white, crystalline solid was collected. (248 mg, 90%). ^{1}H NMR (500 MHz, $CDCl_3$): δ 8.07 – 7.61, (m, 10H) 6.54 – 5.71 (d, 1H) 2.86 (d, 2 H), 1.15 (s, 9H). ^{31}P NMR (202.5 MHz,$CDCl_3$): δ 29.4 (d, J = 488.7).

[(t-Bu)$_2$HPCH$_2$Si(CH$_3$)$_3$]BF$_4$ (17). A flask containing chlorodi-(tertbutyl)phosphine (190 μL, 1 mmol), LiBr (1.70 mg, 0.02 mmol), CuI (1.90 mg, 0.01 mmol), and THF (10 mL) was cooled to 0 °C. Trimethylsilylmethyl lithium (4.9 mL, 3 mmol) was added and the reaction stirred for approximately 15 hours before being concentrated. The resulting solution was diluted with 10 mL of DCM and cooled to 0 °C. HBF_4/H_2O (48 wt%) (5mL) was added and the reaction stirred for 3 hours before being washed with brine, dried over Na_2SO_4, filtered over celite, concentrated, and triturated with hot ether. After filtration a white, crystalline solid was collected. (286 mg,

94%). ^{1}H NMR (500 MHz, $CDCl_3$): δ 6.50 – 5.56 (dt, 1H) 1.50 (d, 18 H) 2.25 (dd, 2H), 0.34 (s, 9H). ^{31}P NMR (202.5 MHz,$CDCl_3$): δ 37.8 (dm).

Preparation of Palladacycles (7, 18, 19):

Phosphonium tetrafluoroborate salts (**13 - 15**) (1 equiv) were dissolved in THF. Sodium *tert*-butoxide (1.2 equiv) was added and the reaction stirred for at least 2 hours. The resulting solution was transferred using a canula to a stirring solution of $Pd(OAc)_2$ in THF. After a period of at least 4 hours the reaction was concentrated and washed with cold pentane to yield a powdered product.

[Pd(*μ*-*κ*^{2}-*O,O*-OAc)(*κ*^{2}-C,P-(*t*-Bu)$_2$PCH$_2$C(Me)$_2$CH$_2$)]$_2$ (7). General procedure for preparing the palladacycles was followed using **13.** ^{1}H NMR (500 MHz, $CDCl_3$): δ 2.33 (br, s, 4H), 1.98 (br, s, 6H), 1.79 m, 4H), 1.40 (*J* = Hz, d, 36H), 1.21, (s, 12H). ^{31}P{^{1}H} NMR (202.5 MHz,$CDCl_3$): δ 93.01.

[Pd(*μ*-*κ*^{2}-*O,O*-OAc)(*κ*^{2}-C,P-(*i*Pr)$_2$PCH$_2$C(Me)$_2$CH$_2$)]$_2$ (18). General procedure for preparing the palladacycles was followed **14.** ^{1}H NMR (500 MHz, $CDCl_3$, 313 K): δ 2.71-2.52 (m, 2H), 2.19 (br s, 2H) 1.85 (br s, 2H), 1.74 (br s, 3H), 1.41 (br s, 6H). 1.32 - 1.21 (m, 12H). ^{13}C NMR (125 MHz, C_6D_6, 295 K) mixture of isomers: δ 181.63, 181.09, 45.77, 45.10, 42.94, 42.84, 42.77, 42.56, 37.75, 37.51, 36.92, 31.81.31.66, 31.61, 31.13, 27.70, 27.20, 25.63, 25.13, 24.93, 23.68, 23.41, 23.20, 19.22, 18.50, 18.19, 17.76, 16.08, 15.79. ^{31}P{^{1}H} NMR (202.5 MHz,$CDCl_3$): δ 72.15 (br s), 71.74 (br s), cis/trans isomers.

[Pd(*μ*-*κ*^{2}-*O,O*-OAc)(*κ*^{2}-C,P-(Cy)$_2$PCH$_2$C(Me)$_2$CH$_2$)]$_2$ (19). General procedure for preparing the palladacycles was followed using **15.** ^{1}H NMR (500 MHz, $CDCl_3$): δ 2.67 (br s, 2H), 2.41-2.13 (m, 6H), 2.02-1.86 (m, 18 H), 1.76-1.16 (m, 44H). ^{13}C NMR (125 MHz, C_6D_6, 295 K) mixture of isomers: δ 181.0, 180.26, 180.14, 44.79, 43.47, 42.11, 42.03, 36.15, 35.92, 33.27, 31.57, 30.50,

29.81, 28.68, 27.80, 27.16, 26.83, 26.01, 25.06, 24.95, 22.65, 22.59, 22.43. $^{31}P\{^{1}H\}$ NMR (202.5 MHz,$CDCl_3$): δ 71.48 (br s), 66.35 (br s), 64.95 (s), mixture of isomers.

General Procedure A- the Coupling of Arylacetylenes with Propargyl Alcohol (20-23):

To a 2 dram borosilicate glass vial was added **7**, **18**, or **19** (0.02mmol; 2 mol %) and a stir bar. The vial was fitted with a septum screw cap and pump-filled with nitrogen three times. Then to the vial was added MeCN (2 mL), arylacetylene (1 mmol, 1 equiv), followed by propargyl alcohol (0.29 mL; 5 mmol; 5 equiv). The reaction mixture was then stirred at 24 °C for 24 h, concentrated under reduced pressure, and subjected directly to flash chromatography on silica gel.

(*E*)-5-Phenylpent-2-en-4-yn-1-ol (20-a) and 2-methylene-4-phenylbut-3-yn-1-ol (20-b): General procedure A was followed using 110 μL of phenylacetylene. A mixture of isomeric cross-coupled products **20-a** and **20-b** were isolated using 10% EtOAc in hexane. **(20-a):** ^{1}H NMR (500 MHz, $CDCl_3$): δ 7.47-7.14 (m, 5H), 6.36-6.30 (dt, *J*= 15.9, 5.2 Hz, 1H), 5.98-5.94 (dt, *J*= 15.9, 1.8 Hz, 1H), 4.23 (s, 2H), 2.54 (br s, 1H). **(20-b):** ^{1}H NMR (500 MHz, $CDCl_3$): δ 7.47-7.14 (m, 5H), 5.61-5.57 (dq, *J*= 15.9, 1.6 Hz, 2H), 4.22 (s, 2H), 2.54 (br s, 1H).

4-(3-Fluorophenyl)-2-methylenebut-3-yn-1-ol (21-b): General procedure A was followed using 115 μL of 1-ethynyl-3-fluorobenzene. Major product **21-b** was isolated using 10-15% EtOAc in hexane. ^{1}H NMR (500 MHz, $CDCl_3$): δ 7.33-6.99 (m, 4H), 5.64-5.60 (dq, *J*= 13.4, 1.5 Hz, 2H), 4.27 (s, 2H), 1.81-1.66 (br s, 1H).

4-(4-Methoxyphenyl)-2-methylenebut-3-yn-1-ol (22-b): General procedure A was followed using 130 μL of 1-ethynyl-4-methoxybenzene. Major product **22-b** was isolated using 30% EtOAc in hexane. ^{1}H NMR (500 MHz, $CDCl_3$): δ 7.40-7.38 (d, *J*= 8.7 Hz, 2H), 6.85-6.83 (d, *J*= 8.7 Hz, 2H), 5.56-5.53 (d, *J*= 13.0 Hz, 2H), 4.22 (s, 2H), 3.81 (s, 3H), 2.00 (s, 1H).

2-Methylene-4-(thiophen-3-yl)but-3-yn-1-ol (23-b): General procedure A was followed using 100 μL of 3-ethynylthiophene. Major product **23-b** was isolated using 25% EtOAc in hexane. ^{1}H NMR (500 MHz, $CDCl_3$): δ 7.47 (d, *J*= 3.0 Hz, 1H), 7.28-7.26 (m, 1H). 7.13-7.12 (d, *J*= 5.0 Hz, 1H), 5.59-5.56 (d, *J*= 14.7 Hz, 2H). 4.23 (s, 2H), 1.62 (s, 1H).

***N*-Propargylphthalimide** (starting material for **24 - 27**): Phthalimide (2.94 g; 20 mmol, 1 equiv), potassium carbonate (6.90 g; 50 mmol; 2.5equiv), acetone (60 mL), and propargyl bromide (80 wt% in toluene, 3.4 mL; 38 mmol; 1.9 equiv) were combined into a Schlenk flask and placed under N_2. The solution was heated to reflux for 24 h. The mixture was allowed to cool to room temperature, water (60 mL) was added, and the mixture was concentrated under reduced pressure to remove the bulk of the acetone. The mixture was then extracted with EtOAc (3 X 50 mL); the combined organic layers were dried over Na2SO4, filtered, and concentrated. The resulting yellow solid was triturated with hexanes to give an off-white solid (3.22 g, 87%). ^{1}H NMR (500 MHz, $CDCl_3$): δ 7.90-7.88 (m, 2H), 7.75-7.74 (m, 2H), 4.47-4.46 (d, *J*= 2.4 Hz, 2H), 2.23-2.22 (t, *J*= 2.5 Hz, 1H).

General Procedure B - The Coupling of Arylacetylenes with *N*-Propargyl Phthalimide:

To a 2 dram borosilicate glass vial was added **7**, **18**, **19** (0.02 mmol; 2 mol %), *N*-propargyl phthalimide (2.5 mmol; 2.5 equiv) and a stir bar. The vial was fitted with a septa screw cap and filled with nitrogen. Then to the vial was added MeCN (2 mL) and arylacetylene (1mmol, 1 equiv). The reaction mixture was then stirred at 60 °C for 24 h, concentrated under reduced pressure, and subjected directly to flash chromatography on silica gel.

(*E*)-2-(5-Phenylpent-2-en-4-yn-1-yl)isoindoline-1,3-dione (24-a) and 2-(2-methylene-4-phenylbut-3-yn-1-yl)isoindoline-1,3-dione (24-b): General procedure B was followed using 110 μL of phenylacetylene. A mixture of isomeric cross-coupled products **24-a** and **24-b** were

isolated using 15% EtOAc in hexane. **(24-a):** ^{1}H NMR (500 MHz, $CDCl_3$): δ 7.88-7.26 (m, 9H), 6.28-6.20 (dt, *J*= 15.8, 6.0 Hz, 1H), 5.99-5.94 (dt, *J*= 15.8 Hz, 1H), 4.40-4.37 (dd, *J*= 6.3, 1.4 Hz, 2H). **(24-b):** ^{1}H NMR (500 MHz, $CDCl_3$): δ 7.88-7.26 (m, 9H), 5.59-5.50 (d, *J*= 32.5 Hz, 2H), 4.48 (s, 2H).

(*E*)-2-(5-(3-Fluorophenyl)pent-2-en-4-yn-1-yl)isoindoline-1,3-dione (25-a) and 2-(4-(3-fluorophenyl)-2-methylenebut-3-yn-1-yl)isoindoline-1,3-dione (25-b): General procedure B was followed using 115 μL of 3-ethynylfluorobenzene. A mixture of isomeric cross-coupled products **25-a** and **25-b** were isolated using 20% EtOAc in hexane. **(25-a):** ^{1}H NMR (500 MHz, $CDCl_3$): δ 7.90-7.86 (m, 2H), 7.75-7.73 (m, 2H), 7.27-6.98 (m, 4H), 6.29-6.23 (dt, *J*= 15.9, 6.2 Hz, 1H), 5.96-5.93 (dt, *J*= 15.9 Hz, 1H), 4.39-4.38 (d, *J*= 6.3 Hz, 2H). **(25-b):** ^{1}H NMR (500 MHz, $CDCl_3$): δ 7.90-7.86 (m, 2H), 7.75-7.73 (m, 2H), 7.27-6.98 (m, 4H), 5.61-5.55 (d, *J*= 33.9 Hz, 2H), 4.48 (s, 2H).

2-(4-(4-Methoxyphenyl)-2-methylenebut-3-yn-1-yl)isoindoline-1,3-dione (26-b): General procedure B was followed using 130 μL of 4-ethynylmethoxybenzene. Product **26-b** was isolated using 10% EtOAc in hexane. ^{1}H NMR (500 MHz, $CDCl_3$): δ 7.89-7.88 (m, 2H), 7.74-7.72 (m, 2H), 7.28-7.26 (d, 2H), 6.80-6.78 (d, *J*= 8.7 Hz, 2H), 5.54-5.45 (d, *J*= 44.2 Hz, 2H), 4.47 (s, 2H), 3.79 (s, 3H).

27-a and 27-b: General procedure B was followed using 100 μL of 3-ethynylthiophene. Products were not isolated.

3.5 Appendix – Chapter 3

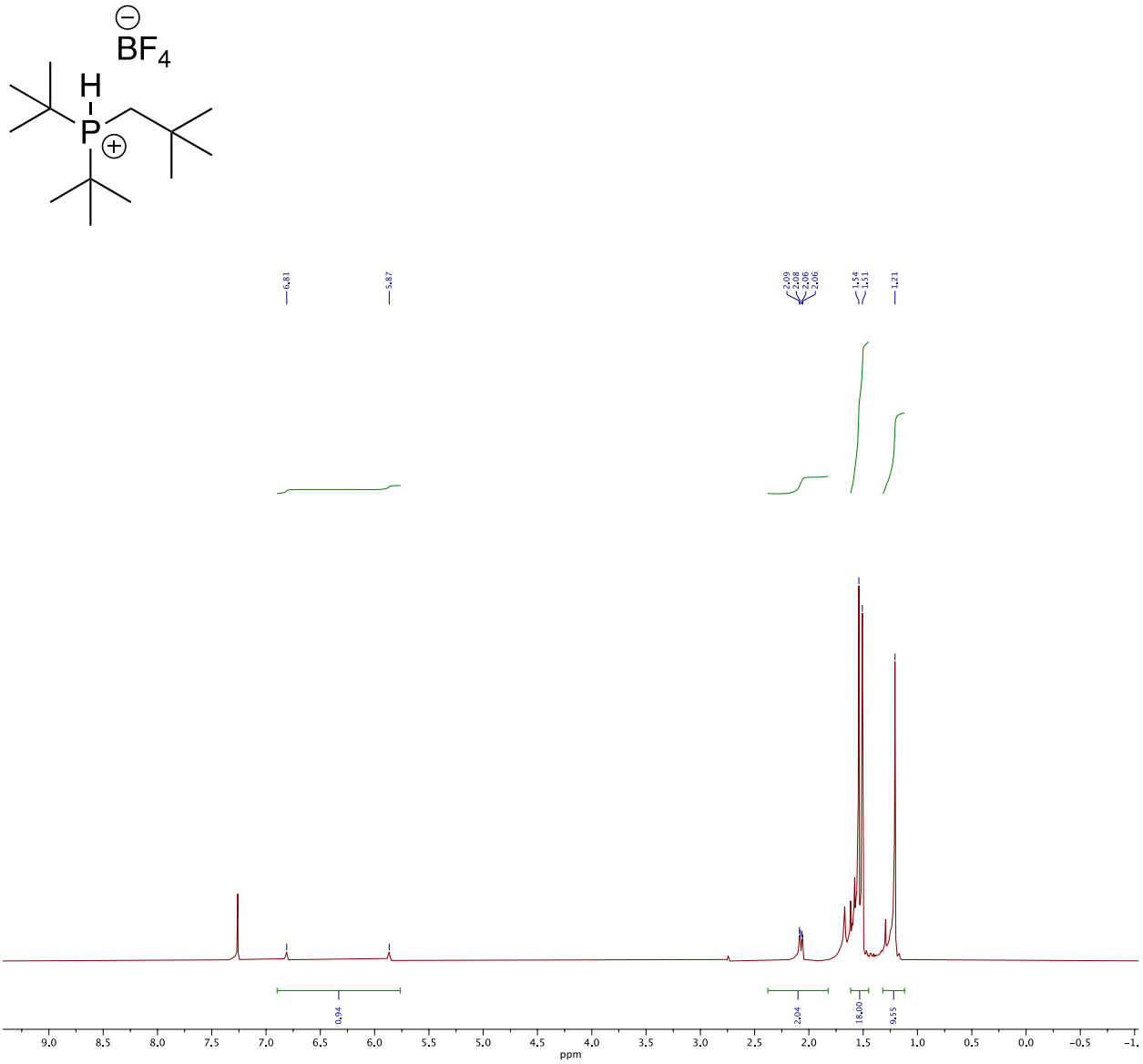

Figure A16: ^{1}H NMR (500 MHz, $CDCl_3$) spectrum of **13**.

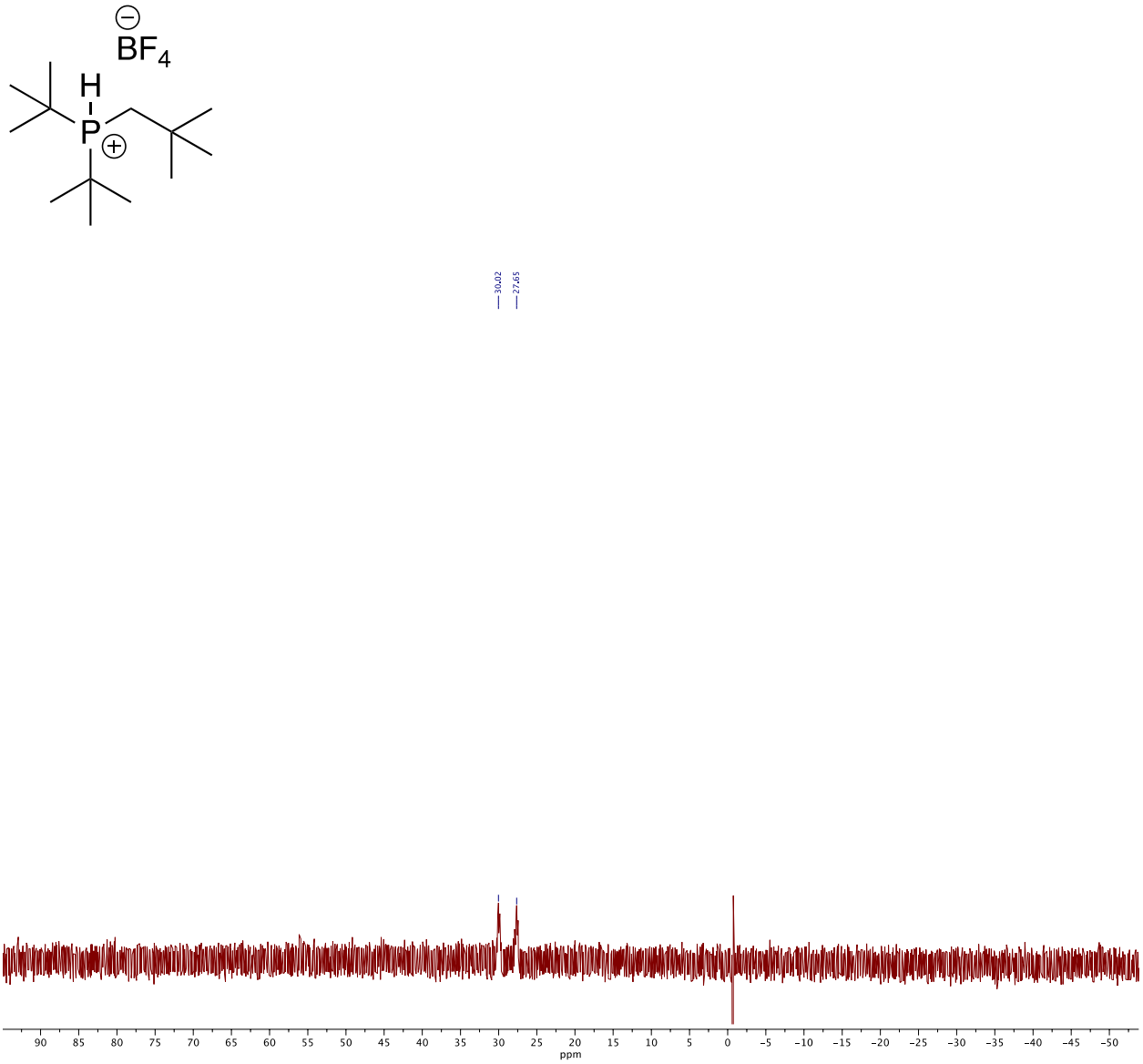

Figure A17: ^{31}P NMR (202.5 MHz,$CDCl_3$) spectrum of **13.**

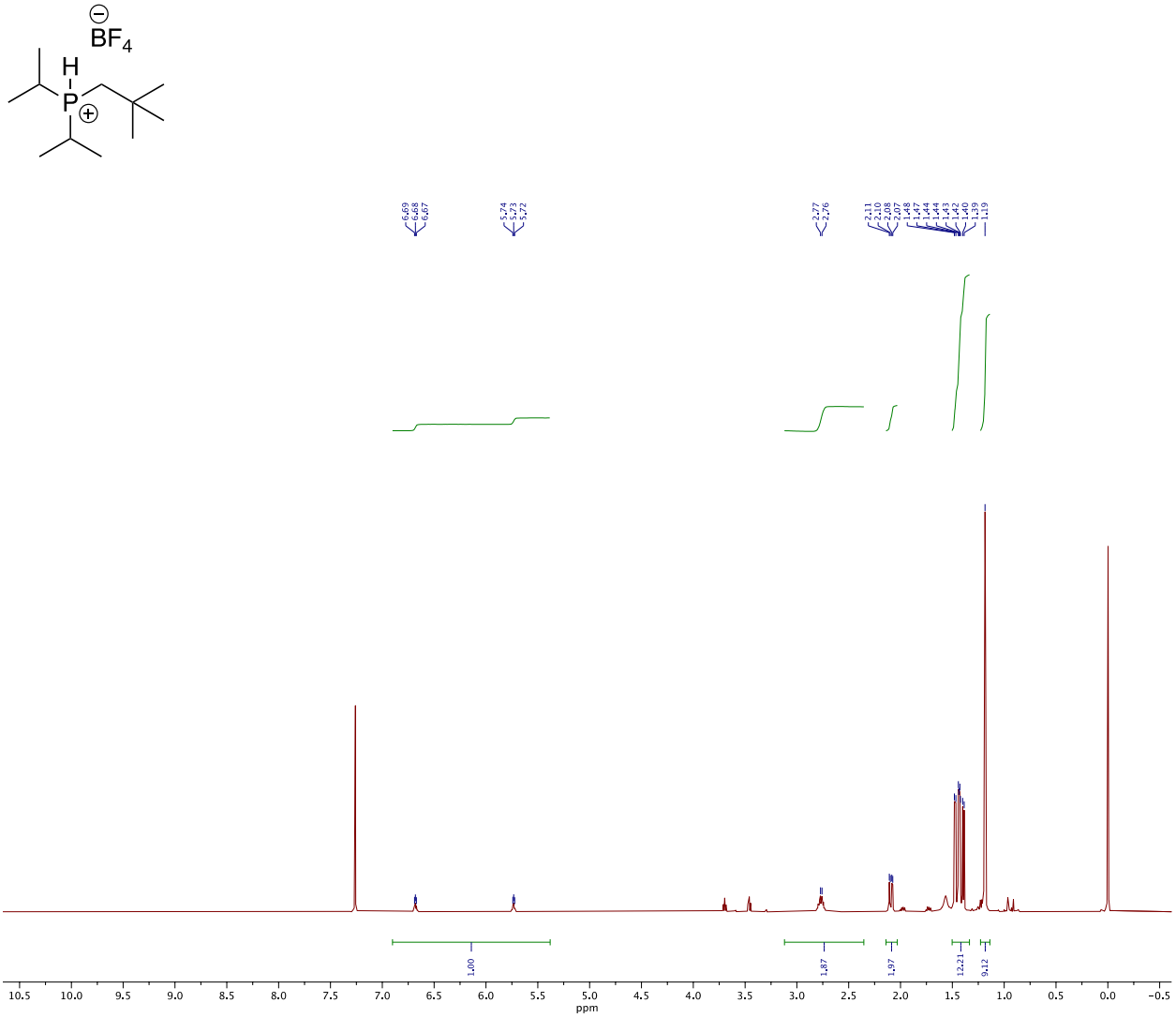

Figure A18: ^{1}H NMR (500 MHz, $CDCl_3$) spectrum of **14**.

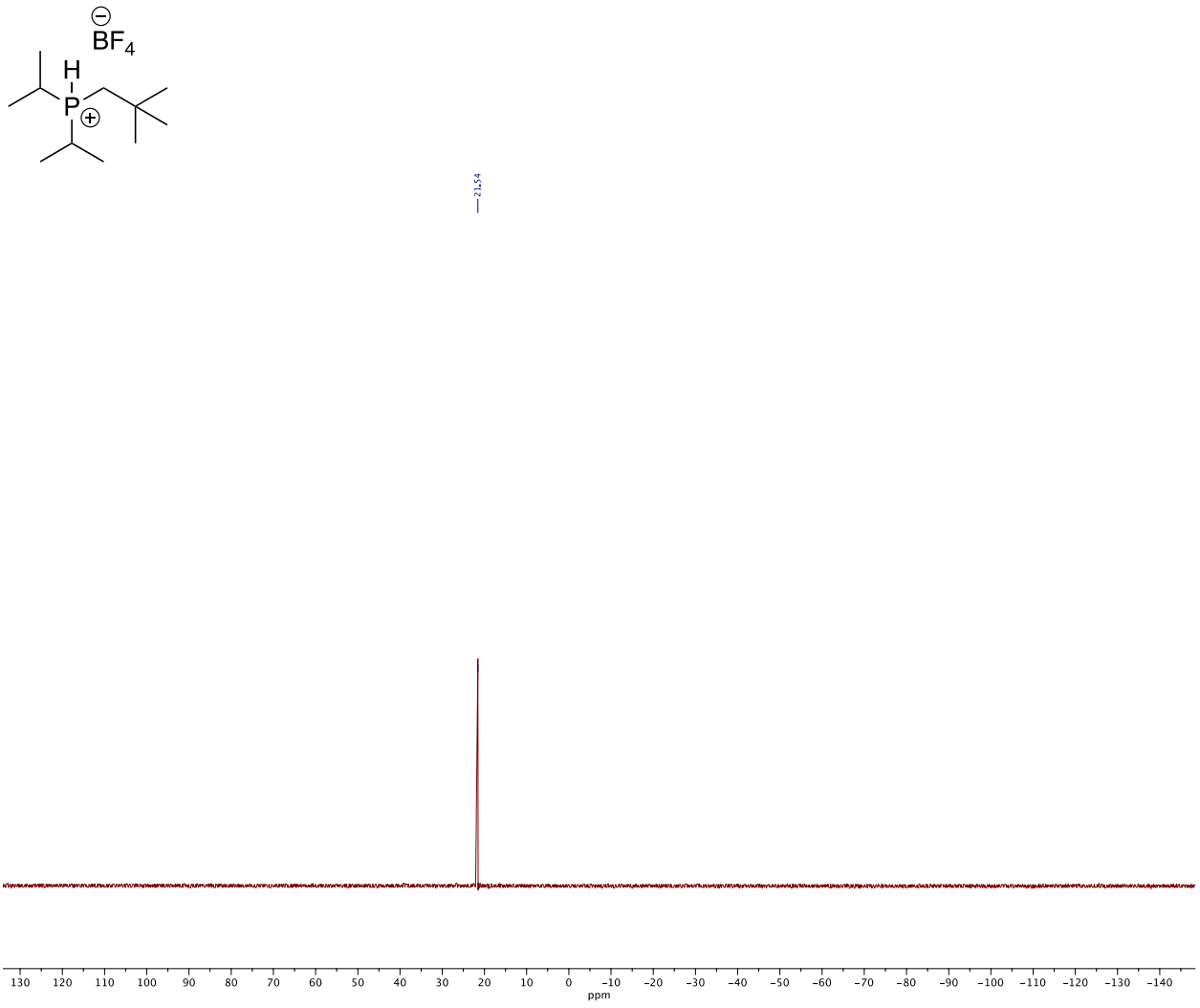

Figure A19: ^{31}P {H} NMR (202.5 MHz,$CDCl_3$) spectrum of **14.**

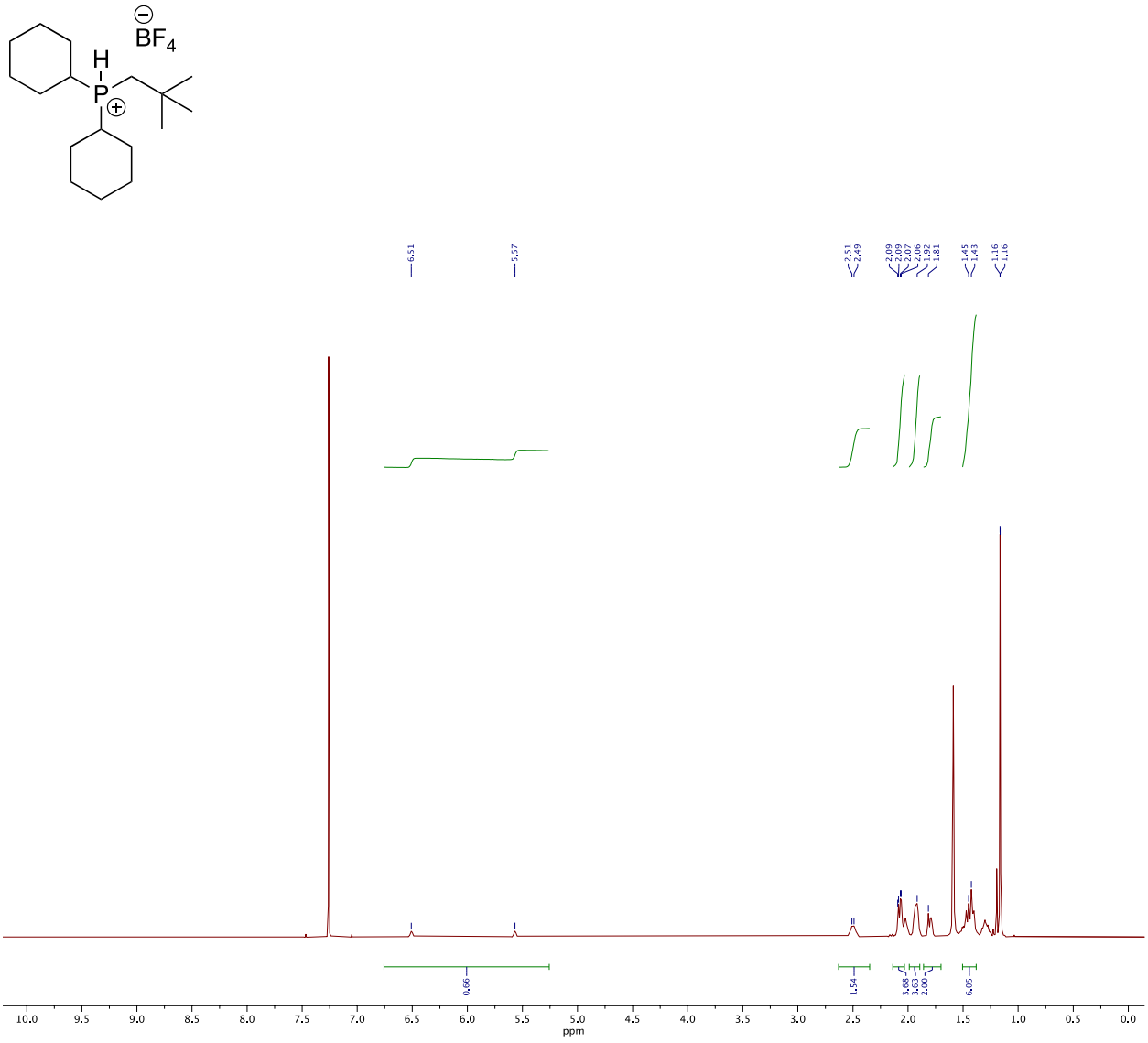

Figure A20: ^{1}H NMR (500 MHz, $CDCl_3$) spectrum of **15**.

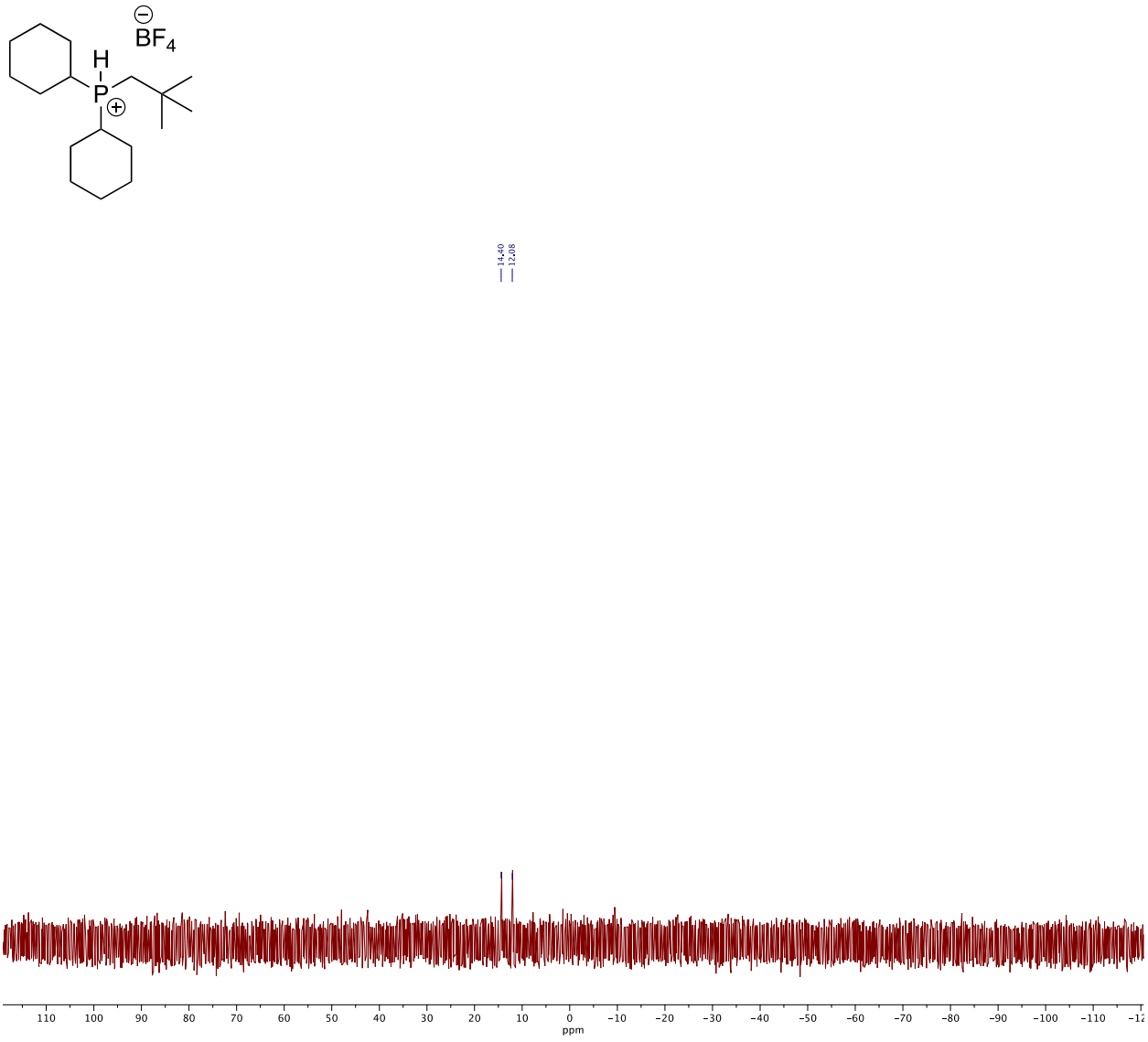

Figure A21: ^{31}P NMR (202.5 MHz,$CDCl_3$) spectrum of **15.**

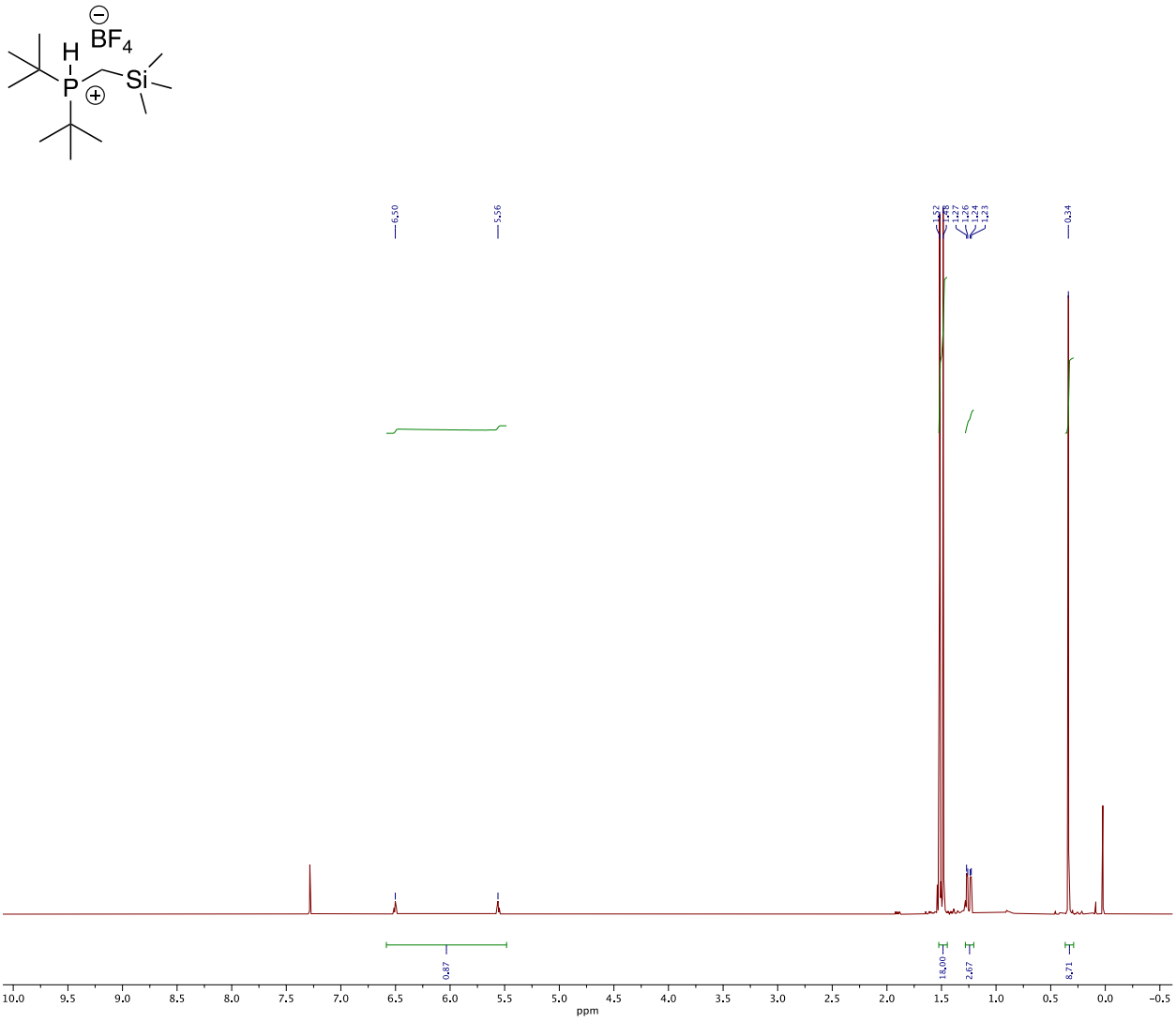

Figure A22: ^{1}H NMR (500 MHz, $CDCl_3$) spectrum of **17**.

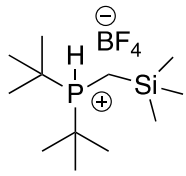

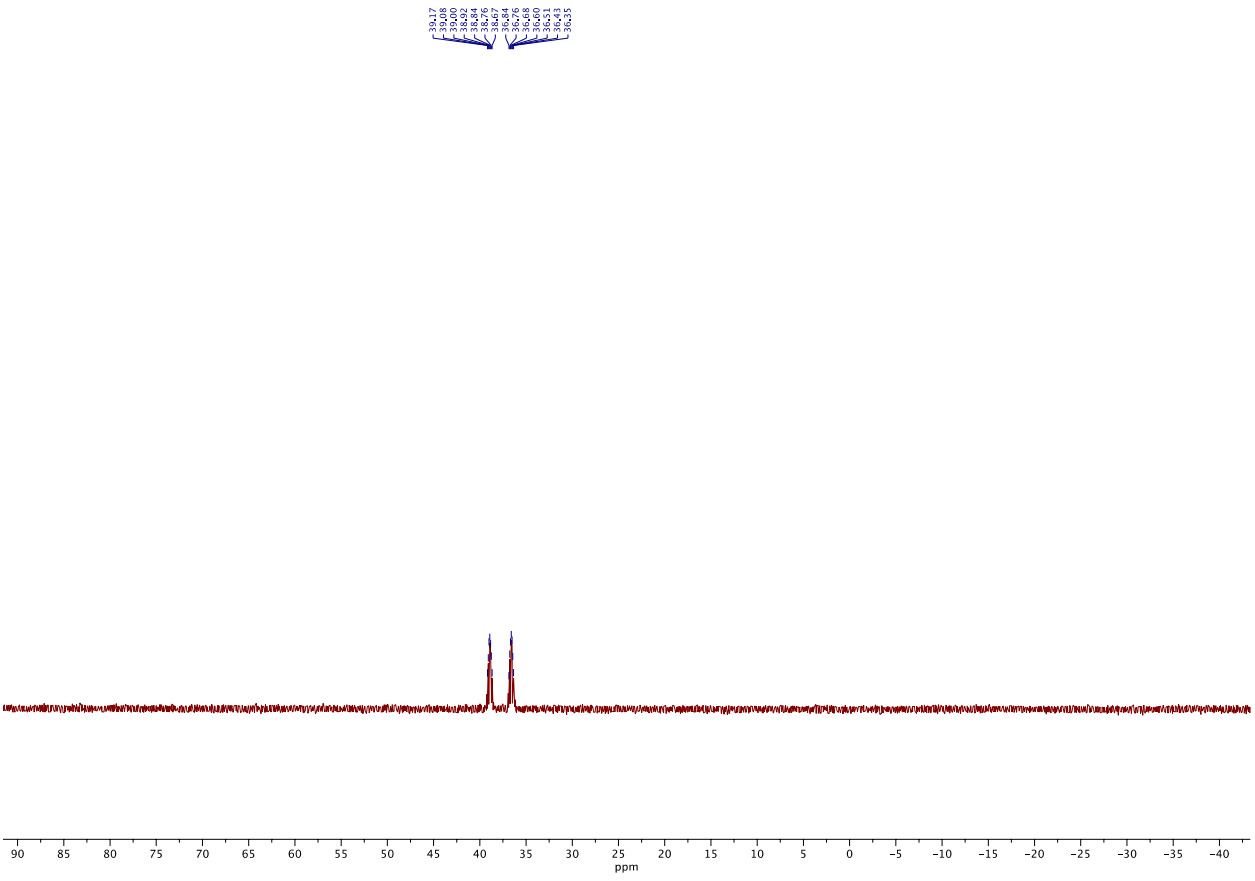

Figure A23: ^{31}P NMR (202.5 MHz,$CDCl_3$) spectrum of **17.**

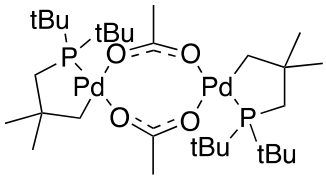

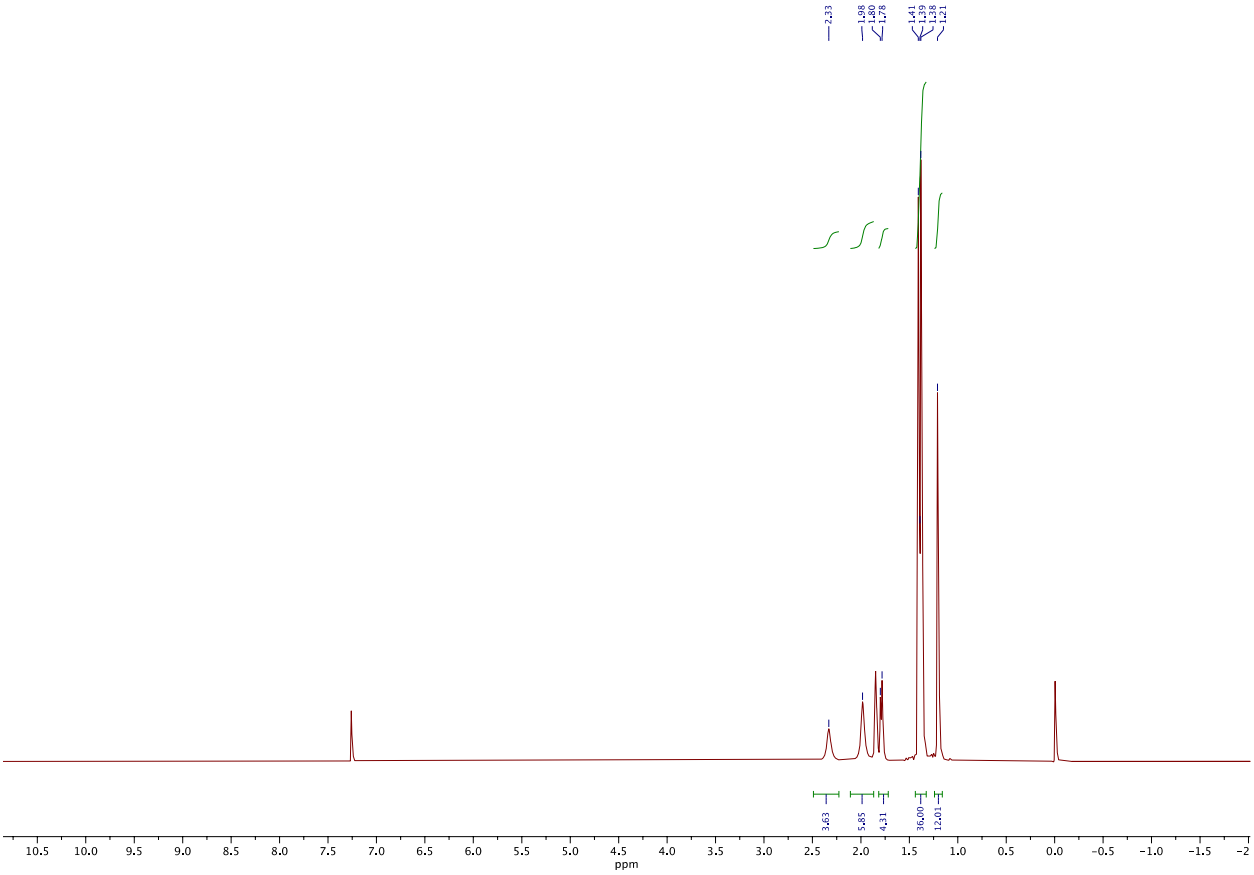

Figure A24: ^{1}H NMR (500 MHz, $CDCl_3$) spectrum of **7**.

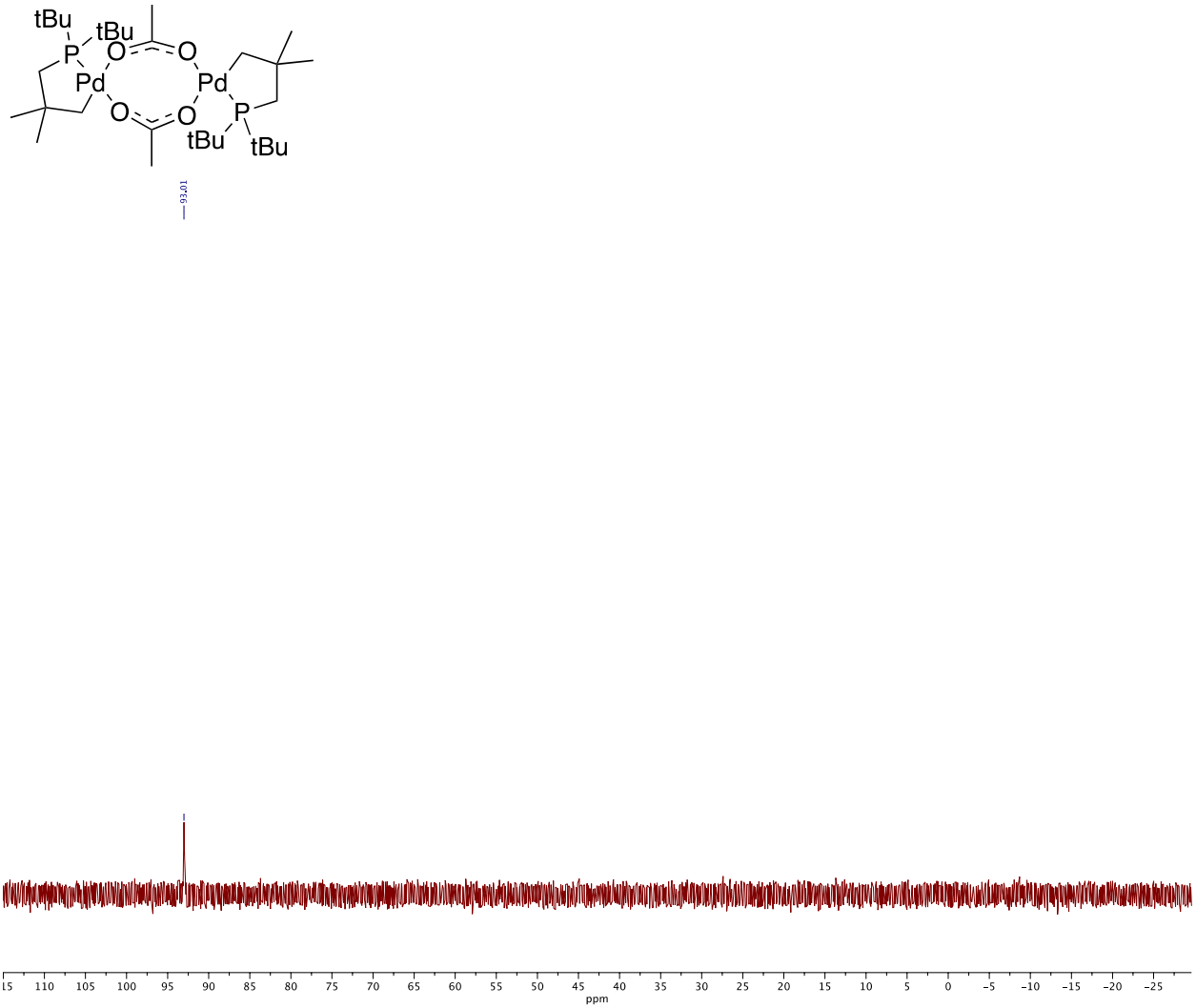

Figure A25: $^{1}P\{H\}$ NMR (202.5 MHz,$CDCl_3$) spectrum of **7.**

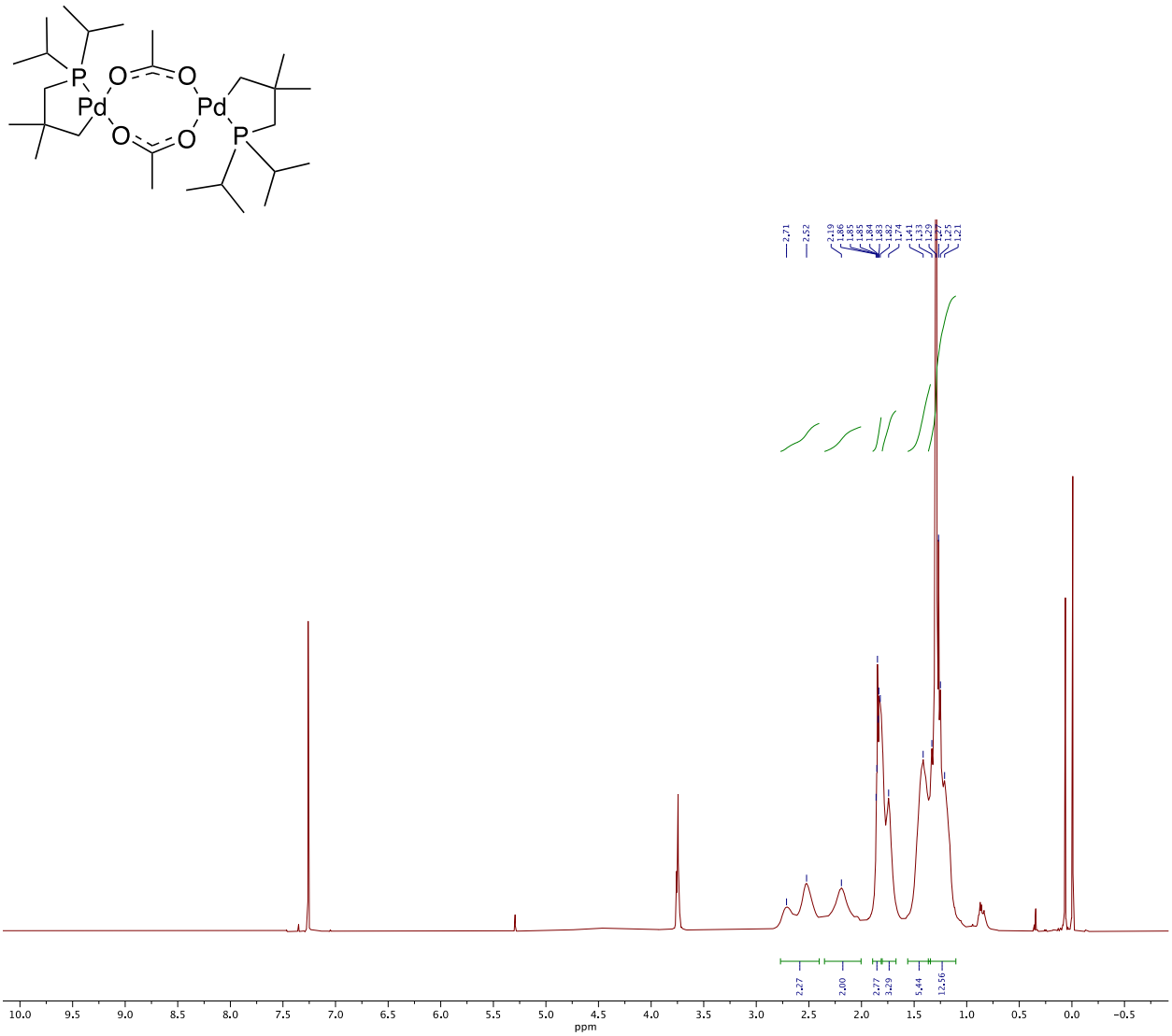

Figure A26: ^{1}H NMR (500 MHz, $CDCl_3$, 313 K) spectrum of **18.**

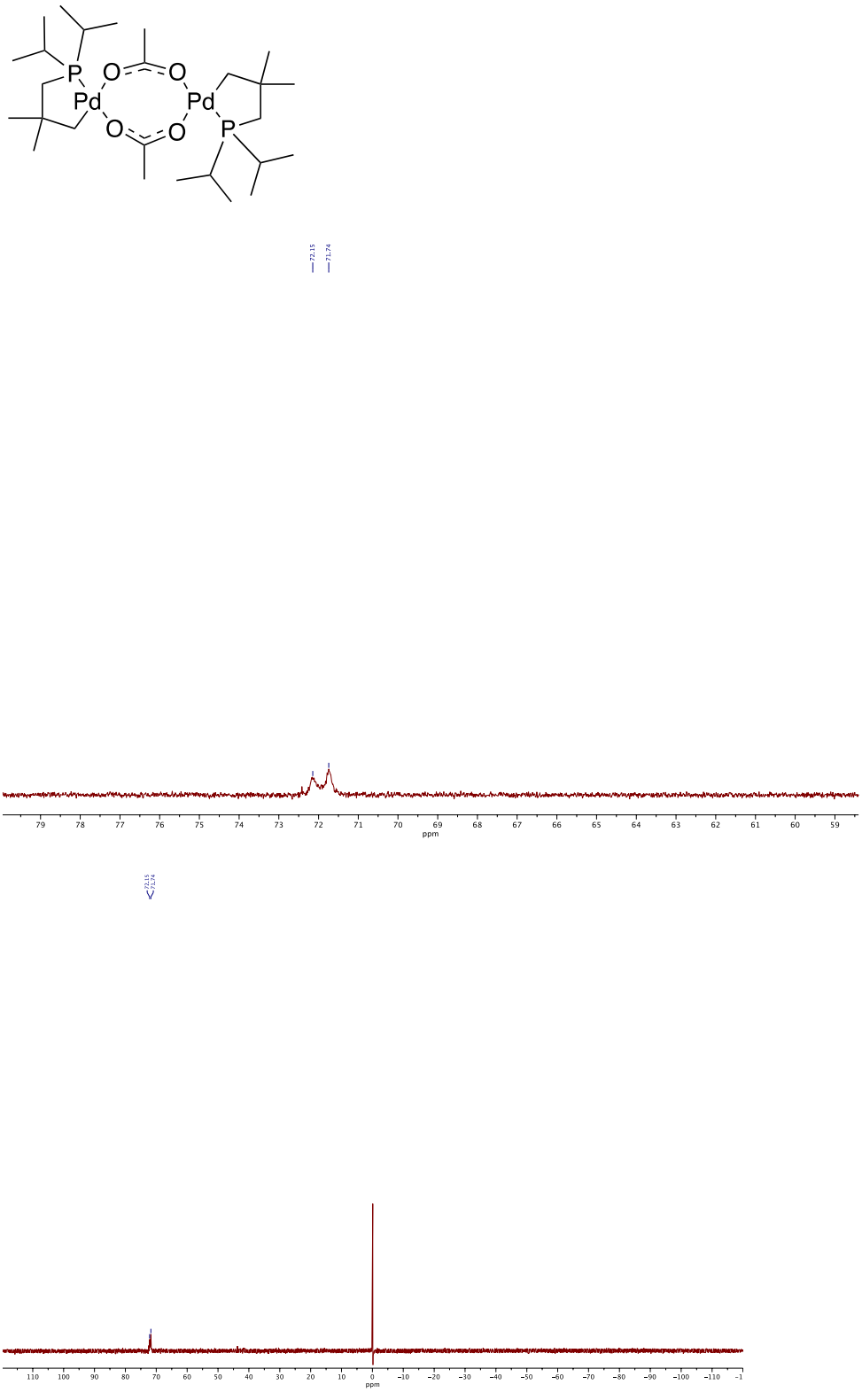

Figure A27: $^{1}P\{H\}$ NMR (202.5 MHz,$CDCl_3$) spectrum of **18** full (bottom) zoomed in (top).

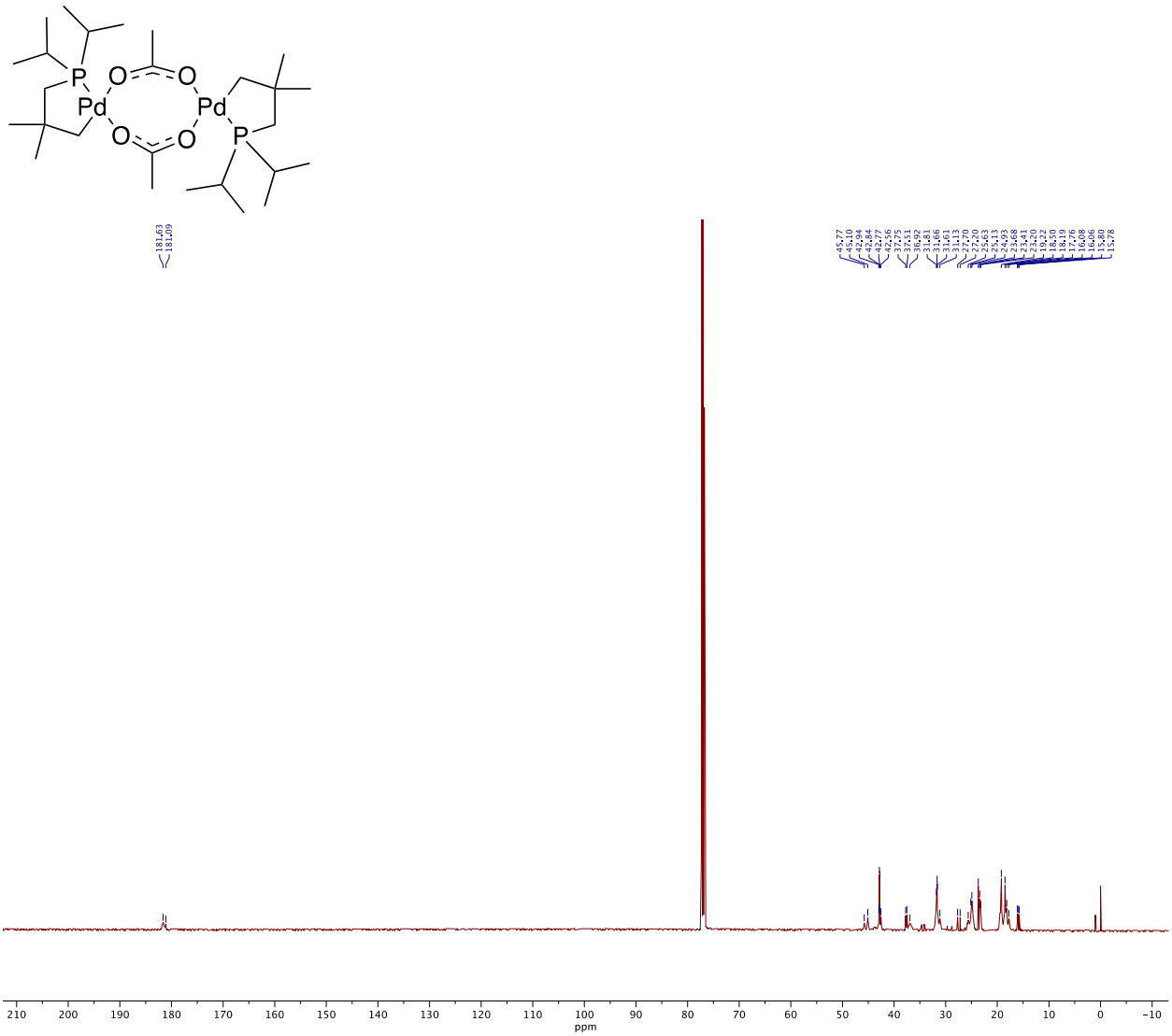

Figure A28: ^{13}C NMR (125 MHz, $CDCl_3$) spectrum of **18.**

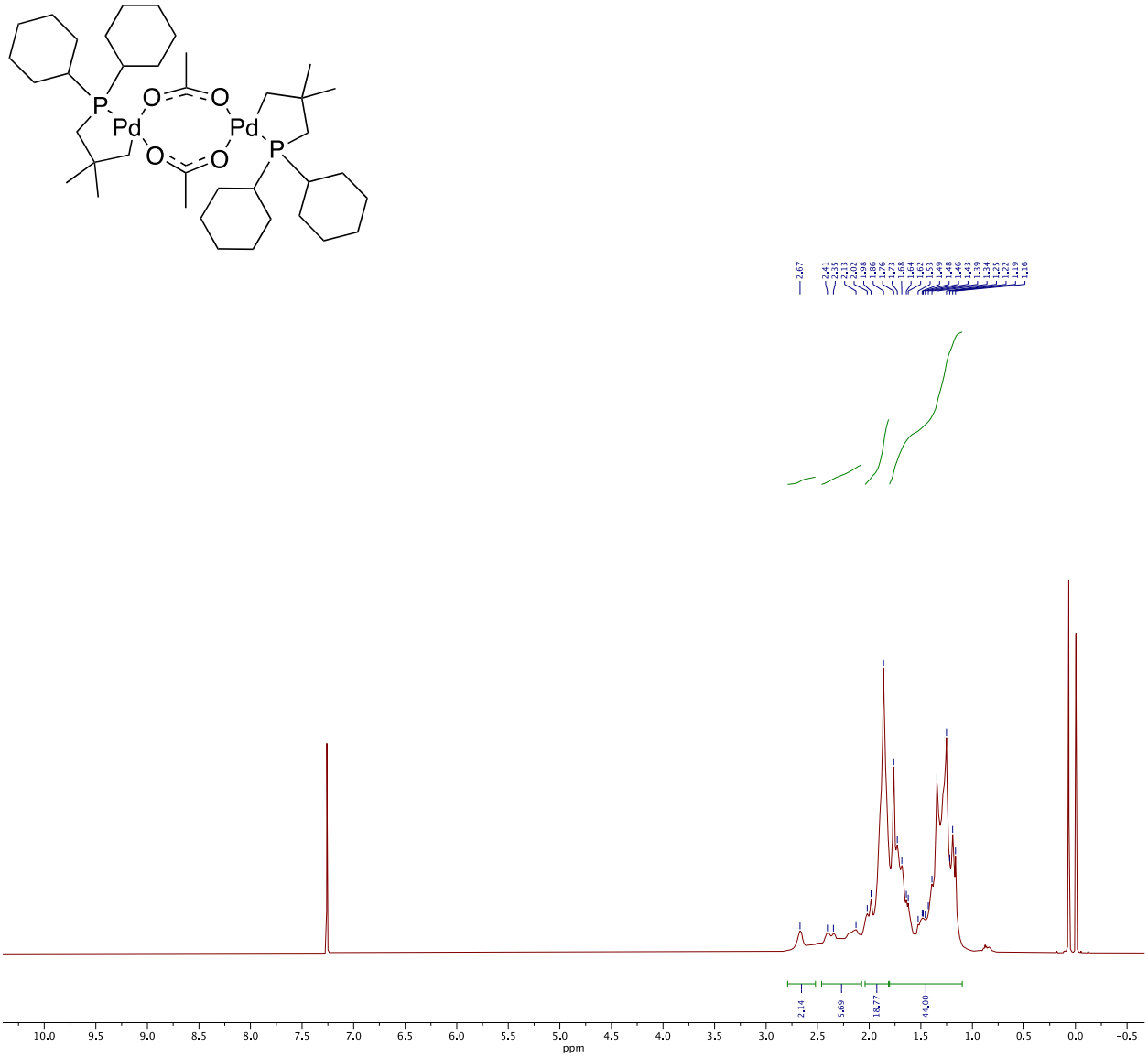

Figure A29: ^{1}H NMR (500 MHz, $CDCl_3$) spectrum of **19.**

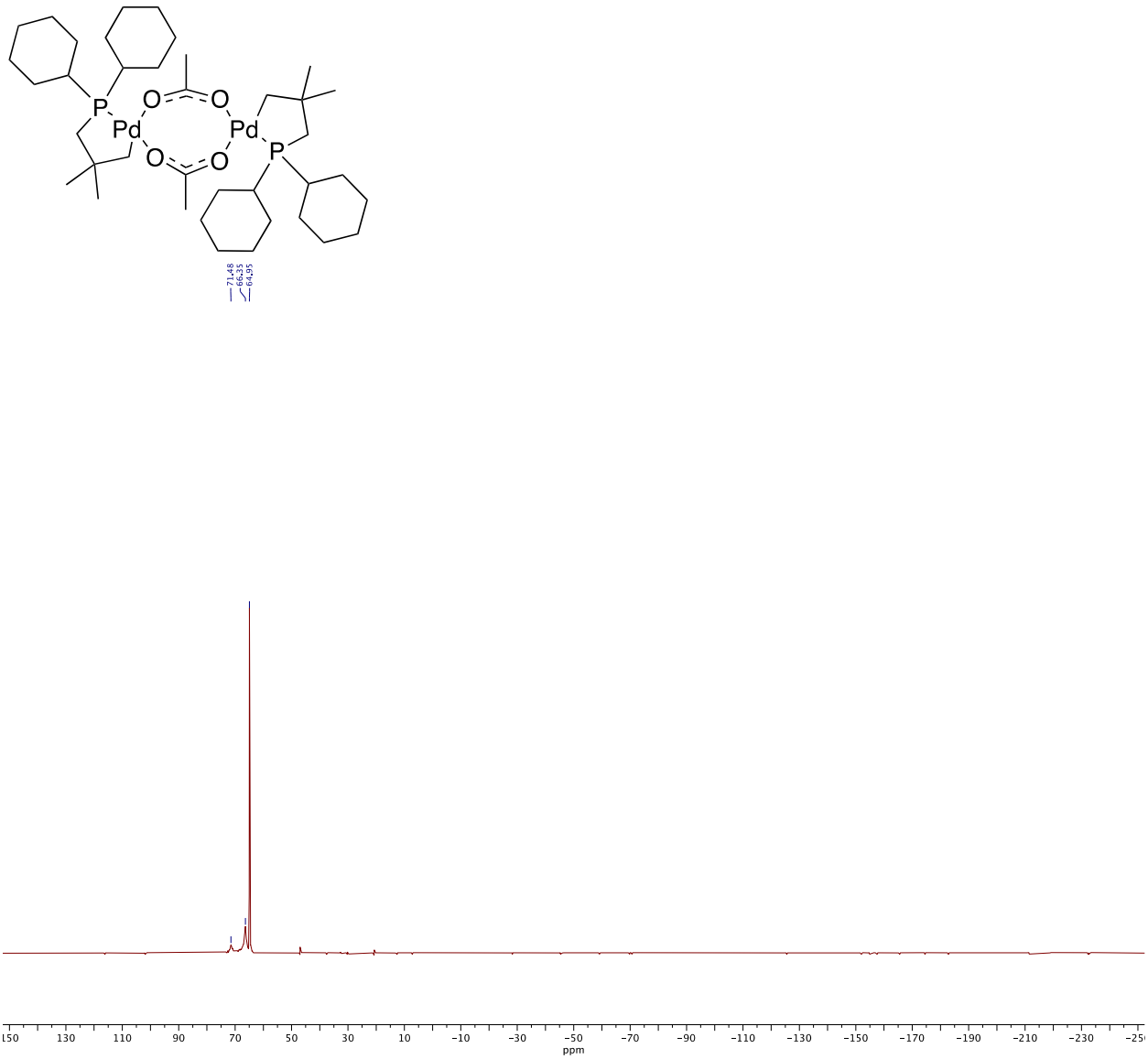

Figure A30: $^{1}P\{H\}$ NMR (202.5 MHz,$CDCl_3$) spectrum of **19.**

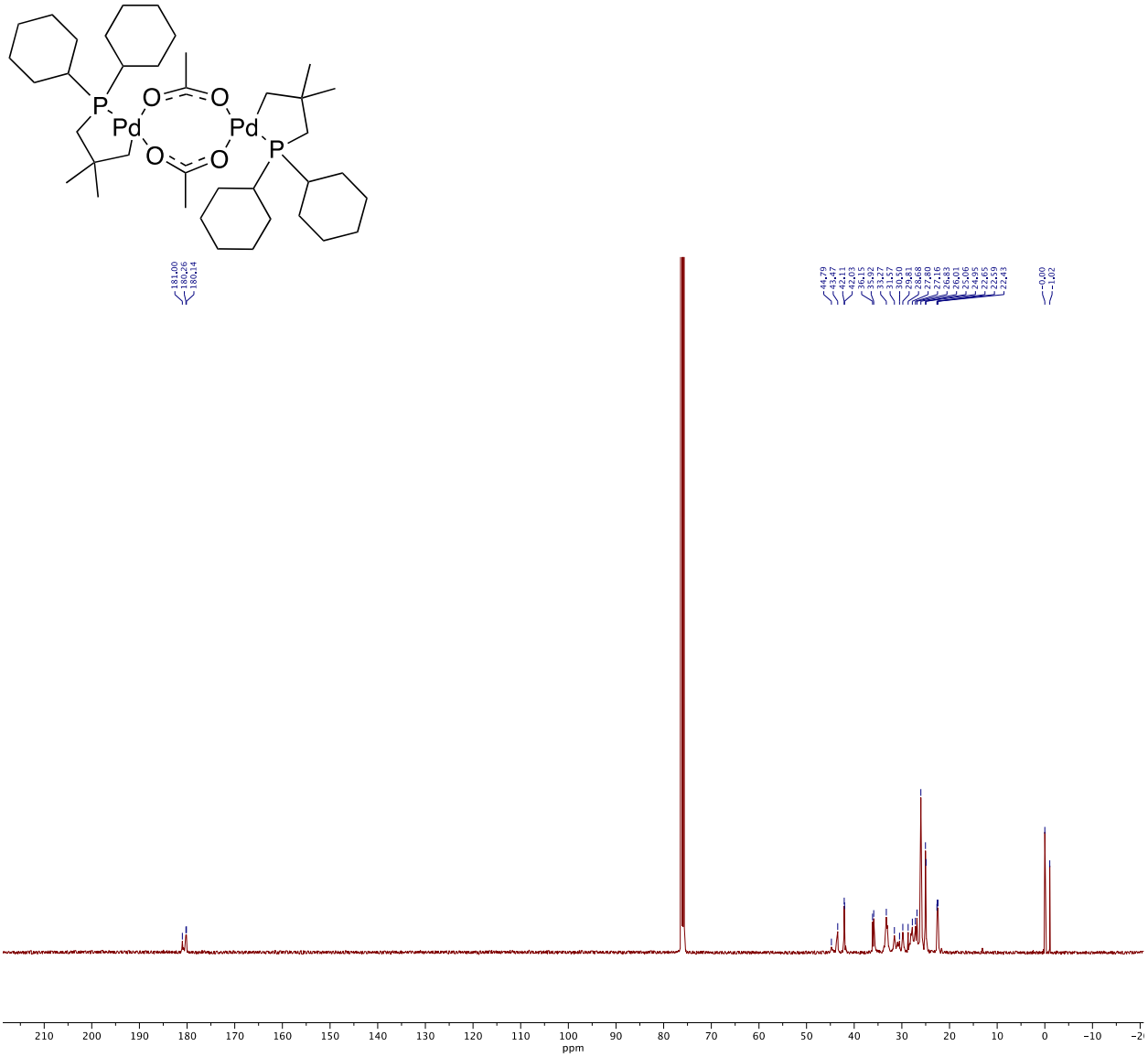

Figure A31: ^{13}C NMR (125 MHz, $CDCl_3$) spectrum of **19.**

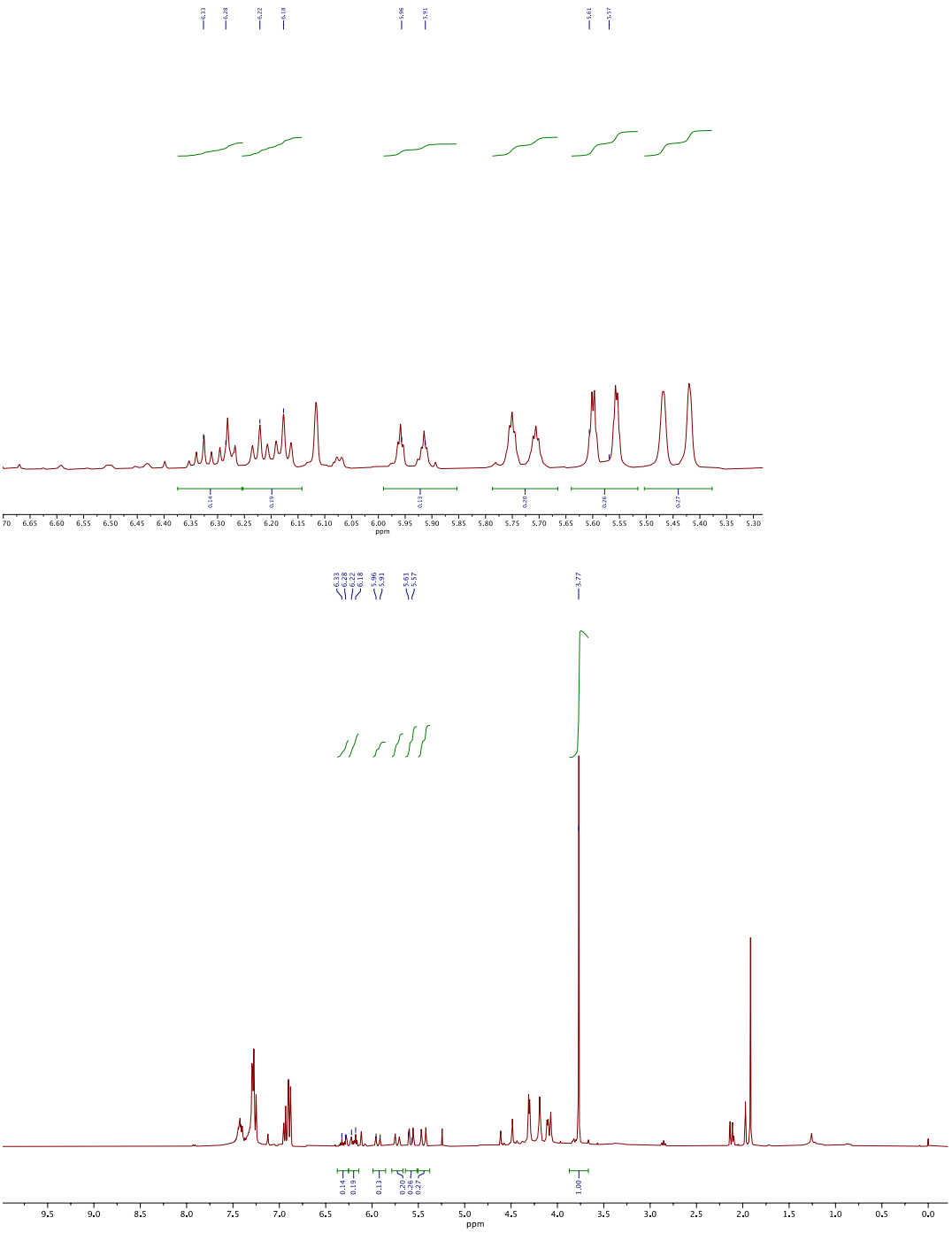

Figure A32: ^{1}H NMR (500 MHz, $CDCl_3$) spectrum of the crude reaction mixture of phenylacetylene with propargyl alcohol catalyzed by **18**.

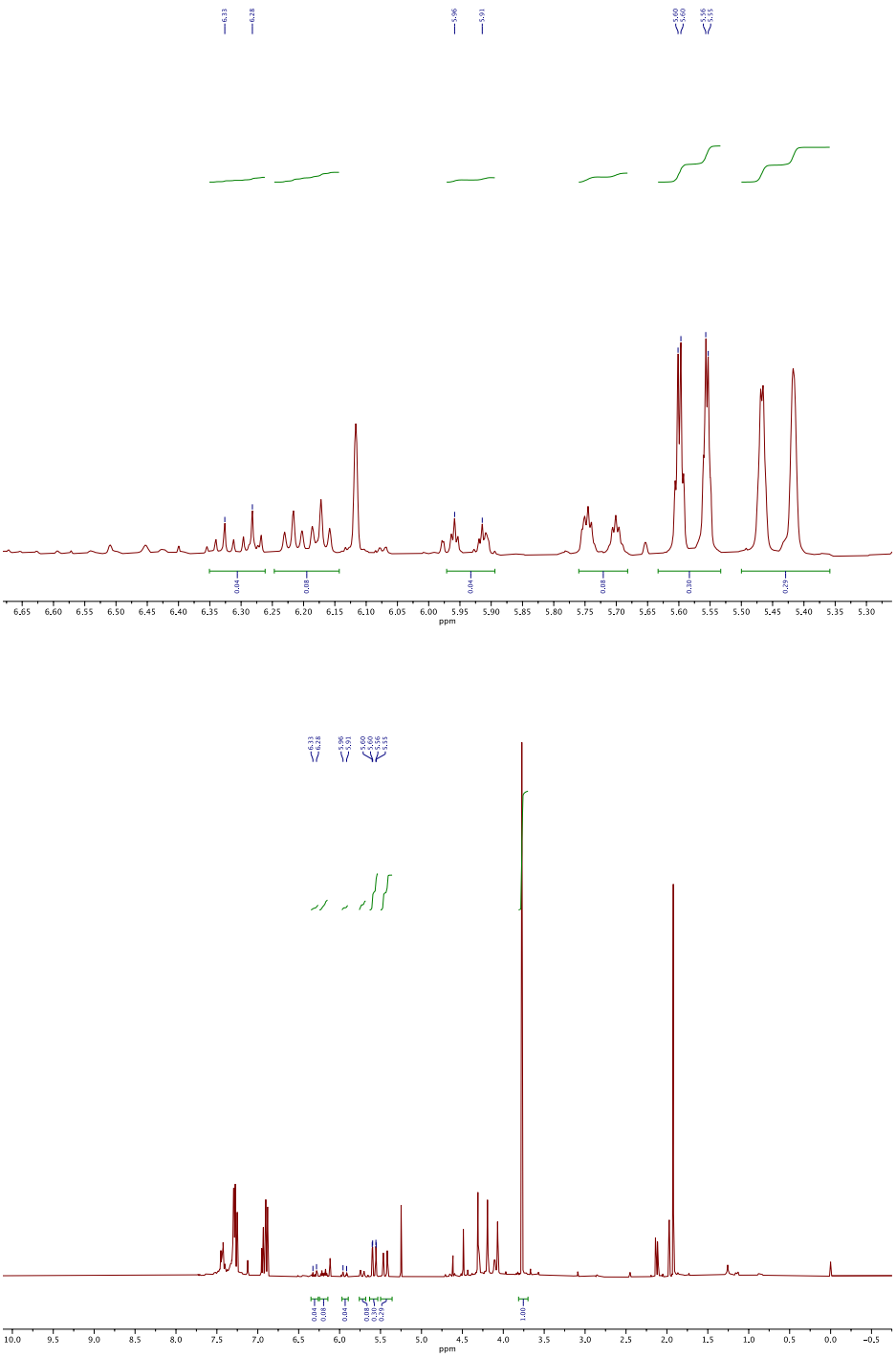

Figure A33: ^{1}H NMR (500 MHz, $CDCl_3$) spectrum of the crude reaction mixture of phenylacetylene with propargyl alcohol catalyzed by **19**.

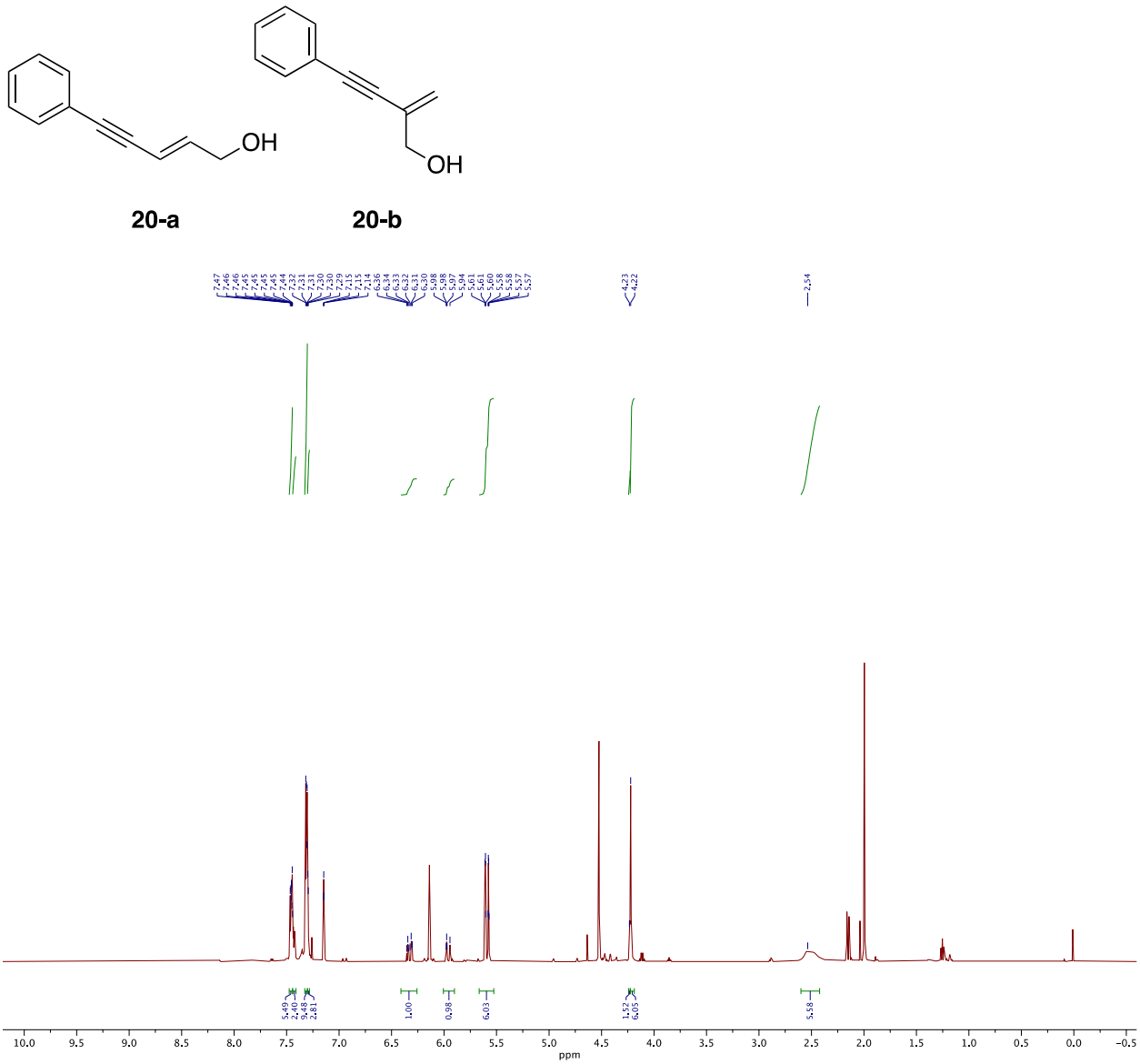

Figure A34: ^{1}H NMR (500 MHz, $CDCl_3$) spectrum of products **20-a** and **20-b**.

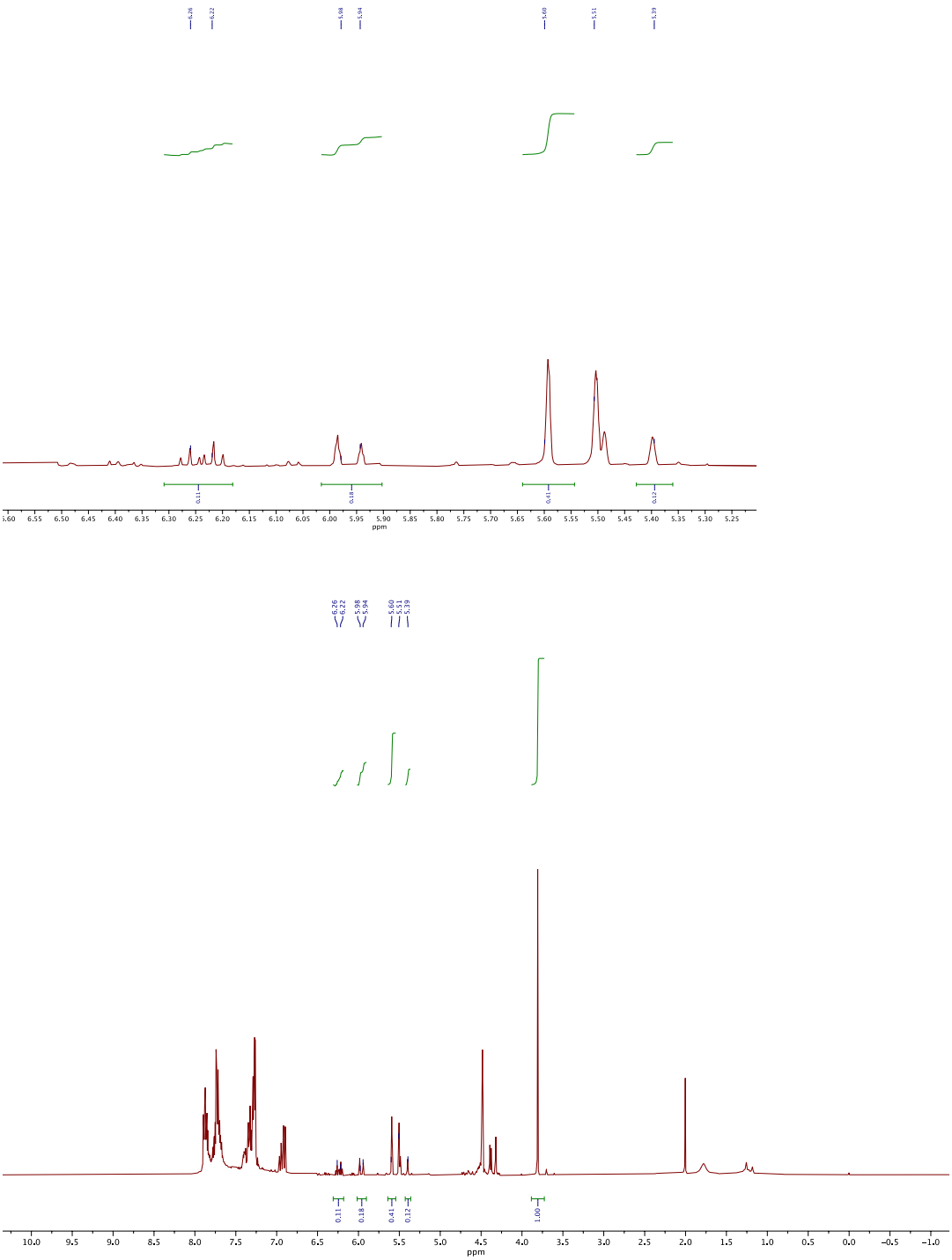

Figure A35: ^{1}H NMR (500 MHz, $CDCl_3$) spectrum of the crude reaction mixture of 3-fluoroethynylbenzene with propargyl alcohol catalyzed by **18**.

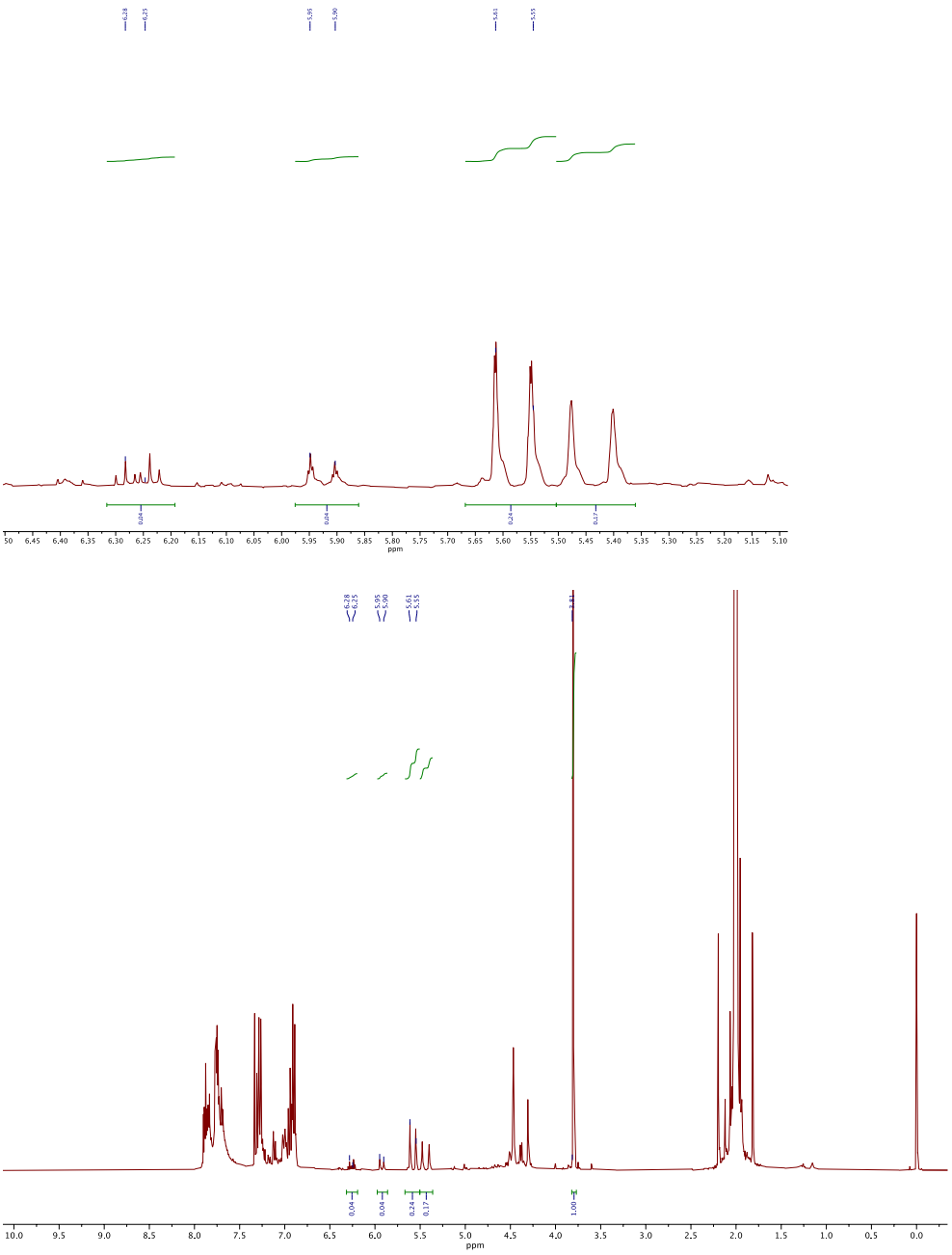

Figure A36: ^{1}H NMR (500 MHz, $CDCl_3$) spectrum of the crude reaction mixture of 3-fluoroethynylbenzene with propargyl alcohol catalyzed by **19**.

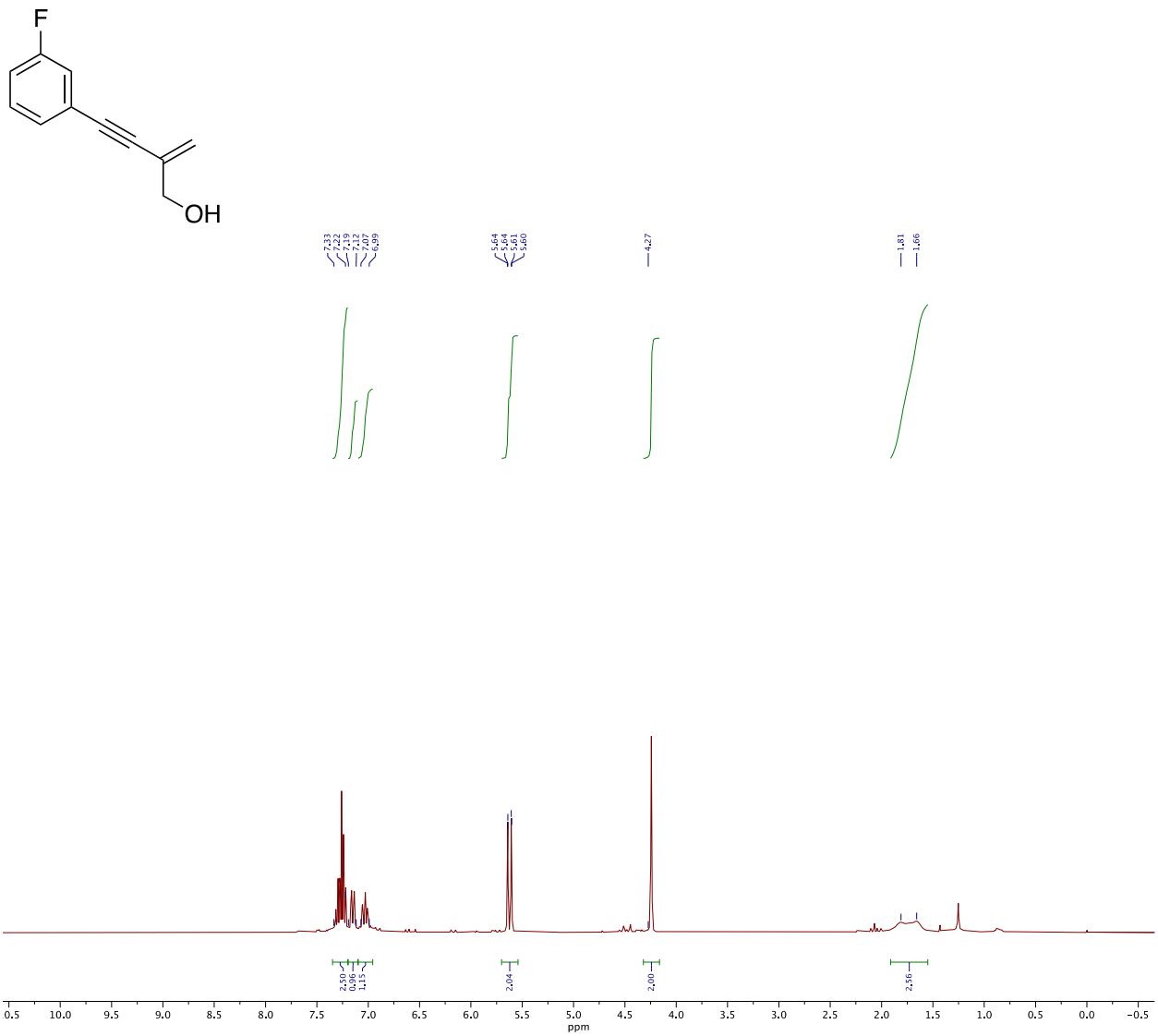

Figure A37: ^{1}H NMR (500 MHz, $CDCl_3$) spectrum of product **21-b**.

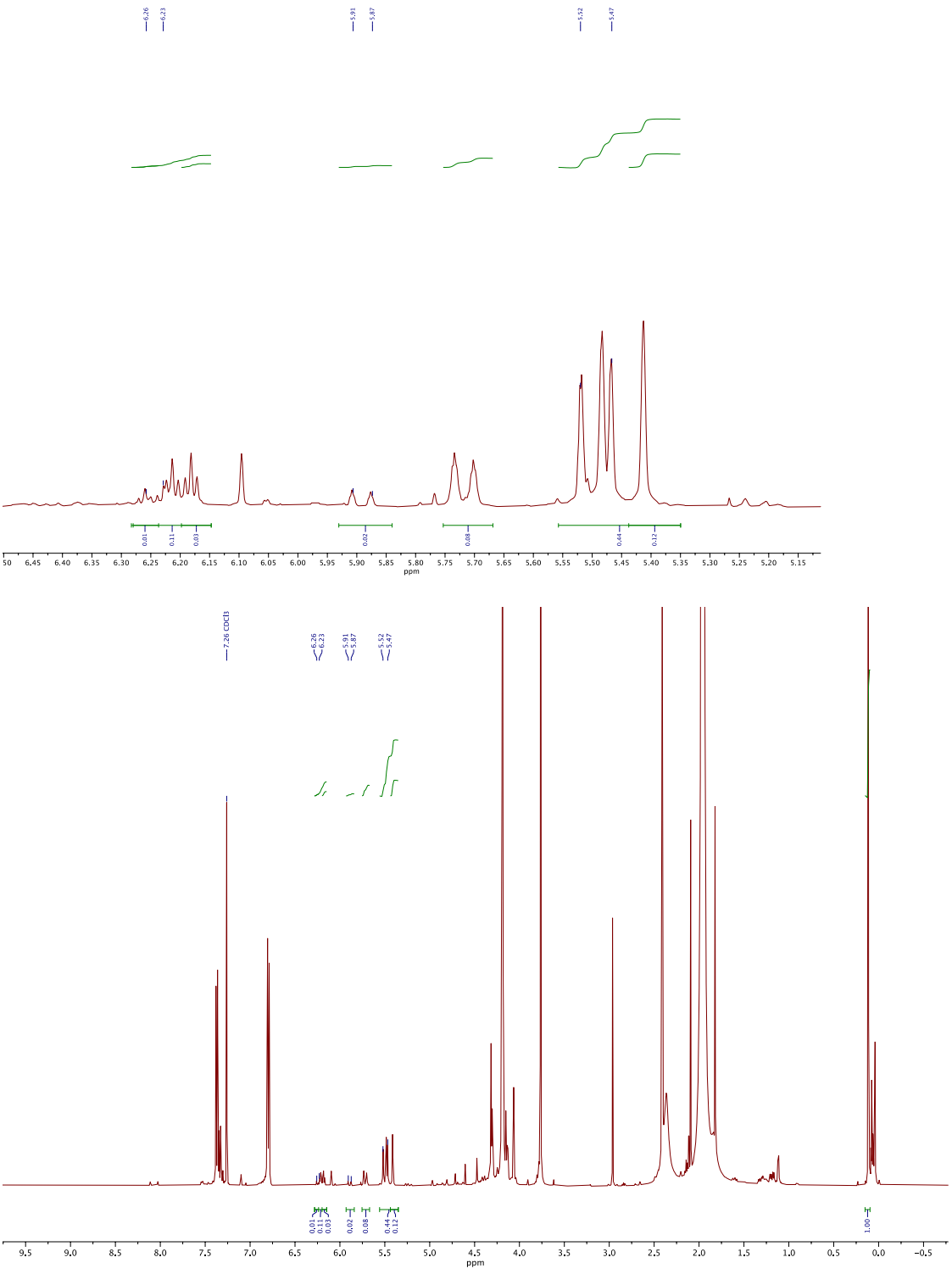

Figure A38: ^{1}H NMR (500 MHz, $CDCl_3$) spectrum of the crude reaction mixture of *p*-methoxy ethynyllbenzene with propargyl alcohol catalyzed by **18**.

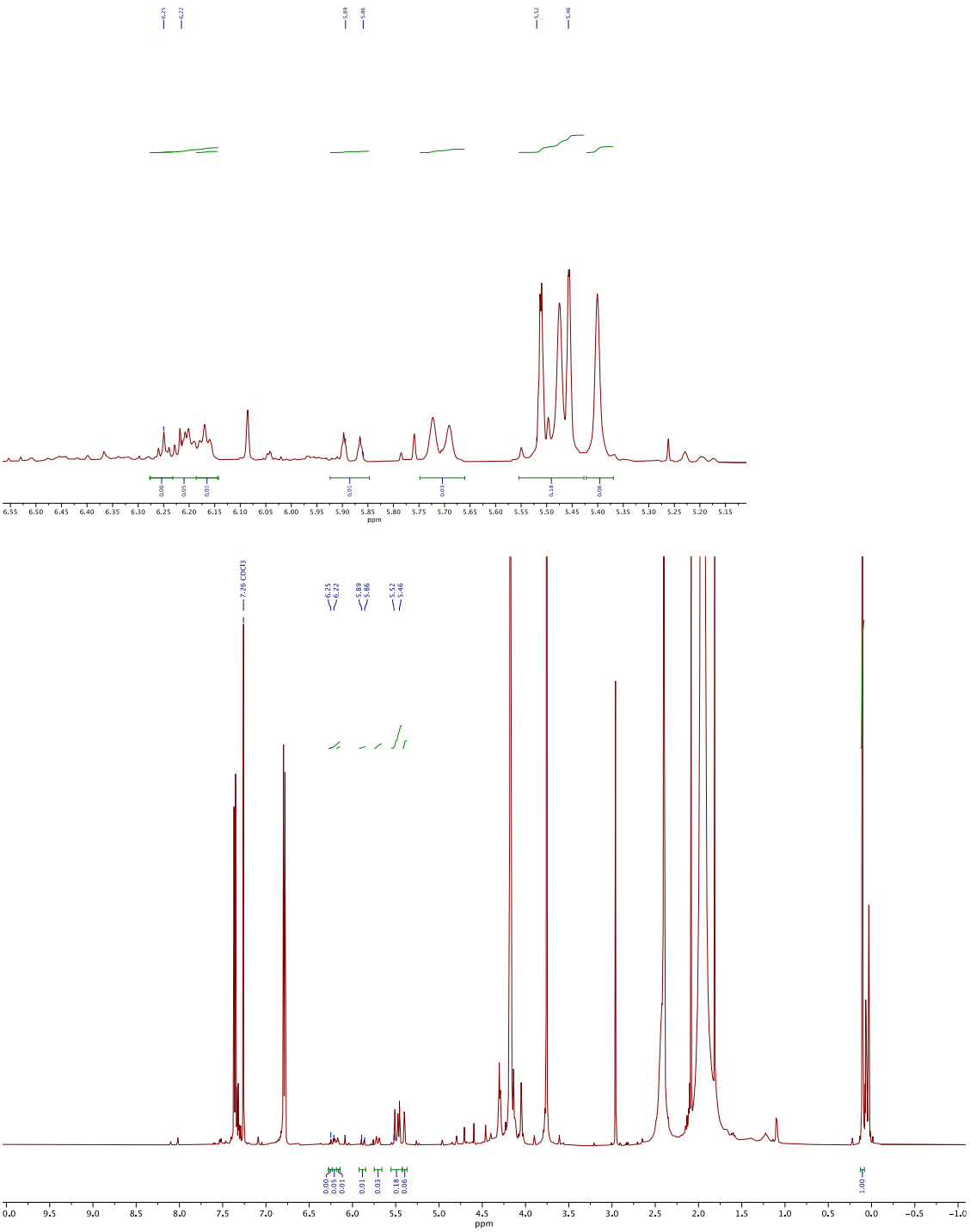

Figure A39: ^{1}H NMR (500 MHz, $CDCl_3$) spectrum of the crude reaction mixture of *p*-methoxy ethynyllbenzene with propargyl alcohol catalyzed by **19**.

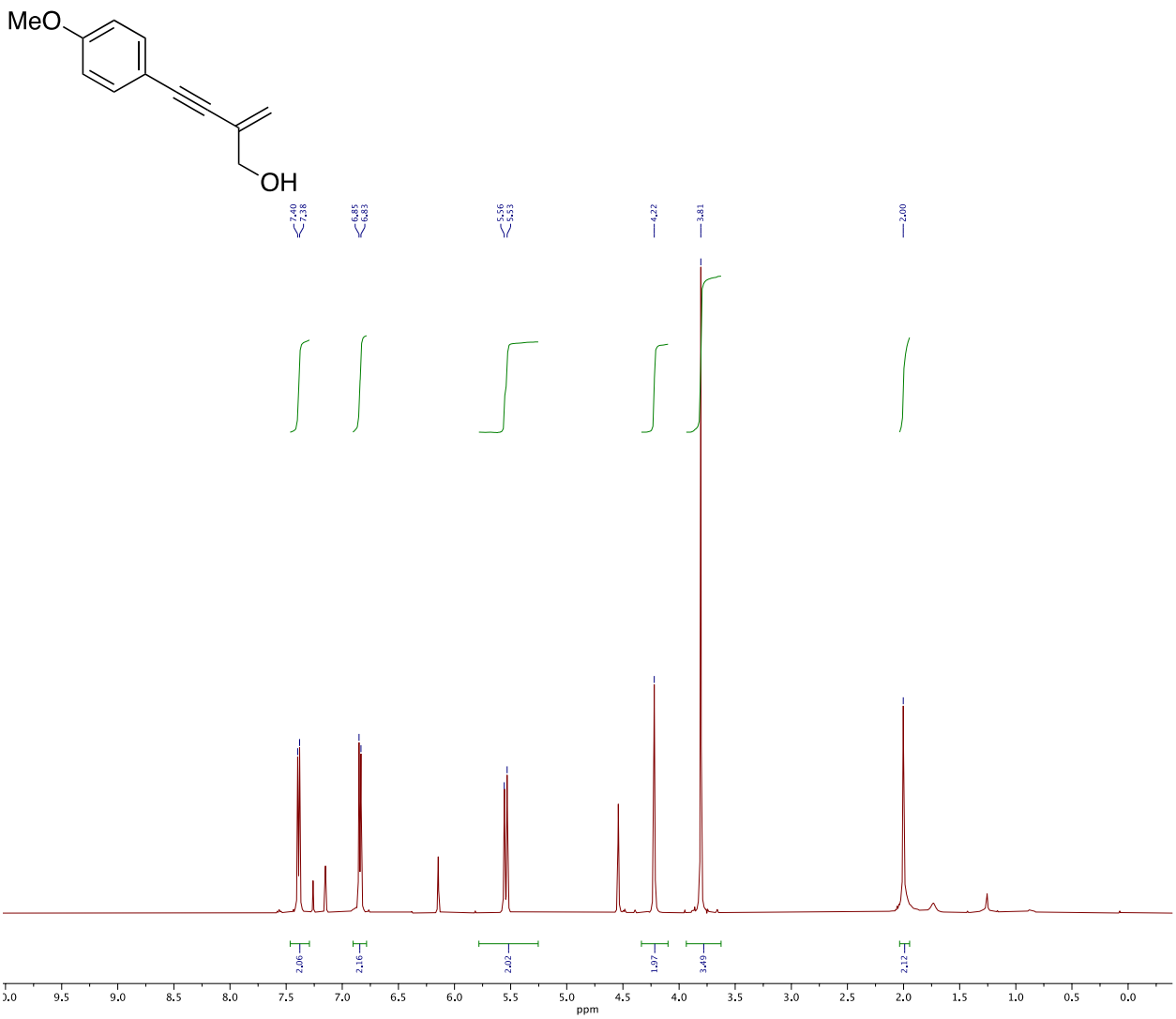

Figure A40: ^{1}H NMR (500 MHz, $CDCl_3$) spectrum of product **22-b**.

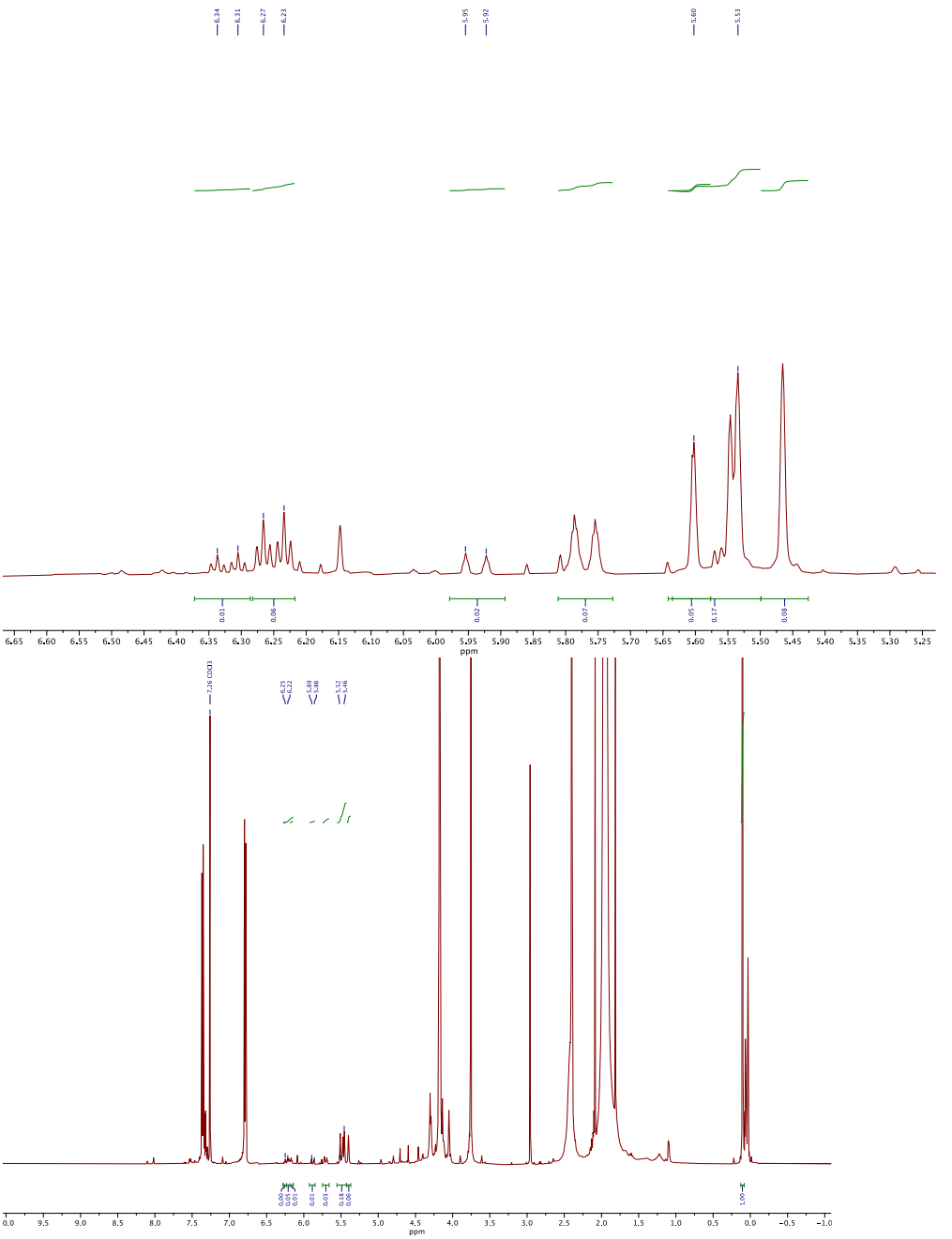

Figure A41: ^{1}H NMR (500 MHz, $CDCl_3$) spectrum of the crude reaction mixture of 3-ethynylthiophene with propargyl alcohol catalyzed by **18**.

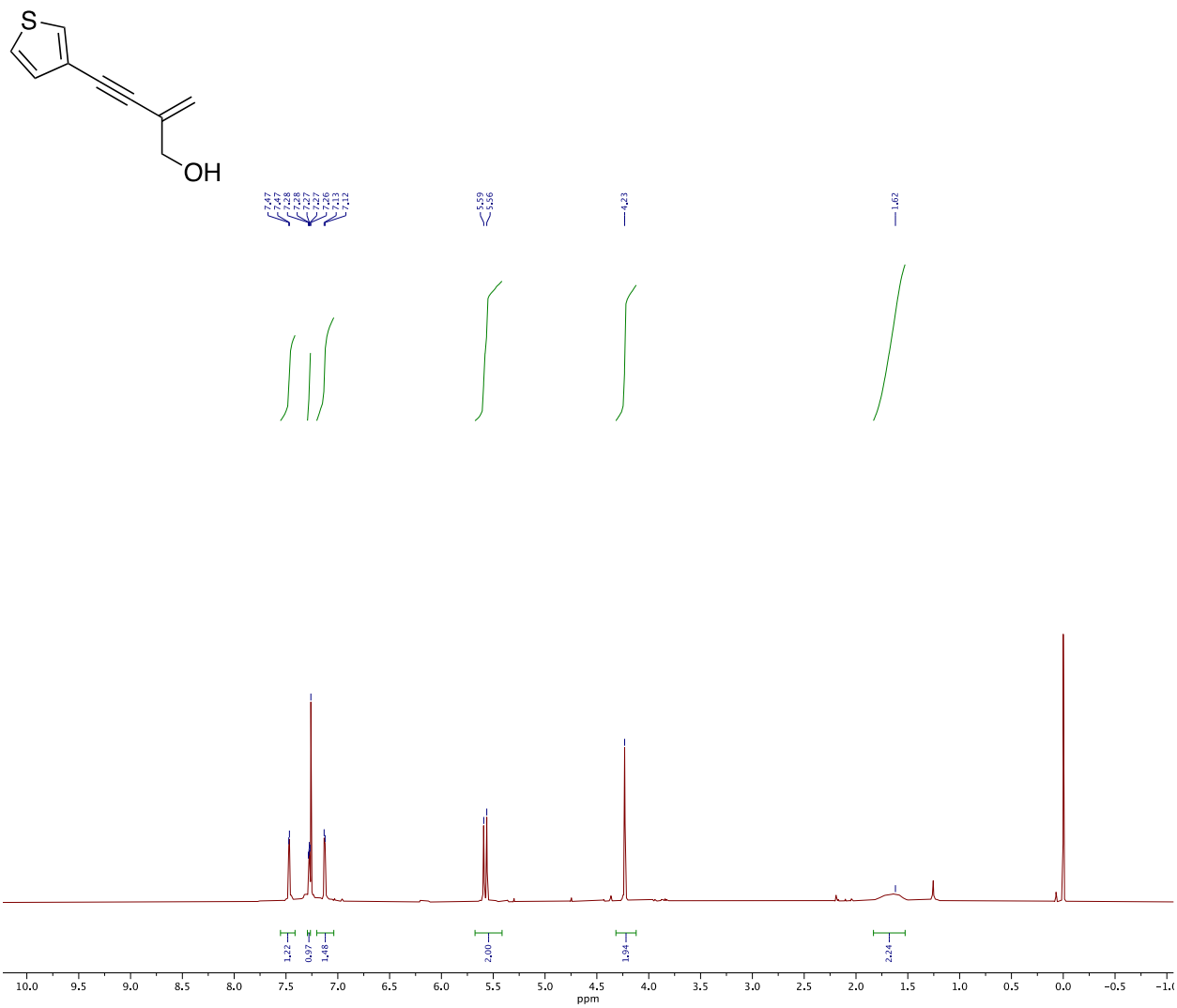

Figure A42: ^{1}H NMR (500 MHz, $CDCl_3$) spectrum of product **23-b**.

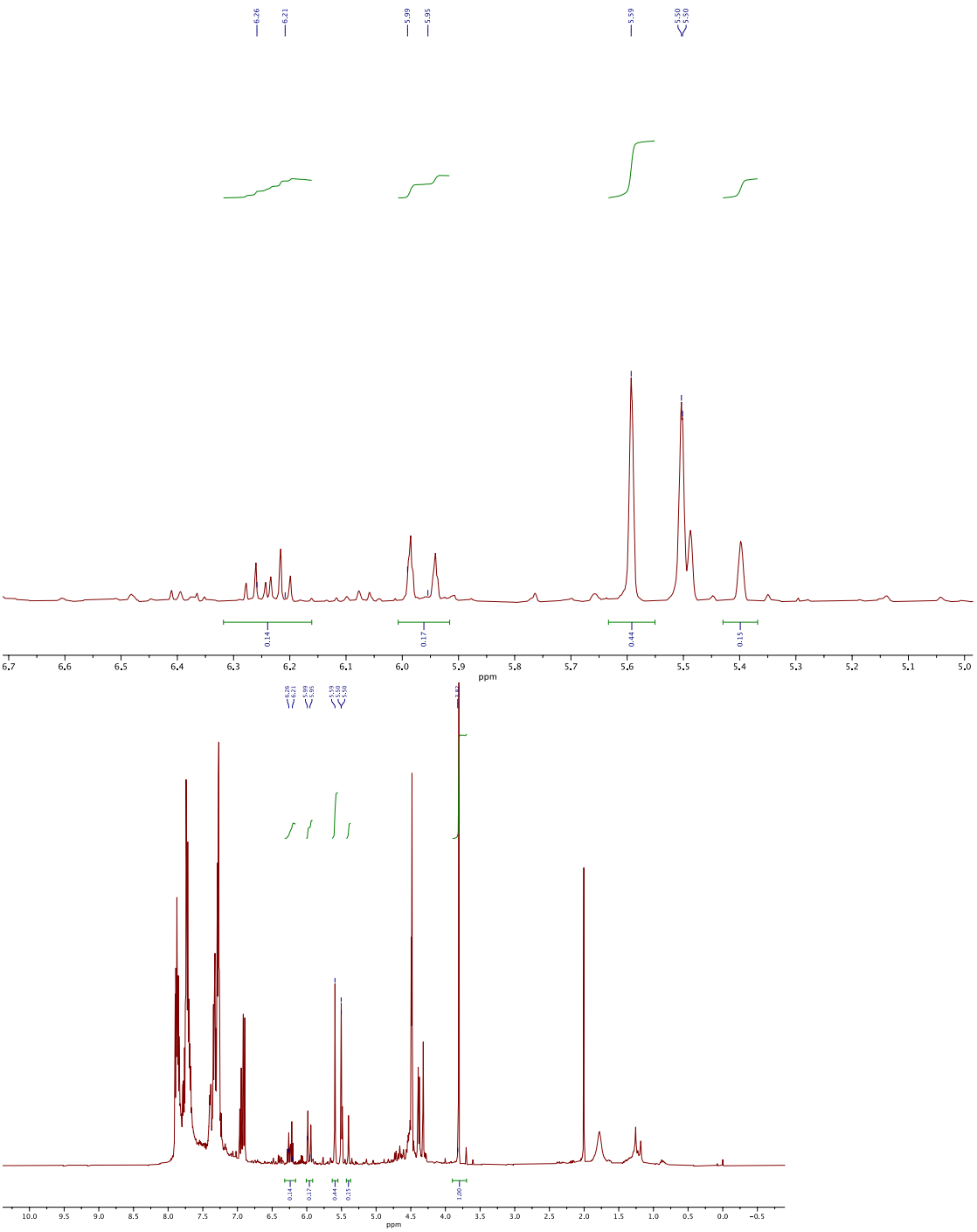

Figure A43: ^{1}H NMR (500 MHz, $CDCl_3$) spectrum of the crude reaction mixture of phenylacetylene with *N*-propargyl phthalimide catalyzed by **18**.

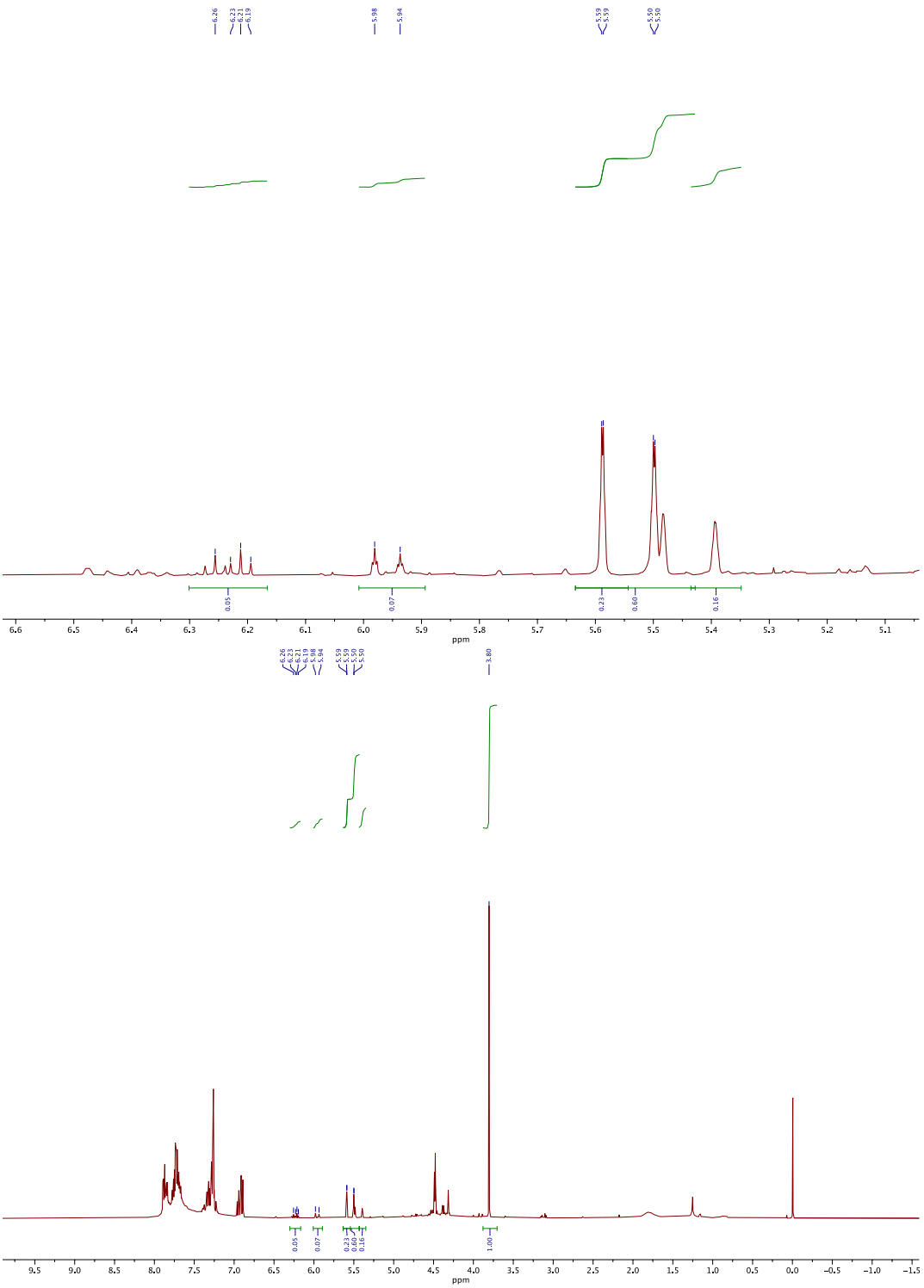

Figure A44: ^{1}H NMR (500 MHz, $CDCl_3$) spectrum of the crude reaction mixture of phenylacetylene with *N*-propargyl phthalimide catalyzed by **19.**

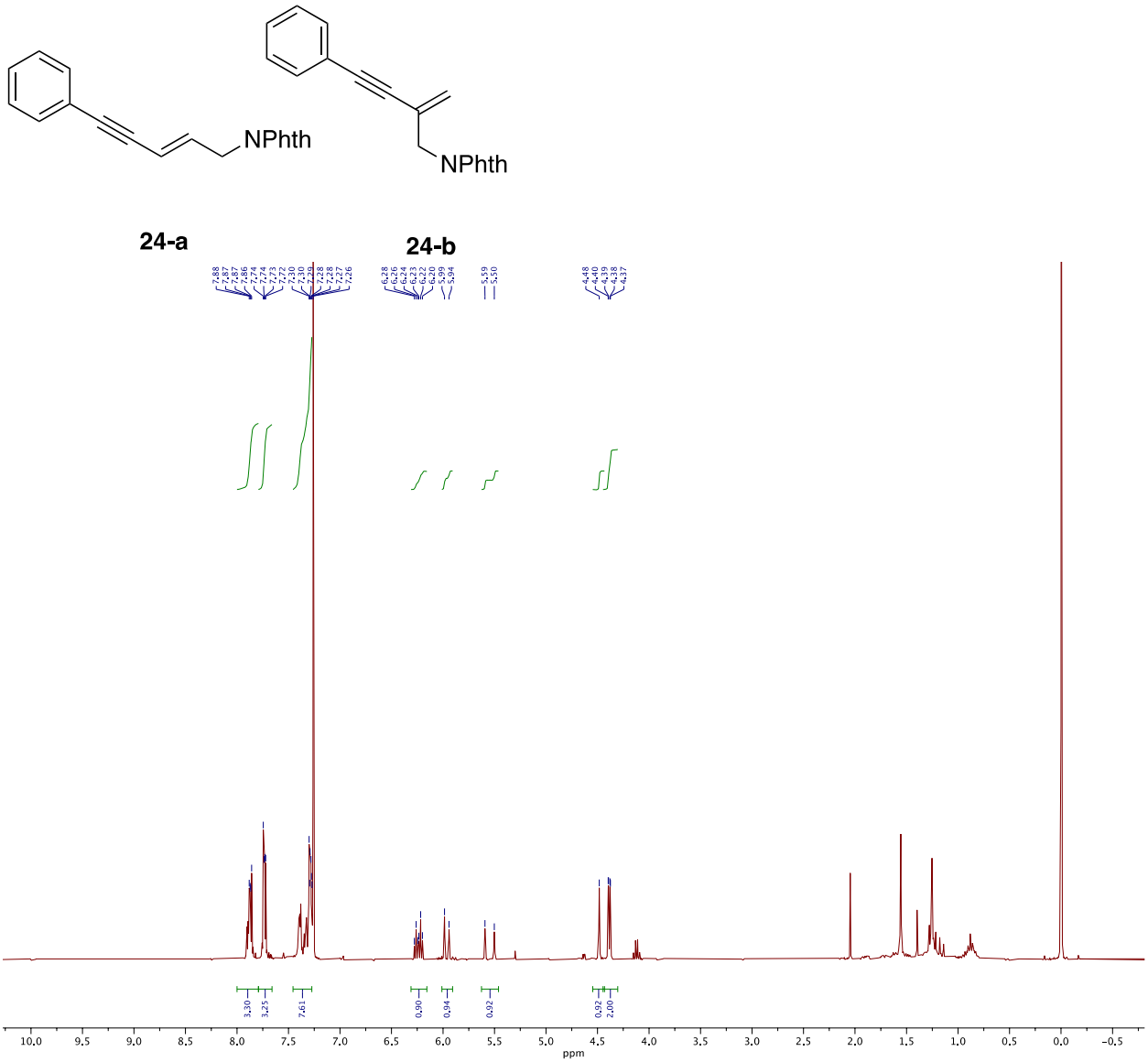

Figure A45: ^{1}H NMR (500 MHz, $CDCl_3$) spectrum of products **24-a** and **24-b**.

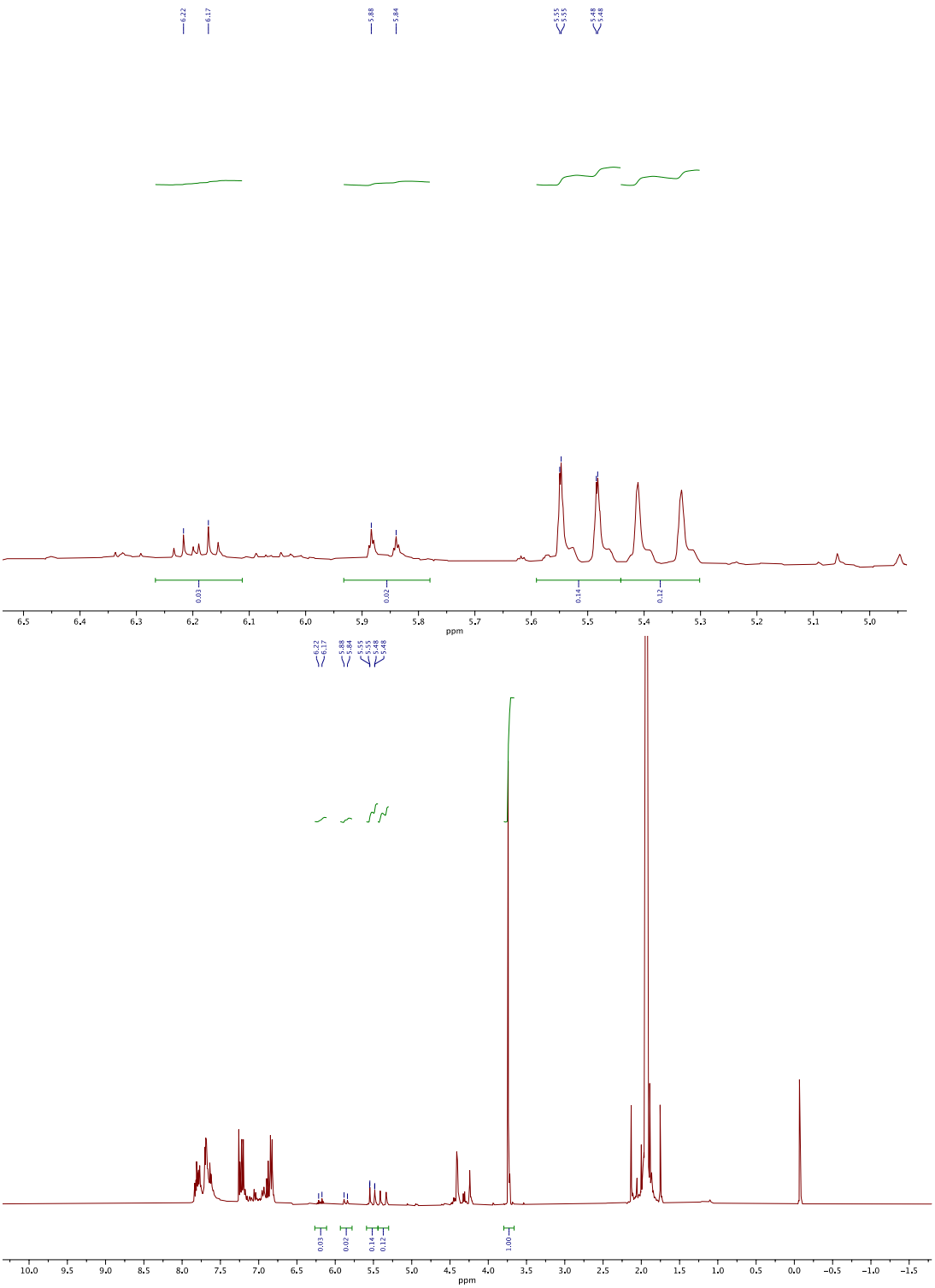

Figure A46: ^{1}H NMR (500 MHz, $CDCl_3$) spectrum of the crude reaction mixture of 3-ethynylfluorobenzene with *N*-propargyl phthalimide catalyzed by **18**.

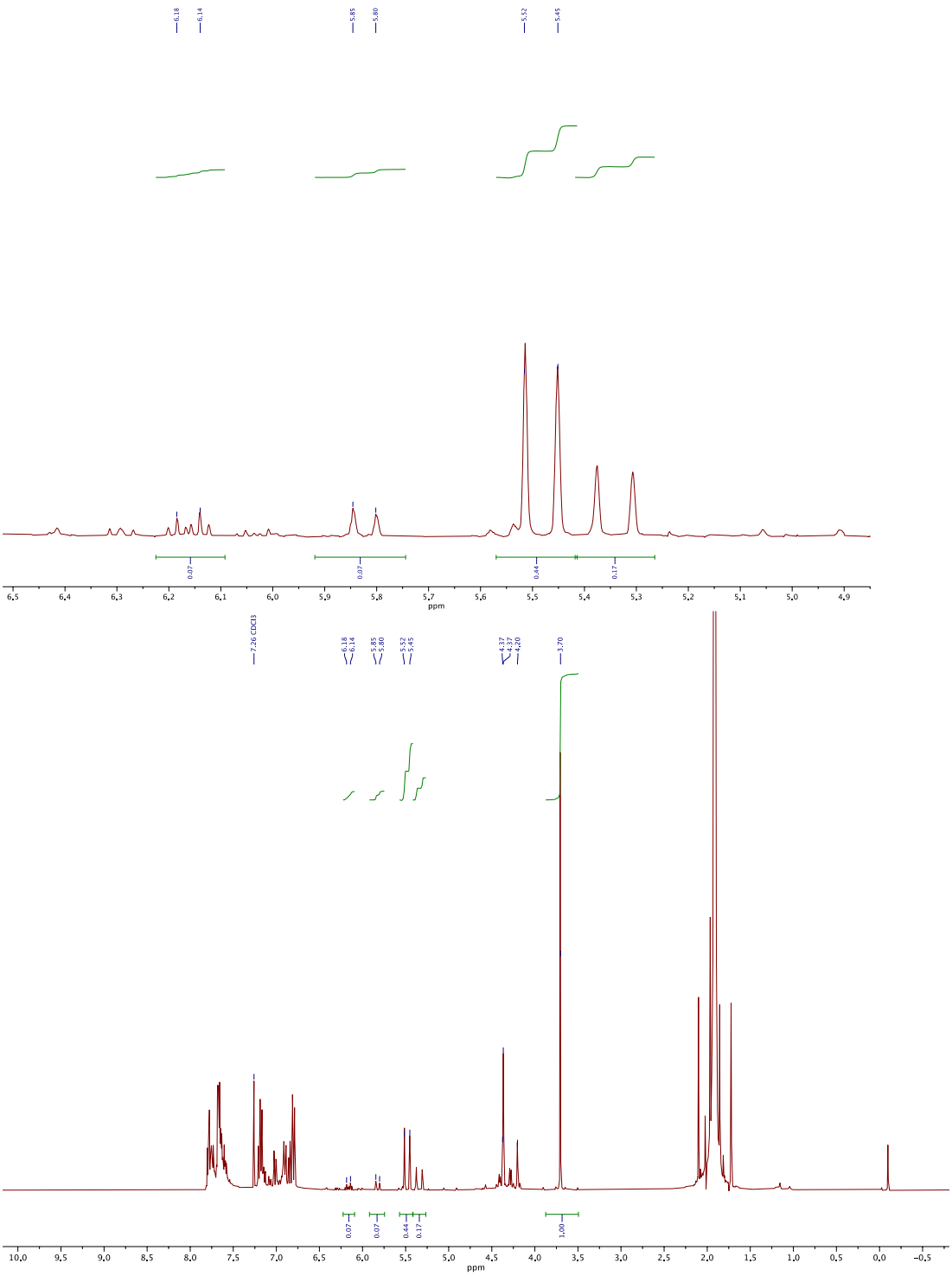

Figure A47: ^{1}H NMR (500 MHz, $CDCl_3$) spectrum of the crude reaction mixture of 3-ethynylfluorobenzene with *N*-propargyl phthalimide catalyzed by **19.**

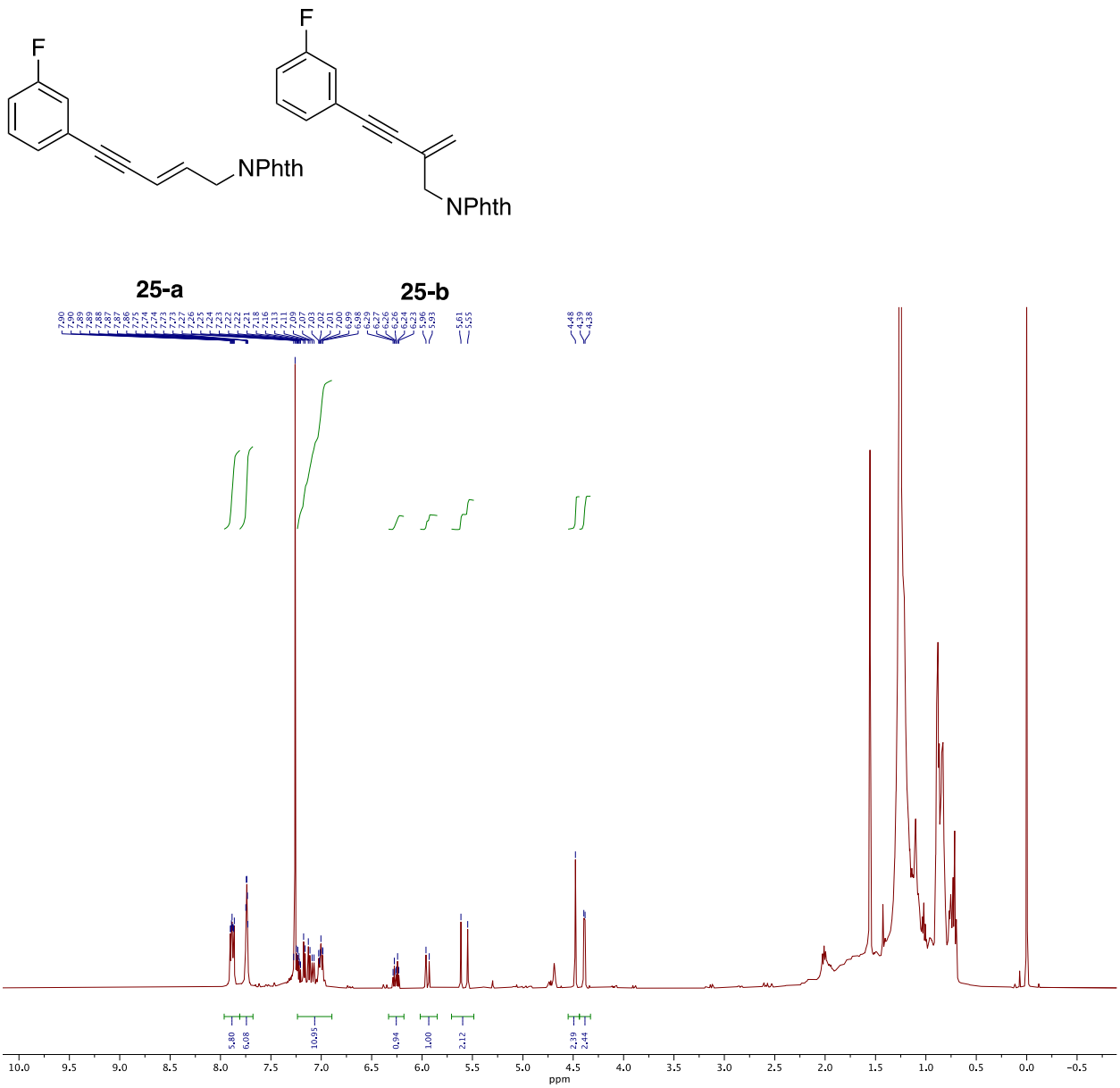

Figure A48: ^{1}H NMR (500 MHz, $CDCl_3$) spectrum of products **25-a** and **25-b**.

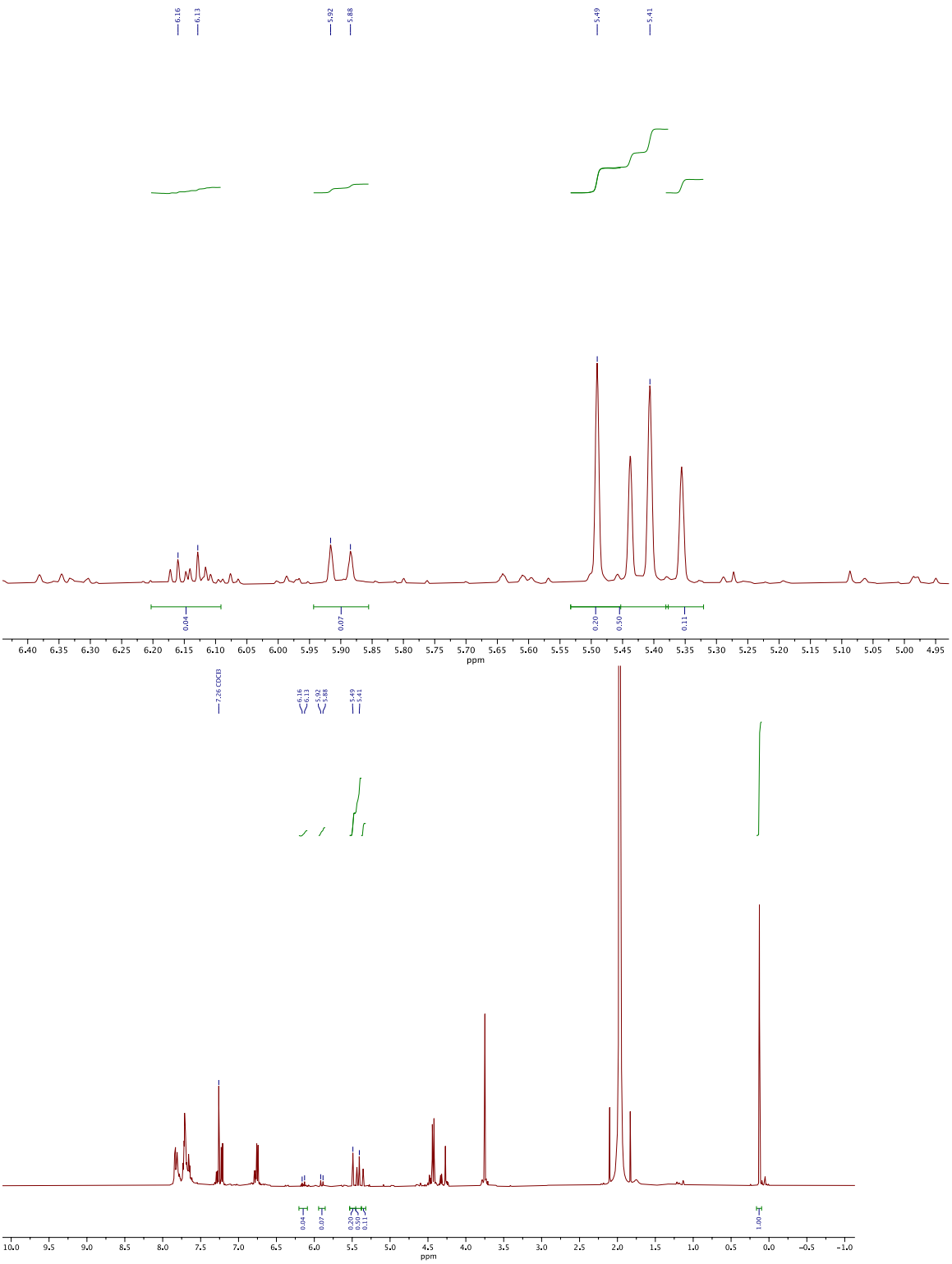

Figure A49: ^{1}H NMR (500 MHz, $CDCl_3$) spectrum of the crude reaction mixture of 4-ethynylmethoxybenzene with *N*-propargyl phthalimide catalyzed by **18.**

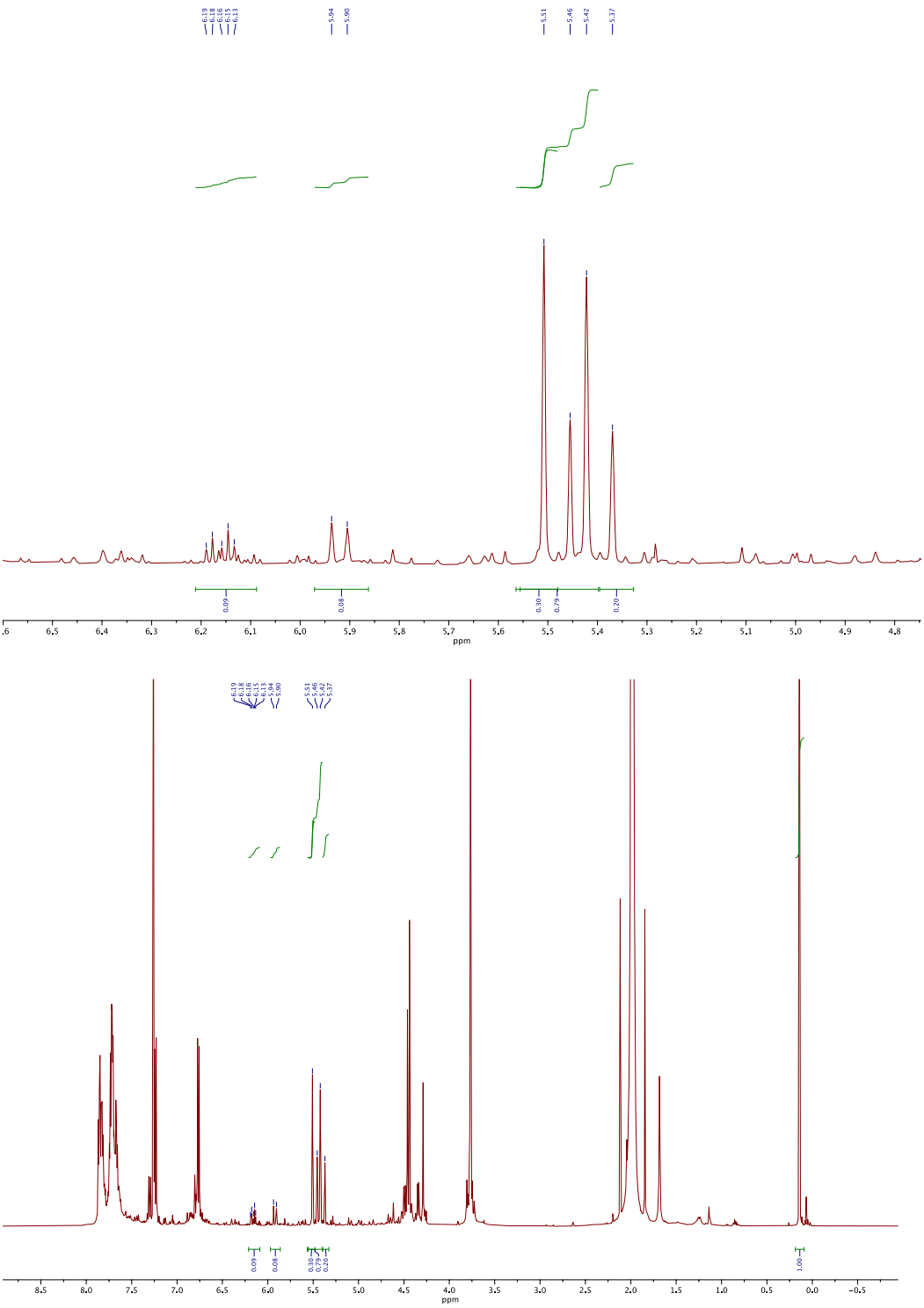

Figure A50: ^{1}H NMR (500 MHz, $CDCl_3$) spectrum of the crude reaction mixture of 4-ethynylmethoxybenzene with *N*-propargyl phthalimide catalyzed by **19.**

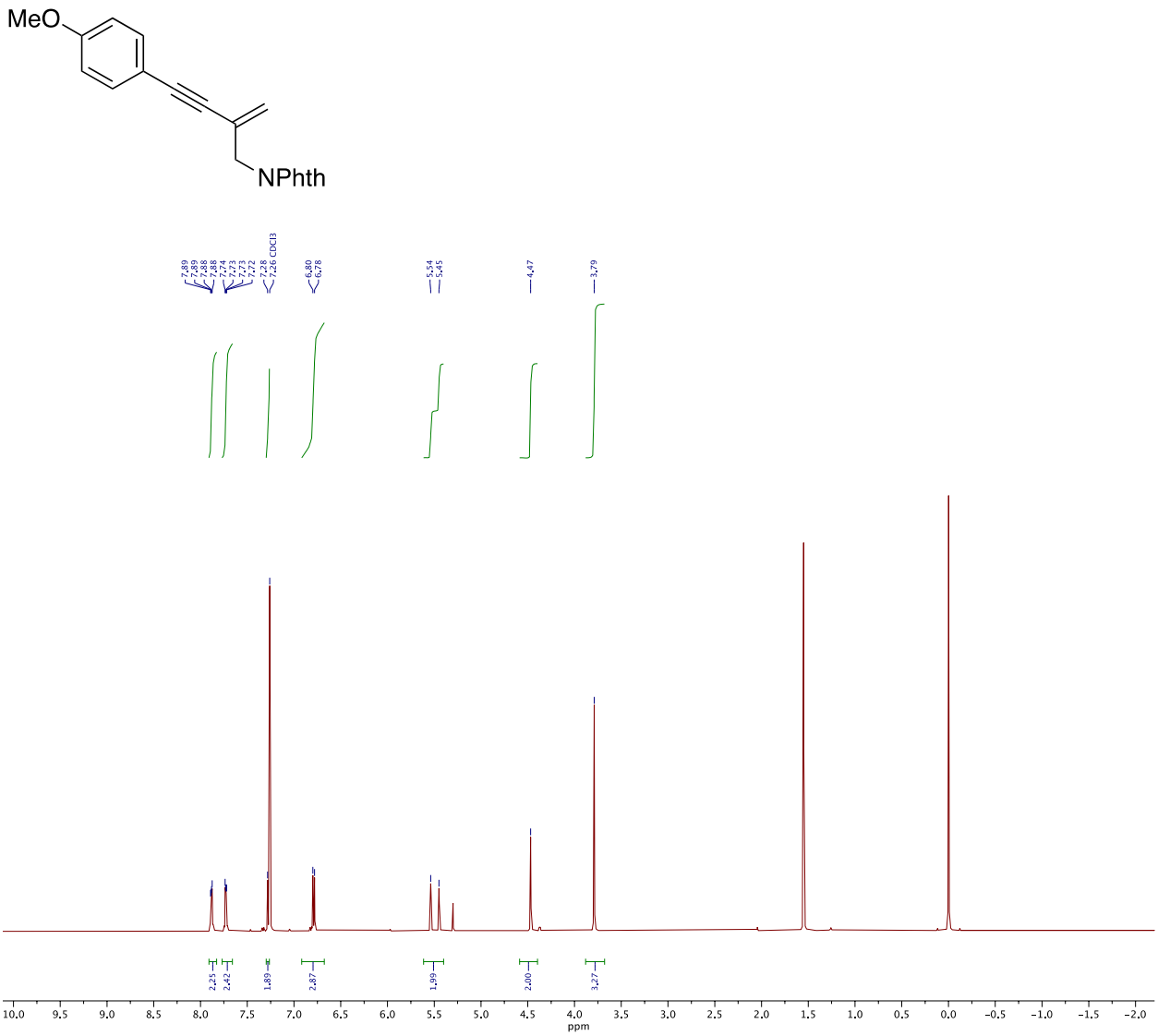

Figure A51: ^{1}H NMR (500 MHz, $CDCl_3$) spectrum of product **26-b**.

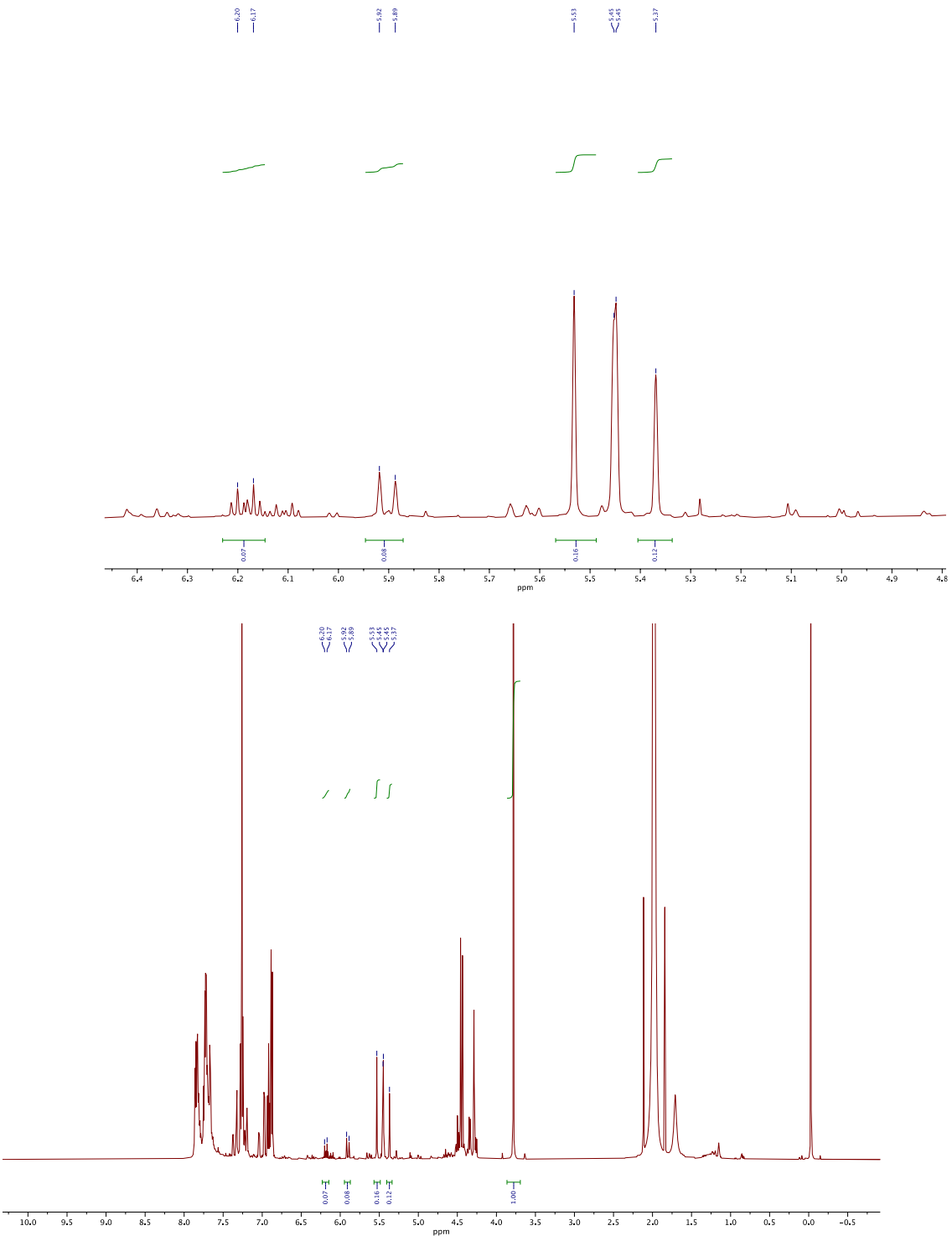

Figure A52: ^{1}H NMR (500 MHz, $CDCl_3$) spectrum of the crude reaction mixture of 3-ethynylthiophene with *N*-propargyl phthalimide catalyzed by **18.**

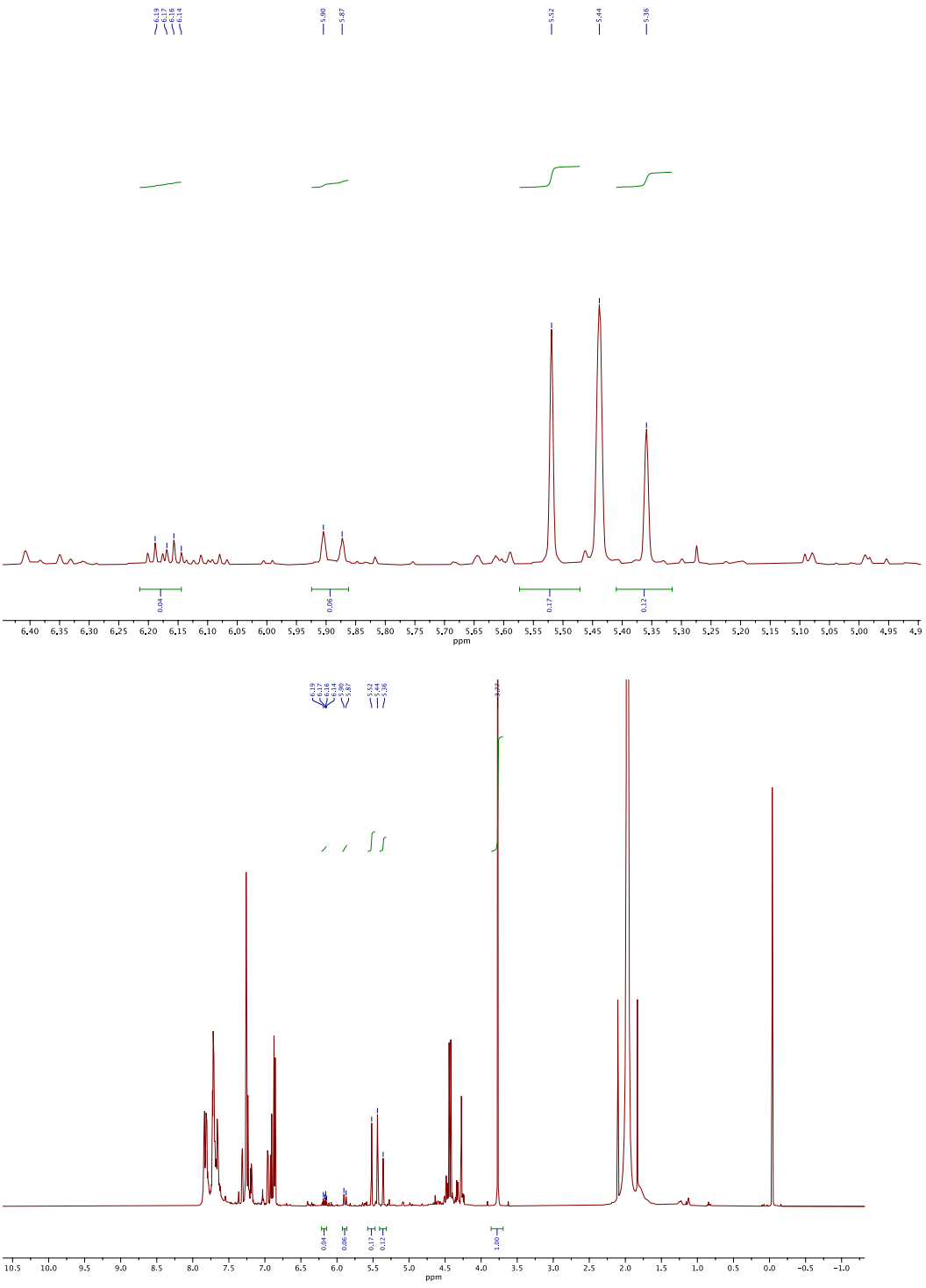

Figure A53: ^{1}H NMR (500 MHz, $CDCl_3$) spectrum of the crude reaction mixture of 3-ethynylthiophene with *N*-propargyl phthalimide catalyzed by **19.**

REFERENCES

1. King, A. O.; Okukado, N.; Negishi, E.-i. Highly general stereo-, regio-, and chemo-selective synthesis of terminal and internal conjugated enynes by the Pd-catalysed reaction of alkynylzinc reagents with alkenyl halides. *J. Chem. Soc., Chem. Commun.* **1977**, 683-684.

2. Miyaura, N.; Yamada, K.; Suzuki, A. A new stereospecific cross-coupling by the palladium-catalyzed reaction of 1-alkenylboranes with 1-alkenyl or 1-alkynyl halides. *Tetrahedron Lett.* **1979,** *20*, 3437-3440.

3. Corriu, R. J. P.; Masse, J. P. Activation of Grignard reagents by transition-metal complexes. A new and simple synthesis of trans-stilbenes and polyphenyls. *J. Chem. Soc., Chem. Commun.* **1972**.

4. Tamao, K.; Sumitani, K.; Kumada, M. Selective carbon-carbon bond formation by cross-coupling of Grignard reagents with organic halides. Catalysis by nickel-phosphine complexes. *J. Am Chem. Soc.* **1972,** *94*, 4374-4376.

5. Sonogashira, K.; Tohda, Y.; Hagihara, N. A convenient synthesis of acetylenes: catalytic substitutions of acetylenic hydrogen with bromoalkenes, iodoarenes and bromopyridines. *Tetrahedron Lett.* **1975,** *16*, 4467-4470.

6. Paul, F.; Patt, J.; Hartwig, J. F. Palladium-catalyzed formation of carbon-nitrogen bonds. Reaction intermediates and catalyst improvements in the hetero cross-coupling of aryl halides and tin amides. *J. Am Chem. Soc.* **1994,** *116*, 5969-5970.

7. Guram, A. S.; Buchwald, S. L. Palladium-Catalyzed Aromatic Aminations with in situ Generated Aminostannanes. *J. Am Chem. Soc.* **1994,** *116*, 7901-7902.

8. Heck, R. F.; Nolley, J. P. Palladium-catalyzed vinylic hydrogen substitution reactions with aryl, benzyl, and styryl halides. *J. Org. Chem.* **1972,** *37*, 2320-2322.

9. Milstein, D.; Stille, J. K. A general, selective, and facile method for ketone synthesis from acid chlorides and organotin compounds catalyzed by palladium. *J. Am Chem. Soc.* **1978,** *100*, 3636-3638.

10. Magano, J.; Dunetz, J. R. Large-Scale Applications of Transition Metal-Catalyzed Couplings for the Synthesis of Pharmaceuticals. *Chem. Rev.* **2011,** *111*, 2177-2250.

11. Devendar, P.; Qu, R.-Y.; Kang, W.-M.; He, B.; Yang, G.-F. Palladium-Catalyzed Cross-Coupling Reactions: A Powerful Tool for the Synthesis of Agrochemicals. *J. Agric. Food. Chem.* **2018,** *66*, 8914-8934.

12. Shang, R.; Liu, L. Transition metal-catalyzed decarboxylative cross-coupling reactions. *Science China Chemistry* **2011,** *54*, 1670-1687.

13. Johansson Seechurn, C. C. C.; Kitching, M. O.; Colacot, T. J.; Snieckus, V. Palladium-Catalyzed Cross-Coupling: A Historical Contextual Perspective to the 2010 Nobel Prize. *Angew. Chem. Int. Ed.* **2012,** *51*, 5062-5085.

14. Vries, J. G. d. The Heck reaction in the production of fine chemicals. *Can. J. Chem.* **2001,** *79*, 1086-1092.

15. Ruiz-Castillo, P.; Buchwald, S. L. Applications of Palladium-Catalyzed C–N Cross-Coupling Reactions. *Chem. Rev.* **2016,** *116*, 12564-12649.

16. Littke, A. F.; Fu, G. C. Palladium-Catalyzed Coupling Reactions of Aryl Chlorides. *Angew. Chem. Int. Ed.* **2002,** *41*, 4176-4211.

17. Scherpf, T.; Steinert, H.; Großjohann, A.; Dilchert, K.; Tappen, J.; Rodstein, I.; Gessner, V. H. Efficient Pd-Catalyzed Direct Coupling of Aryl Chlorides with Alkyllithium Reagents. *Angew. Chem. Int. Ed.* **2020,** *59*, 20596-20603.

18. Hayashi, T.; Konishi, M.; Kumada, M. Dichloro [1, 1′-bis (diphenylphosphino) ferrocene] palladium (II): an effective catalyst for cross-coupling reaction of a secondary alkyl grignard reagent with organic halides. *Tetrahedron Lett.* **1979,** *20*, 1871-1874.

19. Ben-David, Y.; Portnoy, M.; Milstein, D. Chelate-assisted, palladium-catalyzed efficient carbonylation of aryl chlorides. *J. Am Chem. Soc.* **1989,** *111*, 8742-8744.

20. Huser, M.; Youinou, M.-T.; Osborn, J. A. Chlorocarbon Activation: Catalytic Carbonylation of Dichloromethane and Chlorobenzene. *Angew. Chem.* **1989,** *28*, 1386-1388.

21. Louie, J.; Hartwig, J. F. Palladium-catalyzed synthesis of arylamines from aryl halides. Mechanistic studies lead to coupling in the absence of tin reagents. *Tetrahedron Lett.* **1995,** *36*, 3609-3612.

22. Hartwig, J. F.; Kawatsura, M.; Hauck, S. I.; Shaughnessy, K. H.; Alcazar-Roman, L. M. Room-Temperature Palladium-Catalyzed Amination of Aryl Bromides and Chlorides and Extended Scope of Aromatic C-N Bond Formation with a Commercial Ligand. *J. Org. Chem.* **1999,** *64*, 5575-5580.

23. Guram, A. S.; Rennels, R. A.; Buchwald, S. L. A Simple Catalytic Method for the Conversion of Aryl Bromides to Arylamines. *Angewandte Chemie International Edition in English* **1995,** *34*, 1348-1350.

24. Surry, D. S.; Buchwald, S. L. Biaryl Phosphane Ligands in Palladium-Catalyzed Amination. *Angew. Chem. Int. Ed.* **2008,** *47*, 6338-6361.

25. Littke, A. F.; Fu, G. C. A Convenient and General Method for Pd-Catalyzed Suzuki Cross-Couplings of Aryl Chlorides and Arylboronic Acids. *Angew. Chem. Int. Ed. Engl.* **1998,** *37*, 3387-3388.

26. Fu, G. C. The development of versatile methods for palladium-catalyzed coupling reactions of aryl electrophiles through the use of P(t-Bu)3 and PCy3 as ligands. *Acc. Chem. Res.* **2008,** *41*, 1555-64.

27. Zapf, A.; Ehrentraut, A.; Beller, M. A New Highly Efficient Catalyst System for the Coupling of Nonactivated and Deactivated Aryl Chlorides with Arylboronic Acids. *Angew. Chem. Int. Ed.* **2000,** *39*, 4153-4155.

28. Chen, L.; Ren, P.; Carrow, B. P. Tri(1-adamantyl)phosphine: Expanding the Boundary of Electron-Releasing Character Available to Organophosphorus Compounds. *J. Am Chem. Soc.* **2016,** *138*, 6392-6395.

29. Littke, A. F.; Schwarz, L.; Fu, G. C. Pd/P(t-Bu)3: A Mild and General Catalyst for Stille Reactions of Aryl Chlorides and Aryl Bromides. *J. Am Chem. Soc.* **2002,** *124*, 6343-6348.

30. Littke, A. F.; Fu, G. C. A Versatile Catalyst for Heck Reactions of Aryl Chlorides and Aryl Bromides under Mild Conditions. *J. Am Chem. Soc.* **2001,** *123*, 6989-7000.

31. Littke, A. F.; Dai, C.; Fu, G. C. Versatile Catalysts for the Suzuki Cross-Coupling of Arylboronic Acids with Aryl and Vinyl Halides and Triflates under Mild Conditions. *J. Am Chem. Soc.* **2000,** *122*, 4020-4028.

32. Galardon, E.; Ramdeehul, S.; Brown, J. M.; Cowley, A.; Hii, K. K.; Jutand, A. Profound Steric Control of Reactivity in Aryl Halide Addition to Bisphosphane Palladium(0) Complexes. *Angew. Chem. Int. Ed.* **2002,** *41*, 1760-1763.

33. Barrios-Landeros, F.; Carrow, B. P.; Hartwig, J. F. Effect of Ligand Steric Properties and Halide Identity on the Mechanism for Oxidative Addition of Haloarenes to Trialkylphosphine Pd(0) Complexes. *J. Am Chem. Soc.* **2009,** *131*, 8141-8154.

34. Hu, H.; Vasiliu, M.; Stein, T. H.; Qu, F.; Gerlach, D. L.; Dixon, D. A.; Shaughnessy, K. H. Synthesis, Structural Characterization, and Coordination Chemistry of (Trineopentylphosphine)palladium(aryl)bromide Dimer Complexes ([(Np3P)Pd(Ar)Br]2). *Inorg. Chem.* **2019,** *58*, 13299-13313.

35. Raders, S. M.; Moore, J. N.; Parks, J. K.; Miller, A. D.; Leißing, T. M.; Kelley, S. P.; Rogers, R. D.; Shaughnessy, K. H. Trineopentylphosphine: A Conformationally Flexible Ligand for the Coupling of Sterically Demanding Substrates in the Buchwald–Hartwig Amination and Suzuki–Miyaura Reaction. *The Journal of Organic Chemistry* **2013,** *78*, 4649-4664.

36. Hill, L. L.; Smith, J. M.; Brown, W. S.; Moore, L. R.; Guevera, P.; Pair, E. S.; Porter, J.; Chou, J.; Wolterman, C. J.; Craciun, R.; Dixon, D. A.; Shaughnessy, K. H. Neopentylphosphines as effective ligands in palladium-catalyzed cross-couplings of aryl bromides and chlorides. *Tetrahedron* **2008,** *64*, 6920-6934.

37. Hill, L. L.; Moore, L. R.; Huang, R.; Craciun, R.; Vincent, A. J.; Dixon, D. A.; Chou, J.; Woltermann, C. J.; Shaughnessy, K. H. Bulky Alkylphosphines with Neopentyl Substituents as Ligands in the Amination of Aryl Bromides and Chlorides. *The Journal of Organic Chemistry* **2006,** *71*, 5117-5125.

38. Lauer, M. G.; Thompson, M. K.; Shaughnessy, K. H. Controlling Olefin Isomerization in the Heck Reaction with Neopentyl Phosphine Ligands. *The Journal of Organic Chemistry* **2014,** *79*, 10837-10848.

39. Proutiere, F.; Aufiero, M.; Schoenebeck, F. Reactivity and Stability of Dinuclear Pd(I) Complexes: Studies on the Active Catalytic Species, Insights into Precatalyst Activation and Deactivation, and Application in Highly Selective Cross-Coupling Reactions. *J. Am Chem. Soc.* **2012,** *134*, 606-612.

40. Aufiero, M.; Scattolin, T.; Proutière, F.; Schoenebeck, F. Air-Stable Dinuclear Iodine-Bridged Pd(I) Complex - Catalyst, Precursor, or Parasite? The Additive Decides. Systematic Nucleophile-Activity Study and Application as Precatalyst in Cross-Coupling. *Organometallics* **2015,** *34*, 5191-5195.

41. Shaughnessy, K. H. Development of Palladium Precatalysts that Efficiently Generate LPd(0) Active Species. *Isr. J. Chem.* **2020,** *60*, 180-194.

42. Hu, H.; Burlas, C. E.; Curley, S. J.; Gruchala, T.; Qu, F.; Shaughnessy, K. H. Effect of Aryl Ligand Identity on Catalytic Performance of Trineopentylphosphine Arylpalladium Complexes in N-Arylation Reactions. *Organometallics* **2020,** *39*, 3618-3627.

43. Melvin, P. R.; Balcells, D.; Hazari, N.; Nova, A. Understanding Precatalyst Activation in Cross-Coupling Reactions: Alcohol Facilitated Reduction from Pd(II) to Pd(0) in Precatalysts of the Type (η3-allyl)Pd(L)(Cl) and (η3-indenyl)Pd(L)(Cl). *ACS Catalysis* **2015,** *5*, 5596-5606.

44. Lee, H. G.; Milner, P. J.; Buchwald, S. L. An Improved Catalyst System for the Pd-Catalyzed Fluorination of (Hetero)Aryl Triflates. *Org. Lett.* **2013,** *15*, 5602-5605.

45. Hu, H.; Qu, F.; Gerlach, D. L.; Shaughnessy, K. H. Mechanistic Study of the Role of Substrate Steric Effects and Aniline Inhibition on the Bis(trineopentylphosphine)palladium(0)-Catalyzed Arylation of Aniline Derivatives. *ACS Catalysis* **2017,** *7*, 2516-2527.

46. Chen, L.; Francis, H.; Carrow, B. P. An "On-Cycle" Precatalyst Enables Room-Temperature Polyfluoroarylation Using Sensitive Boronic Acids. *ACS Catalysis* **2018,** *8*, 2989-2994.

47. Malapit, C. A.; Bour, J. R.; Laursen, S. R.; Sanford, M. S. Mechanism and Scope of Nickel-Catalyzed Decarbonylative Borylation of Carboxylic Acid Fluorides. *J. Am Chem. Soc.* **2019,** *141*, 17322-17330.

48. Xu, J.; Liu, R. Y.; Yeung, C. S.; Buchwald, S. L. Monophosphine Ligands Promote Pd-Catalyzed C–S Cross-Coupling Reactions at Room Temperature with Soluble Bases. *ACS Catalysis* **2019,** *9*, 6461-6466.

49. Tang, S.-Q.; Bricard, J.; Schmitt, M.; Bihel, F. Fukuyama Cross-Coupling Approach to Isoprekinamycin: Discovery of the Highly Active and Bench-Stable Palladium Precatalyst POxAP. *Org. Lett.* **2019,** *21*, 844-848.

50. Liu, Y.; Scattolin, T.; Gobbo, A.; Beliš, M.; Van Hecke, K.; Nolan, S. P.; Cazin, C. S. J. A Simple Synthetic Route to Well-Defined [Pd(NHC)Cl(1-tBu-indenyl)] Pre-catalysts for Cross-Coupling Reactions. *Eur. J. Inorg. Chem.* **2022,** *2022*, e202100840.

51. Friis, S. D.; Skrydstrup, T.; Buchwald, S. L. Mild Pd-Catalyzed Aminocarbonylation of (Hetero)Aryl Bromides with a Palladacycle Precatalyst. *Org. Lett.* **2014,** *16*, 4296-4299.

52. Stambuli, J. P.; Incarvito, C. D.; Bühl, M.; Hartwig, J. F. Synthesis, structure, theoretical studies, and Ligand exchange reactions of monomeric, T-shaped arylpalladium(II) halide complexes with an additional, weak agostic interaction. *J Am Chem Soc* **2004,** *126*, 1184-94.

53. Meiries, S.; Chartoire, A.; Slawin, A. M. Z.; Nolan, S. P. [Pd(IPr*)(acac)Cl]: An Easily Synthesized, Bulky Precatalyst for C–N Bond Formation. *Organometallics* **2012,** *31*, 3402-3409.

54. Chartoire, A.; Frogneux, X.; Boreux, A.; Slawin, A. M. Z.; Nolan, S. P. [Pd(IPr*)(3-Cl-pyridinyl)Cl2]: A Novel and Efficient PEPPSI Precatalyst. *Organometallics* **2012,** *31*, 6947-6951.

55. Lee, D.-H.; Taher, A.; Hossain, S.; Jin, M.-J. An Efficient and General Method for the Heck and Buchwald–Hartwig Coupling Reactions of Aryl Chlorides. *Org. Lett.* **2011,** *13*, 5540-5543.

56. Reddy, C. V.; Kingston, J. V.; Verkade, J. G. (t-Bu)2PNP(i-BuNCH2CH2)3N: New Efficient Ligand for Palladium-Catalyzed C−N Couplings of Aryl and Heteroaryl Bromides and Chlorides and for Vinyl Bromides at Room Temperature. *The Journal of Organic Chemistry* **2008,** *73*, 3047-3062.

57. Urgaonkar, S.; Verkade, J. G. Scope and limitations of Pd2(dba)3/P(i-BuNCH2CH2)3N-catalyzed Buchwald-Hartwig amination reactions of aryl chlorides. *J. Org. Chem.* **2004,** *69*, 9135-42.

58. Raders, S. M.; Jones, J. M.; Semmes, J. G.; Kelley, S. P.; Rogers, R. D.; Shaughnessy, K. H. Di-tert-butylneopentylphosphine (DTBNpP): An Efficient Ligand in the Palladium-Catalyzed α-Arylation of Ketones. *Eur. J. Org. Chem.* **2014,** *2014*, 7395-7404.

59. Raders, S. M.; Moore, J. N.; Parks, J. K.; Miller, A. D.; Leißing, T. M.; Kelley, S. P.; Rogers, R. D.; Shaughnessy, K. H. Trineopentylphosphine: a conformationally flexible ligand for the coupling of sterically demanding substrates in the Buchwald-Hartwig amination and Suzuki-Miyaura reaction. *J. Org. Chem.* **2013,** *78*, 4649-64.

60. King, R. B.; Cloyd, J. C.; Reimann, R. H. Poly(tertiary phosphines and arsines). XIII. Neopentyl poly(tertiary phosphines). *The Journal of Organic Chemistry* **1976,** *41*, 972-977.

61. Pan, Y.; Young, G. B. Syntheses and spectroscopic characteristics of dialkylpalladium(II) complexes; PdR2(cod) as precursors for derivatives with N- or P-donor ligands. *J. Organomet. Chem.* **1999,** *577*, 257-264.

62. Li, J.; Park, S.; Miller, R. L.; Lee, D. Tandem enyne metathesis-metallotropic [1,3]-shift for a concise total syntheses of (+)-asperpentyn, (-)-harveynone, and (-)-tricholomenyn A. *Org. Lett.* **2009,** *11*, 571-4.

63. Liu, Y.; Luo, P.; Fu, Y.; Hao, T.; Liu, X.; Ding, Q.; Peng, Y. Recent advances in the tandem annulation of 1,3-enynes to functionalized pyridine and pyrrole derivatives. *Beilstein Journal of Organic Chemistry* **2021,** *17*, 2462-2476.

64. Negishi, E.-i.; Anastasia, L. Palladium-Catalyzed Alkynylation. *Chem. Rev.* **2003,** *103*, 1979-2018.

65. Yan, W.; Ye, X.; Akhmedov, N. G.; Petersen, J. L.; Shi, X. 1,2,3-Triazole: Unique Ligand in Promoting Iron-Catalyzed Propargyl Alcohol Dehydration. *Org. Lett.* **2012,** *14*, 2358-2361.

66. Deussen, H.-J.; Jeppesen, L.; Schärer, N.; Junager, F.; Bentzen, B.; Weber, B.; Weil, V.; Mozer, S. J.; Sauerberg, P. Process Development and Scale-Up of the PPAR Agonist NNC 61-4655. *Organic Process Research & Development* **2004,** *8*, 363-371.

67. Jahier, C.; Zatolochnaya, O. V.; Zvyagintsev, N. V.; Ananikov, V. P.; Gevorgyan, V. General and Selective Head-to-Head Dimerization of Terminal Alkynes Proceeding via Hydropalladation Pathway. *Org. Lett.* **2012,** *14*, 2846-2849.

68. Kovalev, I. P.; Yevdakov, K. V.; Strelenko, Y. A.; Vinogradov, M. G.; Nikishin, G. I. Dimerization of 1-alkynes catalyzed by RhCl(PMe3)3. Isolation of the intermediate (alkynyl)(vinyl)rhodium(III) complexes. *J. Organomet. Chem.* **1990,** *386*, 139-146.

69. Ghosh, R.; Zhang, X.; Achord, P.; Emge, T. J.; Krogh-Jespersen, K.; Goldman, A. S. Dimerization of Alkynes Promoted by a Pincer-Ligated Iridium Complex. C−C Reductive Elimination Inhibited by Steric Crowding. *J. Am Chem. Soc.* **2007,** *129*, 853-866.

70. Boese, W. T.; Goldman, A. S. Insertion of acetylenes into carbon-hydrogen bonds catalyzed by rhodium-trimethylphosphine complexes. *Organometallics* **1991,** *10*, 782-786.

71. Platel, R. H.; Schafer, L. L. Zirconium catalyzed alkyne dimerization for selective Z-enyne synthesis. *Chem. Commun.* **2012,** *48*, 10609-10611.

72. Rivada-Wheelaghan, O.; Chakraborty, S.; Shimon, L. J.; Ben-David, Y.; Milstein, D. Z-Selective (Cross-)Dimerization of Terminal Alkynes Catalyzed by an Iron Complex. *Angew. Chem. Int. Ed. Engl.* **2016,** *55*, 6942-5.

73. Azpíroz, R.; Rubio-Pérez, L.; Castarlenas, R.; Pérez-Torrente, J. J.; Oro, L. A. gem-Selective Cross-Dimerization and Cross-Trimerization of Alkynes with Silylacetylenes Promoted by a Rhodium–Pyridine–N-Heterocyclic Carbene Catalyst. *ChemCatChem* **2014,** *6*, 2587-2592.

74. Katagiri, T.; Tsurugi, H.; Satoh, T.; Miura, M. Rhodium-catalyzed (E)-selective cross-dimerization of terminal alkynes. *Chem. Commun.* **2008**, 3405-3407.

75. Albrecht, M. Cyclometalation Using d-Block Transition Metals: Fundamental Aspects and Recent Trends. *Chem. Rev.* **2010,** *110*, 576-623.

76. Henderson, W. H.; Alvarez, J. M.; Eichman, C. C.; Stambuli, J. P. Characterization, Reactivity, and Potential Catalytic Intermediacy of a Cyclometalated Tri-tert-butylphosphine Palladium Acetate Complex. *Organometallics* **2011,** *30*, 5038-5044.

77. Lauer, M. G.; Headford, B. R.; Gobble, O. M.; Weyhaupt, M. B.; Gerlach, D. L.; Zeller, M.; Shaughnessy, K. H. A Trialkylphosphine-Derived Palladacycle as a Catalyst in the Selective Cross-Dimerization of Terminal Arylacetylenes with Terminal Propargyl Alcohols and Amides. *ACS Catalysis* **2016,** *6*, 5834-5842.

78. Netherton, M. R.; Fu, G. C. Air-Stable Trialkylphosphonium Salts: Simple, Practical, and Versatile Replacements for Air-Sensitive Trialkylphosphines. Applications in Stoichiometric and Catalytic Processes. *Org. Lett.* **2001,** *3*, 4295-4298.

79. Stambuli, J. P.; Stauffer, S. R.; Shaughnessy, K. H.; Hartwig, J. F. Screening of Homogeneous Catalysts by Fluorescence Resonance Energy Transfer. Identification of Catalysts for Room-Temperature Heck Reactions. *J. Am Chem. Soc.* **2001,** *123*, 2677-2678.

80. Jover, J.; Cirera, J. Computational assessment on the Tolman cone angles for P-ligands. *Dalton Transactions* **2019,** *48*, 15036-15048.